CIB-W18 Timber Structures

– A review of meetings 1–43

Part 6: Essays

Hans Jørgen Larsen
Jørgen Munch-Andersen (ed.)

Danish Timber Information 2011

CONTENT

TRÆ Information

ESSAY 2.1 H J Larsen
Compression perpendicular to grain

The rules in the ENV version of Eurocode 5 from 1987 were very simple. It had to be verified that

$$\sigma_{c,90,d} \leq k_{c,90} f_{c,90,d} \tag{1}$$

with

$$f_{c,90,k} = 0,014 \rho_k \tag{2}$$

and where $k_{c,90}$ varied from 1 to 1,8 as shown in Table 1 – dependent on the geometry, see Figure 1.

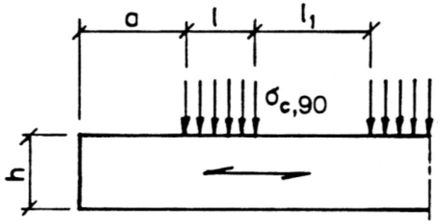

Figure 1. Geometry

Table 1. $k_{c,90}$ dependent on a, l and l_1 in mm.

	$l_1 < 150$ mm	$l_1 \geq 150$ mm	
		$a \geq 100$ mm	$a < 100$ mm
$l \geq 150$ mm	1	1	1
$150 \text{ mm} > l \geq 15$ mm	1	$\sqrt[4]{\frac{150}{l}}$	$1+\left(\sqrt[4]{\frac{150}{l}}-1\right)\frac{a}{100}$
$15 \text{ mm} > l$	1	1,8	$1+\frac{a}{125}$

In about 1995 (see e.g. **Paper 31-6-4**) it became clear that a more realistic value for $f_{c,90,k}$ was

$$f_{c,90,k} = 0,007 \rho_k \tag{3}$$

and research was initiated to verify higher values for $k_{c,90}$.

The result was very complicated rules in the 2004-version of Eurocode 5, but even though the clause on compression perpendicular to grain swelled to 4 full pages, the rules were not exhaustive and, worse, they were not logical having strange $k_{c,90}$-jumps (e.g .from 1 to 4 for marginal changes of the geometric parameters.

Based on a paper by Blass and Görlacher[1] (not published and discussed in CIB W18) the rules were withdrawn and simple and realistic rules were given in an Amendment to Eurocode 5 (A1 from 2006). These rules, that are empirical, are discussed in **Paper 41-6-3.**

Especially for trusses made with punched metal plate fasteners there may be need for higher load-carrying capacity. This can be ensured by re-inforcing the compression zones. This possibility has been investigated by e.g. Kevarinmäki, **Paper 24-14-1.** Based on this paper and recent tests[2] conducted at VTT using the punched metal plates GNT-100S and GNT-150S, the following design method is proposed.

The characteristic load-carrying capacity for a load perpendicular to grain may be determined from:

$$R = R_{90,wood,k} + R_{plate,k} \tag{4}$$

$$R_{plate,k} = 2 l_{p,sup,ef}\, p_{c,\alpha,k} \tag{5}$$

where

$R_{90,wood,k}$	characteristic load-carrying capacity for load perpendicular to grain according to Eurocode 5
$R_{plate,k}$	characteristic contribution from the reinforcement
$l_{p,sup,ef}$	effective support plate length
$p_{c,\alpha,k}$	characteristic reinforcement resistance per unit length of the plate (α = 0º or α = 90º)
α	angle between the plate and the grain direction.

$$l_{p,sup,ef} = \begin{cases} l_{p,\sup} - c & \text{for end supports} \\ l_{p,\sup} + \Delta l & \text{for intermediate supports} \end{cases} \tag{6}$$

where

$l_{p,sup}$ the length of the support plate directly over the support area
c is the allowed misplacement tolerance of the punched metal plate.

---

1. Blass, H.J. and Görlacher, R.: Compression perpendicular to the grain. World Confer-ence Timber Engineering, Finland 2004, Vol. 2, p. 435-440
2. Test results have been published in the reports VTT-S-03764-09 and VTT-S-03766-09.

If the plate covers the whole width of the support then $c = 0$.

$p_{c,\alpha,k}$ and Δl shall be determined from test made with the specific plate and with the same support condition than envisaged, i.e. either with a timber support or with a support (concrete, steel) having a much larger compressive strength than timber perpendicular to the grain. In the former case the contribution for the reinforcement is only about 40 % of the contribution for the latter case.

The support plate length shall be measured as shown in Figure 1.

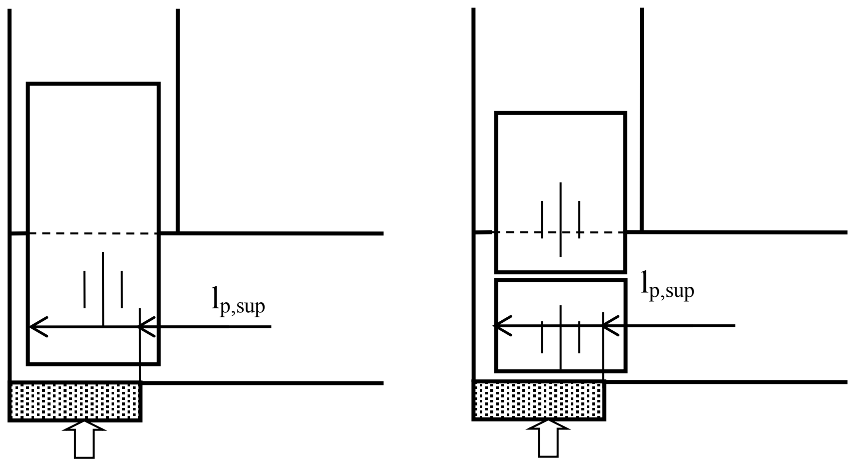

Figure 1. Reinforcement with plates covering the whole depth and with separated plates. α =90º.

The reinforcing punched metal plates shall be identical and be placed in the same way on both sides of the timber member. The extended reinforcement plates may also be used as a connection in the truss according to EN 1995-1-1. The separated punched metal plates are only used as reinforcement.

The reinforcing punched metal plates shall be placed in accordance with the following requirements:

– The principal direction of the punched metal plate shall be either α = 0° (Vertical position) or α = 90° (Horizontal position);
– The lower edge of the punched metal plate shall be between 3 mm and 10 mm away from the lower edge of the timber member;

With the separate reinforcement punched metal plates the gap between the upper and the lower plate shall be less than 10 mm and the height of the lower separate plate shall be at least 40% of the depth of the timber member.

Reinforcement has also been investigated by Korin, **Paper 23-6-1,** who did not find any effect. This may be due to the fact that the plates did not extend completely to the edges.

ESSAY 2.2 H J Larsen
Glulam Strength

The first drafts for standards for the strength of glulam were based on tests made in Norway by Johannes Moe[1]. Based on a small number of tests on 300 mm deep beams made of laminations without joints it was proposed and acceped to calculate the strength as

$$f_{glulam,k} = k\, f_{lamination,k}$$

with k as given in the following table. Note the very high lamination strengths and the corresponding high glulam strengths: between 48 and 28 MPa.

Lamination quality (approximately)	C40	C30	C20
Bending Tension and compression parallel to grain Modulus of elasticity for strength calculations	1,2	1,3	1,4
Shear		1,2	
Other stiffness values		1,2	

Ehlbeck and Colling put in **Paper 19-12-1** forward a more convincing theory for the strength of glulam. They note as a beginning that the bending strength of glulam beams depends especially on the tensile strength of the outer laminations. The tensile strength of a lamination differs, however, in two ways from that in a regular ISO 8375 tension test (strength increasing effects):

a) Lateral displacements of the laminations, occuring in a regular tension test, are prevented when the laminations are part of a glulam beam; this effect can be taken into account by a modification factor k_1
b) Longitudinal strains of a weak zone of the lamination (i.e. zones with knots and low modulus of elasticity) are hindered by the adjacent laminations; let this be taken into account by a modification factor k_2

The bending strength, $f_{m,glulam}$ can therefore be determined by the following equations

$$f_{m,glulam} = k_1 k_2 k_{v,1} f_{t,0}$$

$$f_{m,glulam} = k_1 f_{fj} k_{v,2} f_{t,0,fj}$$

where
$f_{t,0}$ is the tensile strength parallel to grain of the laminations
$f_{t,0,fj}$ is the tensile strength of the finger joints
$k_{v,1}$ and $k_{v,2}$ are factors depending on the varability of strengths

Based on own tests and tests by Larsen[2] the parameters are estimated.

Colling[3] developed in his dissertation from 1990 a model for the strength of glulam beams, the so-called Karlsruhe model.

The Karlsruhe Model uses a subdivision of a glulam beam into cells, (150 mm long and with a depth equal to the lamination thickness). Each cell is assigned random material properties. The calculation model is based on two computer programs, one that simulates glulam beam lay-up, and one that performs finite element calculations.

The beam lay-up simulation program assigns values to each cell along a continuous lamination, The lamination is assumed to consist of two “materials”: wood and finger-joints. First, the position of each finger-joint is determined by sampling from statistical distributions determined by measuring the distance between finger-joints in glulam beams. The density is assumed to be constant within a lamination, but is allowed to vary between laminations. The knot area ratioes (KAR)-value and the density are then used to calculate the stiffness (modulus of elasticity) using regression equations. For each lamination, i.e. for all the cells between two finger-joints, a single basic KAR-value is assigned. This KAR-value is then used within the lamination to assign each cell a specific KAR-value by multiplying the chacteristic lamination-KAR-value by a factor, taken from statistical distributions, its aim being to simulate the influence of multiple knots within a limited zone (= the length of the cell) of the lamination. Following the assigning of KAR-values, each lamination in the beam is assigned a modulus of elasticity in the cells of that lamination. The procedure is shown in below.

---

1. Moe, J.: Strength and stiffness of Glued Laminated Timber Beams, Norsk Skogindustri 1961
2. Larsen, H. J.: Strength of glulam beams, Institute of Building Technology and Structural Engineering, Aalborg University, Report 8201, 1982
3. Collin, M.: Tragfähigkeit von Biegeträgern aus Brettschnittholz in Abhängigkeit von den festigkeitsrelevanten Einflussgrössen. Karlsruhe, 1990

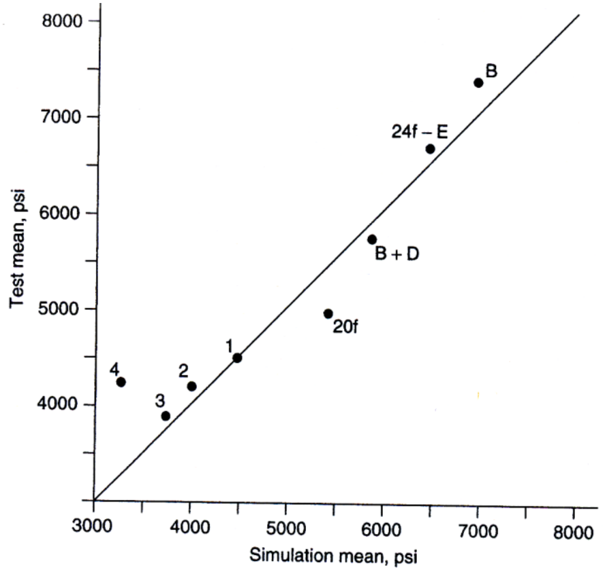

For a given lamination i, and a given KAR-value, the modulus of elasticity is calculated from

$$\ln\left(E_i\right) = \ln\left(E_{reg}\right) + \Delta_{B,i} + X_i$$

where E_i is the modulus according to the regression equation for lamination i. Each such equation gives an expression for the modulus of elasticity as a function of density and KAR-value. Δ_B is defined in the following figure and is a measure of the difference from the average regression equation. Δ_B is assumed to be normally distributed. X_i is a measure of distance from the average regression line to the regression line of the current lamination, and is also assumed to be normally distributed. As an example, the variability for a variable X, is shown as $S_{R,B,1}$.

This procedure is capable of simulating the correlation between KAR-values found within a single lamination. Also, the procedure used means that even if two cells are assigned the same KAR-value, their respective modulus of elasticity need not be the same.

The continuous lamination also contains finger-joints, which are modelled in the same way as described above, but by assigning "finger-joint properties" instead of "wood properties" to the cell that contains a finger-joint.

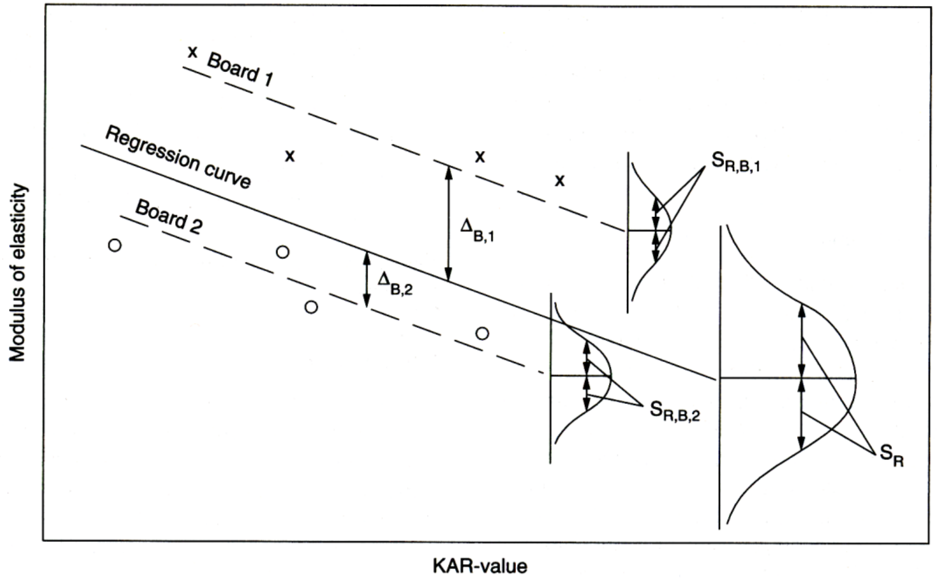

Four different failure criteria are used. These criteria are based on "experience gained during the calibration of the model to beam bending tests":

1. If the stress redistribution due to the removal of a failed element leads to the failure of another element, the beam is assumed to fail. This simulates a brittle failure in tension.
2. If an element fails in tension within a predefined region of a previously failed element, the beam is assumed to collapse. This simulates a failure due to high shear stresses

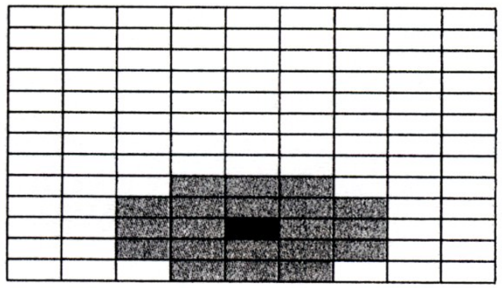

If an element fails close to (grey area) a previously failed element (black) the beam fails.

3. If a finger-joint fails in tension the beam fails. This is motivated by the fact that finger-joints induce a failure across the complete lamination width, and not only a part of it as is the case for knots.
4. If none of the above criteria have been fulfilled, the beam is assumed to fail when the fifth element fails in tension.

The model has been substantiated by many tests both for softwoods, see e.g. **Paper 26-12-1** and hardwoods, see e.g. **Paper 40-12-6.**

An improved model for softwoods is described in **Paper 40-12-2.**

The European Standard for glulam EN 1194 (to be replaced by EN 14080) is partly based on the model but mainly on empirical expressions fitted to data, see e.g. **Paper 28-12-1.**

In USA a completely different approach has been chosen, viz. the so-called I_K/I_G model established in 1954. I_K is moment of inertia of the knot area in a cross-section, and I_G is gross moment of inertia The theory is obscure and relies on several fitting factors/functions based on extensive testing, see **Paper 40-12-4**

ESSAY 2.3 H J Larsen
Shear strength of timber

In Eurocode 5:2000 very simple design rules were given for shear in beams without end notches:

For shear with a stress component parallel to the grain, see Figure 6.5(a), as well as for
shear with both stress components perpendicular to the grain, see Figure 6.5(b), the following
expression shall be satisfied:

$$\tau \leq f_v \tag{6.13}$$

where
τ shear stress
f_v shear strength for the actual condition.

NOTE: The shear strength for rolling shear is approximately equal to twice the tension strength perpendicular to grain.

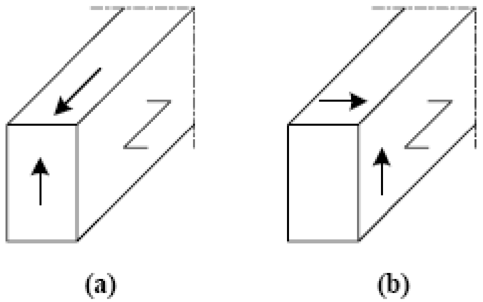

Figure 6.5.(a) Member with a shear stress component parallel to the grain (b) Member with both stress components perpendicular to the grain (rolling shear)

There is thus no size factor and the influence of any end crack is disregarded.
In an amendment (A1 dated 2007) the following is added

For the verification of shear resistance of members in bending, the influence of cracks should be taken into account using an effective width of the member given as:

$$b_{ef} = k_{cr} b \tag{6.13a}$$

where b is the width of the relevant section of the member.

NOTE: The recommended value for k_{cr} is given as
k_{cr} = 0,67 for solid timber
k_{cr} = 0,67 for glued laminated timber
k_{cr} = 1,0 for other wood-based products in accordance with EN 13986 and EN 14374.

Information on the National choice may be found in the National annex.

But still any size effect is disregarded although several researchers have found a size effect at least as big as for tension perpendicular to grain, see **Paper 19-12-3** and **Paper 38-6-3.**

Since rather high shear strengths are given in the present standards EN 338:2003 - Structural timber - Strength classes and EN1194:1999 - Timber structures - Glued laminated timber - Strength classes and determination of characteristic values, the formal safety against shear failure is probably less than for e.g. bending. That shear failures are very rare in timber structures is probably due to that the shear stress distribution at supports deviate from what is normally assumed.

ESSAY 2.4 H J Larsen
Size factors

Timber is a heterogeneous material containing dispersed defects. As a result, the measured bending strength of timber depends on many factors such as the length of the beam, the method of loading, and any bias used in selecting the test beam. The influence of these various factors is often described in terms of two factors: a 'size factor' and a 'load configuration factor'.

These factors are often determined by applying Weibull's weakest link theory although the basic assumptions of the Weibull theory (brittle failure, statistical homogeneity) are not strictly fulfilled.

To estimate the influence of the stress distribution and the size of the stressed volume on the strength, see **Paper 19-12-3**, the two-parameter Weibull-distribution is used. The cumulative frequency is defined by

$$S = 1 - \exp\left[-\int_V \left(\frac{\sigma}{f}\right)^k dV\right] \tag{1}$$

where f and k are the parameters of the Weibull-distribution, and $\sigma = \sigma(x,y,z)$ is the stress distribution over the volume V.

The (constant) width b of a beam with rectangular cross section $b \times h$ is assumed not to influence its strength, so that the integral in (1) may be written:

$$\int_V \left(\frac{\sigma}{f}\right)^k dV = b \int_{x=0}^{L} \int_{y=0}^{h(x)} \left(\frac{\sigma(x,y)^k}{f}\right) dy dx \tag{2}$$

For a beam with constant depth ($k(x) = h$) (2) may be written:

$$\int_V \left(\frac{\sigma}{f}\right)^k dV = bhL\left(\frac{\max\sigma}{f}\right)^k \int_{\varepsilon=0}^{1} F^k(\varepsilon) d\varepsilon \int_{\xi=0}^{1} G^k(\zeta) d\zeta = V\left(\left(\frac{\max\sigma}{f}\right)^k \lambda_L \lambda_h\right)^k \tag{3}$$

with

V stressed volume

max σ maximum stress occurring over the volume V

$F(\varepsilon), G(\zeta)$ dimensionless stress distribution over the length and depth respectively related to max σ

λ_L, λ_h parameters, denoted fullness parameters by Colling, to describe the fullness of the stress-distributions. A value of λ near 1 stands for a nearly constant stress-distribution.

Table 1 gives expressions for λ.

The exponent k depends only on the variation of the distribution and may approximately be determined by

$$k = \frac{1{,}15}{\text{COV}} \tag{4}$$

In the case of shear and tension perpendicular to grain k = 5 may be assumed corresponding to a coefficient of variation of COV = 0,23.

For structural timber beams in bending the size effect is in most cases expressed as a depth effect that covers as well the depth influence proper as the length effect, i.e. the depth factor k_h is nomally given as

$$k_h = \left(\frac{h_{ref}}{h}\right)^c \tag{5}$$

where

h beam depth

h_{ref} a reference depth

c a constant

In Europe a reference depth of h_{ref} = 150 mm and c = 0,2 has been chosen. In North America h_{ref} = 150 mm and c = 0,4 covering also a length effect.

For glulam a reference depth of h_{ref} = 600 mm and c = 0,1 mm has been chosen.

Some researchers doubt any depth effect for glulam; see **Paper 28-12-2.** The chosen reference depth makes it very costly to make tests that can unequivocally determine the depth effect for glulam.

Table 1. Fullness-parameter λ as a function of the exponent k of the two-parameter Weibull distribution.

Stress-distribution		λ
1	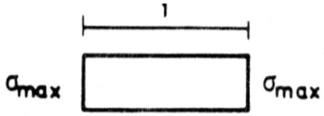	1,0
2		$\left(\frac{1}{k}\right)^{1/k}$
3	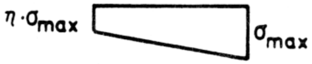	$\left(\frac{1}{k+1}\cdot\frac{1+\lvert\eta\rvert^{k+1}}{1+\lvert\eta\rvert}\right)^{1/k}$
4	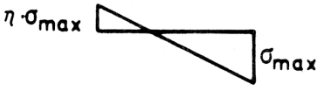	$\left(\frac{1}{k+1}\cdot\frac{1-\eta^{k+1}}{1-\eta}\right)^{1/k}$
5	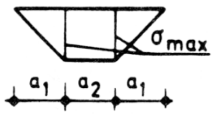	$\left(\frac{1}{k+1}\left(1+a_2k\right)\right)^{1/k}$
6	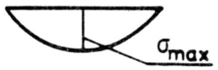	$\sim\Big(\; [illegible] \; +0,345k-0,027k^2+0,0013k^3\big)\Big)^{1/k}$

EN 408 – Timber structures – Structural timber and glued laminated timber – Determination of some physical and mechanical properties, specifies that the bending strength shall be determined from tests on beams with geometry as shown in Figure 1.

EN 384, Structural timber – Determination of characteristic values of mechanical properties and density requires that the bending and tensile strength shall be adjusted to 150 mm depth or width by dividing by

$$k_h = \left(\frac{150}{h}\right)^{0,2} \tag{6}$$

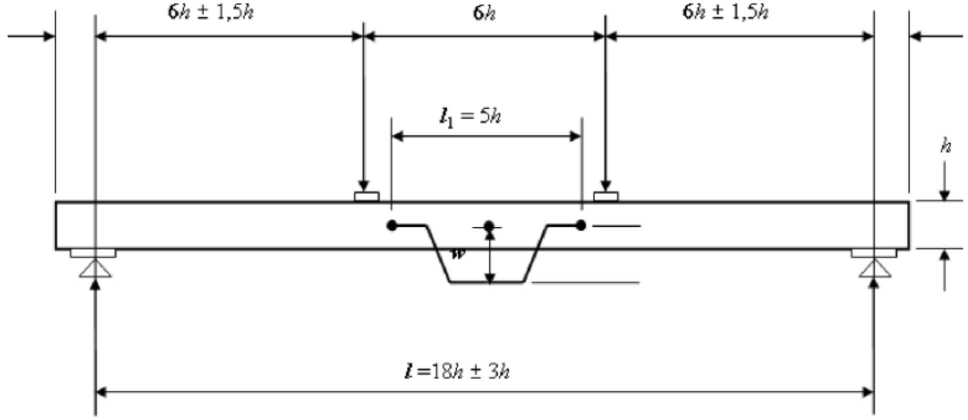

Figure 1 — Test arrangement for measuring local modulus of elasticity in bending

When the bending test arrangement is not as shown (i.e. span, $l = 18h$ and distance between inner points, $a_1 = 6h$) then the bending strength shall be adjusted by dividing by

$$k_l = \left(\frac{l_{es}}{l_{et}}\right)^{0,2} \tag{7}$$

where l_{es} and l_{et} are calculated as

$$l_{es} \text{ or } l_{et} = l + 5a_f \tag{8}$$

and l and a_f have the respective values for the standard test procedure and the test.

Apparently the depth rules are identical for design and test. However, (7) applies for all depths, while (5) only applies for $h \le 150$ mm, reflecting Eurocode 5´s attitude to size effect for beams. The missing symmetry makes it possible to cheat with the strength values.

Eurocode 5 does not take the effect of load configuration into account. This is in practice not feasible, even the simplest beam design would become very complicated.

As shown in **Paper13-6-2** there is also a size effect for longitudinal shear and here has been proposals for including the effect in Eurocode 5.

As for configuration effect this has been estimated to be too complicated, especially since shear is seldom decisive in practice.

For a curved beam it shall be verified that

$$\sigma_{t,90} \leq k_{dis} k_{vol} f_{t,90}$$

where

$$k_{vol} = \left(\frac{V_0}{V}\right)^{1/k} = \left(\frac{V_0}{V}\right)^{1/5}$$

where

- V *is* the stressed volume and V_0 is the reference volume for which $f_{t,90}$ is defined. According to EN 1194 - Timber structures - Structural timber and glued laminated timber - Determination of some physical and mechanical properties, the reference volume is 0,01 m^3.
- k_{dis} is a factor that takes into account the stress distribution.

For a curved beam with constant moment where the stresses $\sigma_{t,90}$ varies parabollically over the depth k_{dis} is theoretically 1,22. Eurocode 5 gives k_{dis} = 1,4 for all curved beams and tapered beams with straight underside and k_{dis} = 1,7 for pitched-cambered beams.

Tension perpendicular to grain

For a uniformly stressed volume V, the design criterion is

$$\sigma_{t,90} \leq f_{t,90} \left(\frac{V_{ref}}{V}\right)^{1/k}$$

where V_{ref} is the reference volume for which $f_{t,90}$ is determined and k is the parameter of the Weibull distribution (in Eurocode 5 a value of k = 5 is normally used.

ESSAY 3.1 H J Larsen
Stresses around holes in beams

The placement of holes in glulam beams represents a frequent necessity in timber construction practice in order to enable the penetration of pipes and wires. The disturbance of the stress flow around a hole creates tension stresses perpendicular to grain which may reduce the load bearing capacity of beams with unreinforced holes considerably. In general a hole reinforcement is inevitable to provide sufficient shear force capacity. Invisible internal reinforcements, such as glued-in steel rods and screws, especially self-tapping screws, are very often preferable from architectural points of view.

In a draft for Eurocode from 2002 there was a proposal for design rules. It was based on the assumption that the load-carrying was the same as for a corresponding notched beam, see the figure.

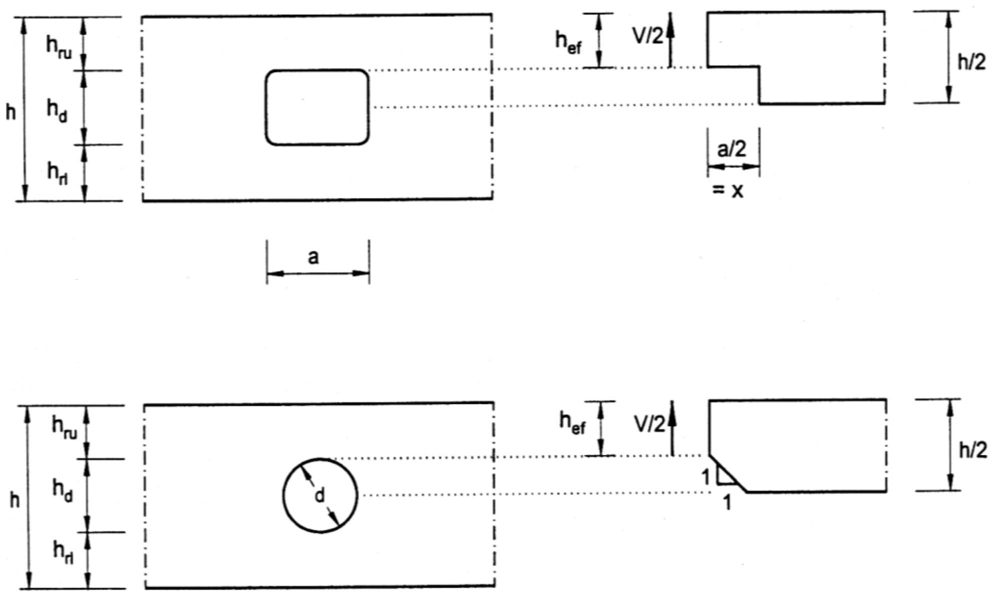

Dimensions of holes in beams and the notched beam approximations for rectangular and round holes.

The analogy seams obvious, however tests has shown that the method is very much on the unsafe side and it is not found in the final (2004) Eurocode 5.

Another method was put forward in a draft (2000) for the German Timber Design Code: DIN 1052. The method is below described for a round hole (the design for rectangular holes is in principle the same). The method is a classical strength of material approach: The design tension force perpendicular to the grain at the hole periphery, $F_{t,90,d}$ is compared to the design value of the resistance $R_{t,90,d}$

$$\frac{F_{t,90,d}}{R_{t,90,d}} = \frac{F_{t,90,d}}{0,5 l_{t,90} b f_{t,90,d}} \le 1 \qquad (1)$$

where (in case of round holes)

$$l_{t,90} = 0,353 h_d + 0,5 h \qquad (2)$$

is the distribution length of the assumed triangular stress distribution perpendicular to grain. b is beam width and $f_{t,90,d}$ is the design tension strength perpendicular to grain, see the figure. Rewritten as the ratio of a design stress $\sigma_{t,90,d}$ versus design strength, (1) reads:

$$\frac{\sigma_{t,90,d}}{f_{t,90,d}} \le 1 \qquad (1b)$$

where

$$\sigma_{t,90,d} = \frac{F_{t,90,d}}{0,5 l_{t,90} b} \qquad (3)$$

The design value of the tension force is composed of two additive parts bound to the separate actions of the shear force and the bending moment

$$F_{t,90,d} = F_{t,V,d} + F_{t,M,d} \qquad (4)$$

where (in the case of round holes)

$$F_{t,V,d} = \frac{V_d \cdot 0,7 h_d}{4h}\left[3 - \frac{(0,7 h_d)^2}{h^2}\right] = \eta V_d \qquad (5)$$

$$F_{t,M,d} = 0,008 \frac{M_d}{h_r} \qquad (6)$$

V_d and M_d are the absolute values of design shear force and moment at the hole edge (hole centre $\pm d/2$): sign of $\pm d/2$ to be chosen so as to give unfavourable results and

$$h_r = \min\{h_{ru} + 0{,}15 h_d, h_{rl} + 0{,}15 h_d\}^2 \tag{7}$$

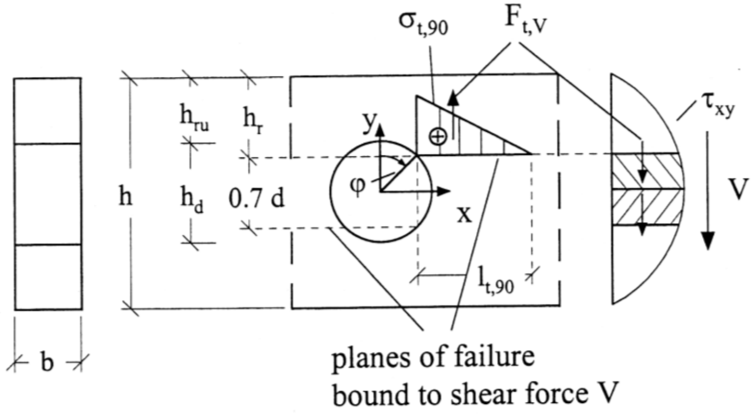

Geometry notations of a round hole in a glulam beam according to DIN 1052 and schematic illustration of the derivation of the tension force $F_{t,v}$ bound to shear force V.

Further, the maximum/minimum restrictions $h_d \le 0{,}4h$ and $h_{ro(ru)} \ge 0{,}25h$ apply.

However, the tests reported, support neither the DIN nor the Eurocode methods and they have both been withdrawn. For the time being there is no recognized design method and it is generally necessary to avoid the problem by using a reinforcement at the hole edges.

There is, however in **Paper 42-12-1** a new draft for a design method. It is copied below.

Design and construction rules for internally reinforced holes according to DIN 1052

Figure 6 gives the geometry notations used in the present German timber design code DIN 1052:2008-10. In detail Fig. 6a specifies the dimensions of the hole within the beam and indicates the relevant crack planes, similarly relevant for unreinforced and reinforced holes. Figure 6 b gives the dimensional notations of the internal reinforcement rods and the respective (edge) distances. The following construction rules/limits for the permissible position and sizes of round holes (see Fig. 6a) apply:

- $\ell_v \ge h$
- $\ell_A \ge h/2$
- $h_{ro(ru)} \ge h/4$
- $h_d \le 0{,}3\, h$ (internal reinforcements, i. e screws, glued-in rods)
- $h_d \le 0{,}4\, h$ (external reinforcements, i. g. glued-on plywood plates)

For the position of the reinforcement bars (d_r = nominal /outer diameter) the following (edge) distances are prescribed:

- $a_{1,c}$: $2{,}5\, d_r \le a_{1,c} \le 4\, d_r$
- a_2: $a_2 \ge 3\, d_r$
- $a_{2,c}$: $a_{2,c} \ge 2{,}5\, d_r$

The design verification of the rod is given as

$$F_{t,90,d} \le R_{ax,d} \tag{1}$$

where

$$F_{t,90,d} = F_{t,90,k} \cdot \gamma_L = F_{t,V,d} + F_{t,M,d} \tag{2a}$$

design (d) resp. characteristic (k) tension force perpendicular to grain due to stress disturbance in the hole vicinity

and

$$F_{t,V,d} = \frac{V_d \cdot 0{,}7 h_d}{4 \cdot h}\left[3 - \frac{(0{,}7\, h_d)^2}{h^2}\right], \quad F_{t,M,d} = 0{,}008\,\frac{M_d}{h_r} \tag{2b,c}$$

$$h_r = \min\{h_{ro} + 0{,}15\, h_d ; h_{ru} + 0{,}15 h_d\} \tag{3}$$

k_{mod} — modification factor for accumulated load duration and service class;

γ_L, γ_M — partial safety factors for loading and materials

And on the resistance side, in case of screws

$R_{ax,d} = R_{ax,k} \cdot (k_{mod} / \gamma_M)$ — axial design (d) resp. characteristic (k) tension capacity of the rod (4a)

In case of (self-tapping) screws the characteristic axial capacity at 90 degrees vs. fiber direction is (head pull through situation not regarded here)

$$R_{ax,k} = \min\left\{f_{1,k} \cdot \ell_{ad} \cdot d_r \,;\, R_{t,u,k}\right\} \quad (4b)$$

and (ρ_k in kg/m^3)

$f_{1,k} = 80 \cdot 10^{-6} \cdot \rho_k^2$ in N/mm^2 — characteristic value of pull out parameter of wood screw (load capacity class 3) or of self tapping screw acc. to Z-9.1-519 (4c)

$R_{t,u,k}$ — characteristic axial steel tension load capacity

In case of glued-in rods the design capacity is

$$R_{ax,d} = \min\ \{\pi \cdot d_r \cdot \ell_{ad} \cdot f_{k1,d}\ ;\ f_{y,d} \cdot A_{ef}\} \quad (5a)$$

where

$f_{k1,d} = f_{k1,k} \cdot (k_{mod}\ \gamma_M)$ — design (d) resp. characteristic (k) bond strength between rod and timber (values for $f_{k1,k}$ given in Tab. F. 23 of DIN 1052:2008, see below) (5b)

$f_{y,d} = f_{y,k} / \gamma_M$ — design (d) resp. characteristic (k) yield stress of rod

The effective anchorage length ℓ_{ad} of the rod, accounting for the possible slight eccentricity of the hole vs. mid-depth and the respective minimum value are

$$\ell_{ad} = h_{ru} + 0{,}15\ h_d \quad \text{or} \quad \ell_{ad} = h_{ro} + 0{,}15\ h_d, \quad \ell_{ad,min} = \max\left\{0{,}5 d_r^2 ; 10 d_r\right\} \quad (5c,d)$$

The basic idea of the design equations (1) and (2a-c) is sketched schematically in Fig. 7, which exclusively addresses the redistribution of the shear stresses which can not be transferred in undisturbed manner due to the missing cross-section in the hole area [Kolb and Epple, 1984; Blaß and Steck, 1999a-c].

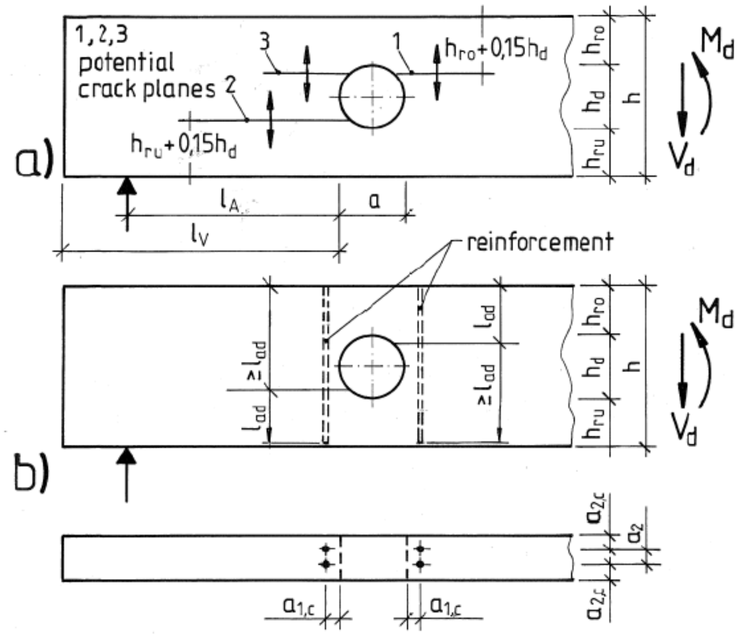

Fig. 6: Geometry notations and endangered/potential crack planes of unreinforced and reinforced glulam beams acc. to DIN 1052:2008

ESSAY 3.2 H J Larsen
Bracing of compression members

The theory on which the bracing rules in Eurocode 5 are based is the following.

Single column

The free length of a single column with length $2a$ shall be reduced to a by a support in the middle. A requirement for this is that the support has sufficient strength and stiffness. The requirements are as shown in the figure found by investigating a column that in the middle has the maximum permissible deflection e_{2a}. The force F that the lateral support shall be able to exert depends among other properties on its (spring)- stiffness C.

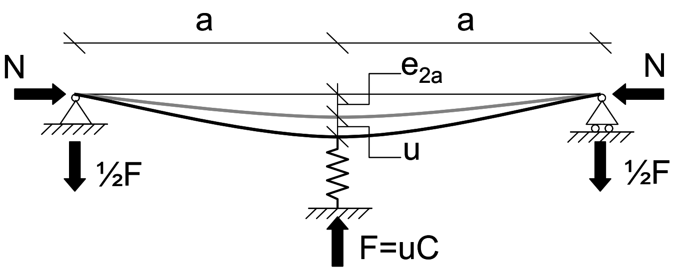

Compression loaded column over two spans with initial mid-height deflection e_{2a} laterally supported at mid-height by a spring with stiffness C, u is the resulting deflection and F the reaction force perpendicular to the column in the elastic support.

The axial force N results in a mid point moment of $N(e_{2a}+u)$ where u is the elastic deflection. This moment is counteracted by a force $2aF/4$. Since $u = F/C$, $N\left(e_{2a} + F/C\right) = Fa/2$ or

$$F = \frac{e_{2a}}{\frac{a}{2N} - \frac{1}{C}}$$

Theoretically, the minimum stiffness of the bracing member should be

$$C = k_s \frac{N_d}{a} = 2\left(1 + \cos\frac{\pi}{m}\right)\frac{N_d}{a}$$

where m is the number of spans. For two-spans it is thus required that k_s = 2 and for several spans k_s = 4.

For $e_{2a}/2a$ = 1/300 that is the maximum permitted value for structural timber and for $e_{2a}/2a$ = 1/300 that is the maximum permitted the maximum permitted deviation from straightness for glulam, the required strength is given in the table depending on C.

Theoretical requirements to the strength F expressed as F/N for different C-values.

	$e_{2a}/2a$	C		
		$2N/a$	$4N/a$	∞
Structural timber	1/300	∞	1/37,5	1/75
Glulam	1/500	∞	1/63	1/125

Based on experience other values may be found in the National Application Documents.

ESSAY 3.3 H J Larsen
Timber columns

Solid columns

The first draft for the CIB code (the predecessor for Eurocode 5) was based on **Paper 2-2-1**. The departure for this paper was a straight linear elastic column loaded with a sinusoidal deviation from straightness with an eccentricity in the middle of

$$e = e_1 + e_2 = a + b\lambda \quad (1)$$

where λ is the geometrical slenderness ratio:

$$\lambda = l/i \quad (2)$$

where
l column length/buckling length
i radius of gyration

A very simple failure criterion was used:

$$\sigma_c/f_c + \sigma_m/f_m = 1 \quad (3)$$

where
σ_c axial stress
σ_m bending stress
f_c compression strength
f_m bending strength

The column factor is defined as

$$k_c = \frac{\sigma_{cr}}{f_c} \quad (4)$$

where
σ_{cr} column failure stress

σ_{cr} was determined for various assumed eccentricities used in timber codes in Canada, France, Germany, The Netherlands, Norway, Switzerland, Sweden, UK and USA. In UK $a = 0$ has been used, leading to the so-called Perry Robertson formula from 1925.

In **Paper 4-2-1** results of tests with 120 columns of Nordic Spruce of C18 and C30 and with deflection both in the weak and the strong direction are reported.

The main conclusion is that the theory described in **Paper 2-2-1** is satisfactory and that the eccentricity independent of timber grade and direction may reasonably be put at:

$$e = (0{,}1 + 0{,}005\lambda)r \quad (5)$$

where
r is the core radius.

In **Paper 20-2-2** it is criticised that the design of timber columns is based on the elastic theory assuming that collapse occurs when an elastic limit state stress is reached. Research has shown that this failure criterion is conservative and that a considerably higher load-carrying capacity may be found – especially for laterally loaded columns – by taking the plastic behaviour into account. This is also pointed out in e.g. **Paper 17-2-1 and Paper 30-2-1.**

A computer model for the ultimate load of glued laminated columns is described and used to determine characteristic values of the load-carrying capacity of timber compression members. Monte-Carlo-simulations are used to calculate the ultimate load by a second order plastic analysis, assuming for both glued laminated and solid timber columns the stress-strain-diagram shown in Figure 1.

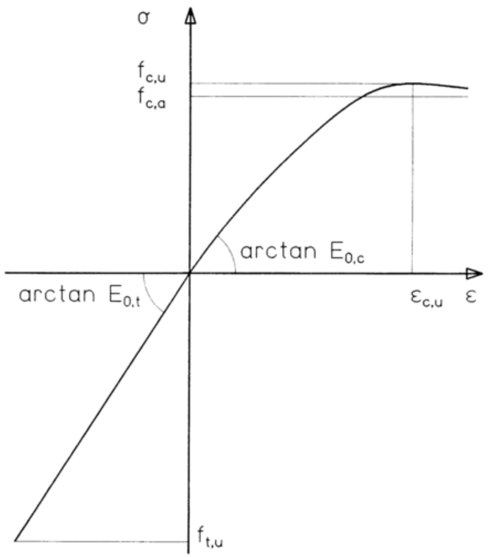

Figure 1. Stress-strain diagram. $f_{c,d} = 0{,}85 f_{c,u}$; $\varepsilon_{c,u} = 1{,}25 f_{c,u}/E_{0,c}$.

In the case of solid timber the properties were determined for cross-sections spaced 150 mm using the following structural attributes: density, knot area ratio, moisture content, and portion of compression wood. For glulam the properties were determined for cross-sections spaced 150 mm in each lamination and further the strength of finger joints were taken into consideration.

An example of a calculated k_{cr} -curve is shown in Figure 2.

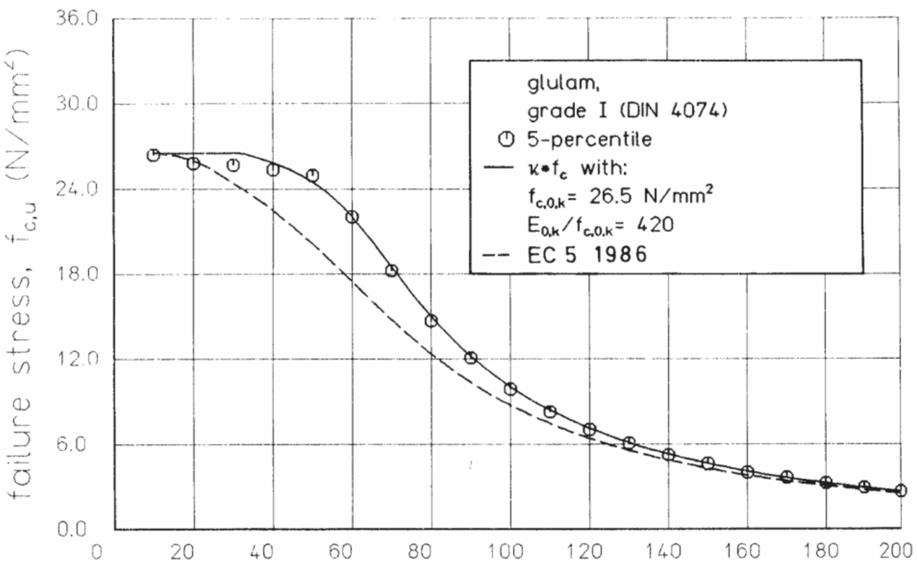

Figure 2. k_{cr} as function of the relative slenderness for timber with the assumed properties for grade 1 according to DIN 4074 together with the curve found from Eurocode 5. It is seen that Eurocode 5 is on the safe side.

The curves have been approximated by analytical expressions that happen to be the same as those given in Eurocode 3 for steel columns,

The Eurocode 3/Eurocode 5-curves may formally be found by the method described in **Paper 2-2-1** with an initial deviation from straightness given by:

$$\frac{e}{r} = \frac{f_m}{f_c} \beta\left(\lambda_{rel} - \lambda_{rel,0}\right) \tag{5}$$

where

β constant

λ_{rel} relative slenderness

$\lambda_{rel,0}$ the relative slenderness for the test specimens from which the compression strength is found

$$\lambda_{rel} = \frac{\lambda}{\pi}\sqrt{\frac{f_c}{E}} \tag{6}$$

$$\lambda_{rel,0} = 0,3$$

$$\beta = \begin{cases} 0,2 & \text{for structural timber} \\ 0,1 & \text{for glulam} \end{cases}$$

Since the curves have been approximated by analytical expressions of the same type as in **Paper 2-2-1**, the difference for centrally loaded columns is marginal. For laterally loaded columns, however the plastic method leads to significantly higher load-carrying capacities than the elastic approach for slenderness ratios below about 80, see Figure 3.

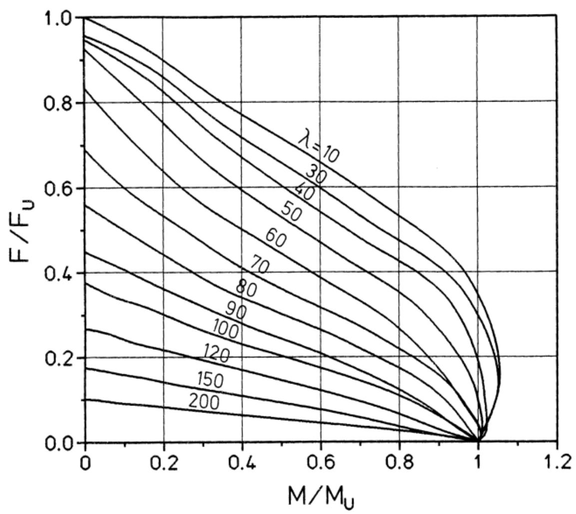

Figure 3. Combinations of axial forces and moments. F/F_u and M/M_u are in (7) and (8) denoted σ_c/f_c and $\sigma_{m,y}/f_{m,y}$.

This is, however, not taken into consideration in the general column expressions in Eurocode 5, where linear interaction expressions are prescribed, but only in the expressions for cross-section verification for combined compression and bending where for all slenderness ratios it is required that it shall be verified that

$$\left(\frac{\sigma_c}{f_c}\right)^2 + \frac{\sigma_m}{f_m} \leq 1 \quad \text{Eurocode (6.19)-(6.20)} \tag{7}$$

Leicester presents in **Paper 21-2-1** a very simplistic approach to instability problems. It is based on the fact that it is generally possible to determine the load-carrying capacity for the two extremes: slender members where the elastic solution (for columns e.g. the Euler load) and members without stability problems where the strength corresponds to the failure load of the cross-section. His thesis is then that any reasonable interaction curve supported by a few test is sufficiently accurate for practice. This approach is in Eurocode 5 used for lateral beam instability.

Built-up columns

Built-up columns, Eurocode 5, Annex C) are treated in **Paper 3-2-1**. Reference is made to the general theory for built-up structures where expressions for an effective moment of inertia I_e are given. It has been shown by testing that the load-carrying capacity for slender perfect columns is determined by the Euler formula using the effective moment of inertia. It is then suggested that the load-carrying capacity can generally be based on the usual expression, but with the slenderness ratio determined from I_e and not from the total moment of inertia I. The justification for this is discussed.

Expressions for the effective moments of inertia for various types of columns: continuously jointed columns, spaced columns with glued; nailed or bolted packs, spaced columns with glued or nailed battens (Vierendeel columns) and glued or nailed lattice columns are given based on tests with the said types of columns, partly to assess the applicability of the proposed theoretical expressions and partly to determine the rigidity of the connections.

The paper contains the expressions found in Eurocode 5, Annex C.

ESSAY 3.4 H J Larsen
Lateral instability of beams

High slender beams can fail due to lateral deflection and torsion even when they are loaded in pure bending as shown in Figure 1.

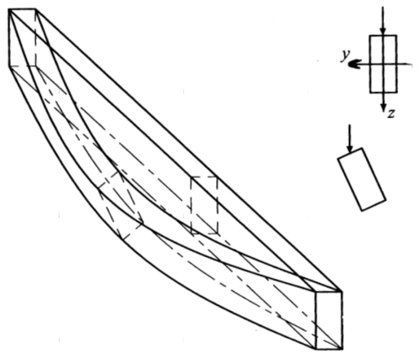

Figure 1. Deflected beam.

To calculate the load-carrying capacity of a straight elastic and simply supported beam, it is assumed that the torsion is prevented at the end supports and that the beam is loaded by two equal bending moments $M = M_y$ at the beam end. Under these conditions the beam will be stable for loads below a critical value $M = M_y$. If this moment is exceeded, the beam will deflect as shown in figure 1 and 2.

In the deflected state there will in addition to the moment about the *y*-axis be a moment M_z about the *z*-axis and a twisting moment M_x about the *x*-axis. Since the angles are small: $\sin\phi \sim \phi$ and $\cos\phi \sim \cos\theta \sim 1$, and

$$M_y = -EI_y \frac{d^2u}{dx^2} = M$$

$$M_z = M\phi = -EI_z \frac{d^2v}{dx^2} \qquad (1)$$

$$M_x = -M\theta$$

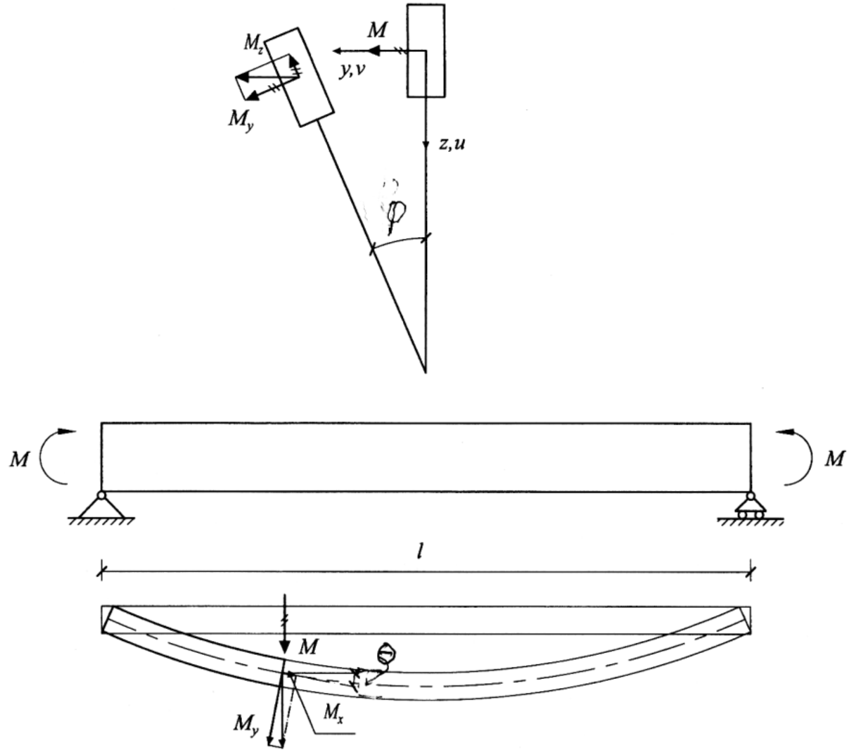

Figure 2. Beam deflected in torsion and lateral deflection instability

The differential equation for twisting (torsion) about the *x*-axis is:

$$M_x = GI_{tor}\frac{d\phi}{dx} - EI_w \frac{d^3\phi}{dx^3} \qquad (2)$$

where
I_{tor} is the torsional moment of inertia
I_w is the warping moment of inertia

By differentiation of (2) and inserting in (1):

$$-\frac{M^2\phi}{EI_z} = GI_{tor}\frac{d^2\phi}{dx^2} - EI_w \frac{d^4\varphi}{dx^4} \qquad (3)$$

A solution that fulfils the boundary conditions $\phi = 0$ for $x = 0$ and $x = l$ is:

$$\phi = \phi_0 \sin \frac{\pi x}{l} \tag{4}$$

where ϕ_0 is the twist angle at the beam middle. By inserting (4) in (3) you find:

$$\frac{M^2}{EI_z} \phi_0 \sin \frac{\pi x}{l} = GI_{tor} \phi_0 \left(\frac{\pi}{l}\right)^2 \sin \frac{\pi x}{l} + EI_w \phi_0 \left(\frac{\pi}{l}\right)^4 \sin \frac{\pi x}{l} \tag{5}$$

giving

$$M = M_{cr} = \frac{\pi}{l} \sqrt{EI_z GI_{tor} \left(1 + \left(\frac{\pi}{l}\right)^2 \frac{EI_w}{GI_{tor}}\right)} \tag{6}$$

The last term is only of importance for open thin-walled cross-sections. For the cross-sections common in timber structures $I_W / I_{tor} \sim 0$, i.e.

$$M_{cr} = \frac{\pi}{l} \sqrt{EI_y GI_{tor}} \tag{7}$$

The case with equal end moments is one of the few where there is an analytical solution. In most cases numerical methods, e.g. based on strain energy methods are required. Examples on solutions may be found in e.g. S. P. Timoshenko and J. M. Gere: Theory of Elastic Stability
The solutions may all be written as:

$$M_{cr} = \frac{\pi}{l_{ef}} \sqrt{EI_y GI_{tor}} \tag{8}$$

where l_{ef} is an effective length. Examples on l_{ef} are given in Table 1.

As is apparent from figures 1 and 2, the critical moment depends on the location of the load in the cross-section. The higher the location, the bigger the driving effect and the smaller the critical load. Loads acting below the axis of rotation will even have a stabilizing effect. This is taken into account in Eurocode 5 by reducing/increasing l_{ef} as shown by $0.5h$ and $2h$ respectively.

Lateral stability shall be verified both for M_y alone and for M_y together with an axial compression force N_c

Table 1. Effective length, l_{ef}, as a function of beam length l and beam depth h

	Load acts in		
	the bottom of the beam	the centerline	the top of the beam
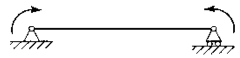		l	
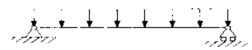	$0.9l - 0.5h$	$0.9l$	$0.9l + 2h$
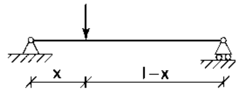	$0.8\alpha l - 0.5h$	$0.8\alpha l$	$0.8\alpha l + 2h$
$\alpha = 4\frac{x}{l}\left(1 - \frac{x}{l}\right)$			
	$0.6l - 0.5h$	$0.6l$	$0.6l + 2h$

For M_y alone, it shall be verified that

$$\sigma_m \leq k_{crit} f_m \tag{9}$$

where:

σ_m is the bending stress
f_m is the bending strength
k_{crit} is a factor that takes account of the reduced load-carrying capacity when failure is caused by lateral instability

The critical bending stress may be found from (8) as:

$$\sigma_{m,crit} = \frac{M_{y,crit}}{W_y} = \frac{\pi\sqrt{EI_z GI_{tor}}}{l_{ef} W_y} \tag{10}$$

where:

W_y is the section modulus.

For solid softwood, $\sigma_{m,crit}$ is approximately:

$$\sigma_{m,crit} = \frac{0,78\,b^2}{h\,l_{ef}} E_{0,05} \tag{11}$$

Acccording to Eurocode 5

$$k_{crit} = \begin{cases} 1 & & \lambda_{rel,m} \le 0,75 \\ 1,56 - 0,73\lambda_{rel,m} & \text{for} \quad 0,75 < & \lambda_{rel,m} \le 1,4 \\ \dfrac{1}{\lambda_{rel,m}^2} & \quad 1,4 < & \lambda_{rel,m} \end{cases} \tag{12}$$

where the relative slenderness $\lambda_{rel,m}$ has been introduced by

$$\lambda_{rel,m} = \sqrt{\frac{f_{m,k}}{\sigma_{m,crit}}} \tag{13}$$

In (12) the expression in the first line is the cross-section strength, the last expression is the instability strength according to the theory of elasticity and the middle expression is an interpolation proposed and verified in R F Hooley and B Madsen: Lateral instability of glued laminated timber beams, Journal of the Structural Division , ASCE, Vol. 90, No. ST3, 1964.

ESSAY 3.5 H J Larsen
System effects in Eurocode 5

Eurocode 5 states:

6.6 System strength
(1) When several equally spaced similar members, components or assemblies are laterally connected by a continuous load distribution system, the member strength properties may be multiplied by a system strength factor k_{sys}.
(2) Provided the continuous load-distribution system is capable of transferring the loads from one member to the neighbouring members, the factor k_{sys} should be 1,1.
(3) The strength verification of the load distribution system should be carried out assuming the loads are of short-term duration.

NOTE: For roof trusses with a maximum centre to centre distance of 1,2 m it may be assumed that tiling, battens, purlins or panels can transfer the load to the neighbouring trusses provided that these load distribution members are continuous over at least two spans, and any joints are staggered.

(4) For laminated timber decks or floors the values of k_{sys} given in Figure 6.12 should be used.

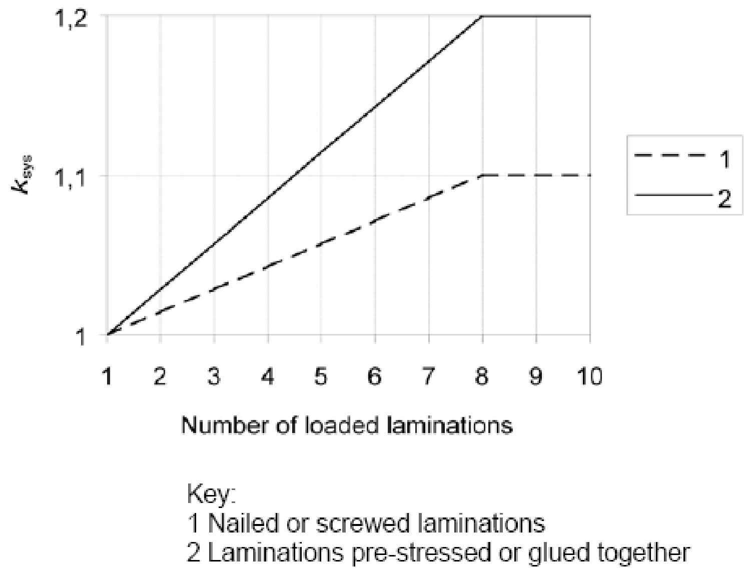

Figure 6.12 – System strength factor k_{sys} for laminated deck plates of solid timber or glued laminated members

* * *

There are 3 reasons why the strength of systems is increased.

- Initial failure in a cross-section or a joint may be counteracted or stopped because battens, laths and other secondary elements due to resulting deflections transfer part of its load to the neighbouring structures
- In statically indeterminate structures there is a possibility of load redistribution from weak to stronger elements.
- In e.g. trusses the moment distribution is characterised by localised moment peaks at supports and nodes. The probability that moment peaks and weak sections, e.g. due to knots, coincide is small.

Although it is unlikely that the secondary elements really are able to transfer a considerable part of a load on an element to the neighbouring elements, especially the situation mentioned in the NOTE is very unrealistic for trusses because of their high stiffness, Eurocode 5 takes only effect 1 into consideration and disregards effect 2, that is probably the most important and reliable effect.

ESSAY 3.6 H J Larsen
Mechanically jointed beams

Mechanically jointed built-up members were used to some extent until about 1950 but are now completely replaced by glued members, e.g. glulam and light I-beams with webs of panel materials. The reason why there is still interest in the topic in CIB-W18 is that the same theory applies to composite T-members with wooden webs and concrete flanges, both in new structures (e.g. bridges) and especially in old buildings where a new concrete slab on top of the existing beams can ensure an upgrading of the strength and also the fire resistance.

Figure 1 shows a symmetric, simply supported beam with two members (lamellas).

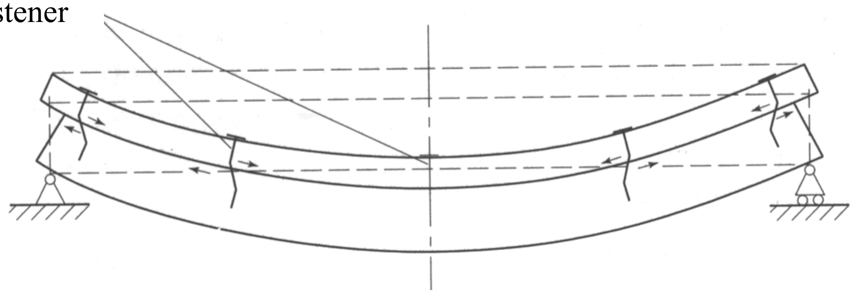

Figure 1. Simply supported composite (built-up) beam).

To transfer load between the lamellas there must be a slip in the joint, increasing from zero in the middle (due to symmetry) to a maximum value at the ends. The result is compression stresses in the top and tension in the bottom taking up any beam moment. The stiffer the connection, the more effective becomes the transfer between the two parts. If the connection is very stiff (glue), the situation corresponds to a solid beam. If the connection is very flexible, the strength and stiffness correspond to the sum of the members.

It is possible, see e.g. **Paper 3-2-1**, to derive relatively simple expressions for a general cross-section as shown in Figure 2, but in practice only T-cross-sections as shown in Figure 3, with 2 lamellas placed on top of each other are used and only these cross-sections will be dealt with in de tail in the following. However, at the end the Eurocode three expressions for I-cross-sections is derived.

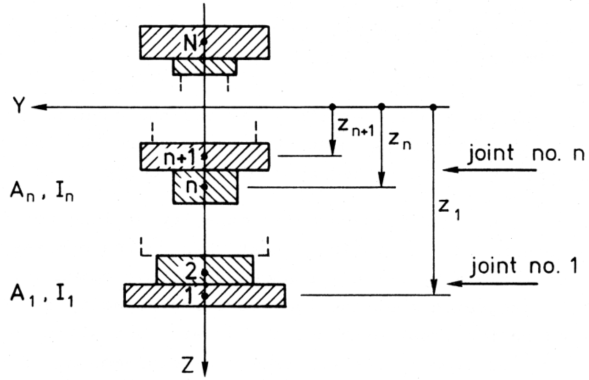

Figure 2. Cross-section with N lamellas.

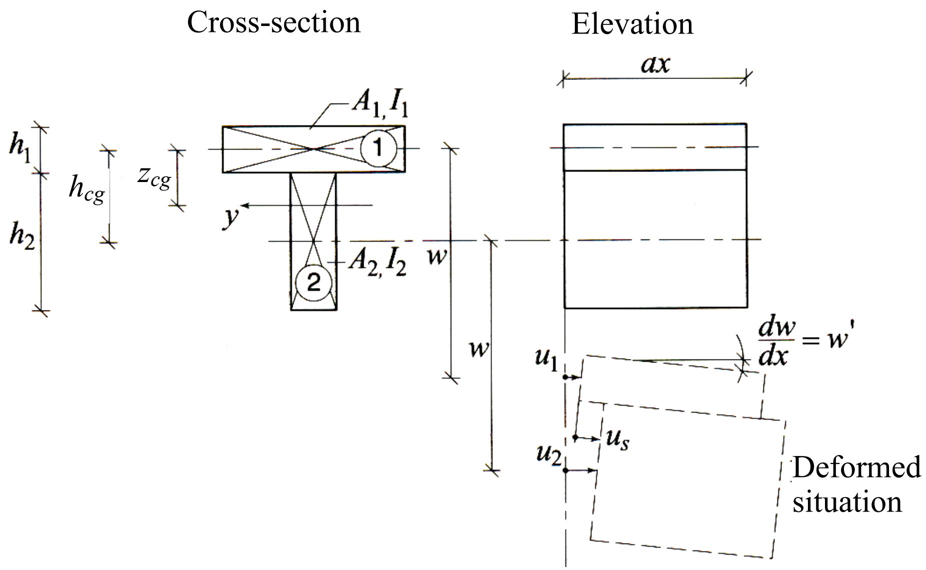

Figure 3. T- Cross-section.

T-cross-section

It is assumed that the lamellas are linear elastic. The lamination areas are A_1 and A_2. The second moments of area (moments of inertia) about there own centres of gravity are I_1 and I_2. If the modulus of elasticity vary, the theory applies if E_1 is taken as reference and the following geometrical values are used:

$$A_1,\ \frac{E_2}{E_1}A_2,\ I_1 \text{ and} \frac{E_2}{E_1}I_2. \tag{1}$$

The theory will be set up both for fasteners having a linear-elastic load-slip curve and for fasteners having a linear-elastic/ideal-plastic behaviour.

The centre of gravity is placed at

$$z_{cg} = h_{cg}\frac{A_2}{A_1 + A_2} \tag{1}$$

The total geometrical moment of inertia is

$$I = I_1 + I_2 + A_1 z_{cg}^2 + A_2\left(h_{cg} - z_{cg}\right)^2 = I_0 + h_{cg}^2 A_r \tag{2}$$

where

$$I_0 = I_1 + I_2 = \beta^2 I \tag{3}$$

$$A_r = \frac{A_1 A_2}{A_1 + A_2} \tag{4}$$

The deformation of the beam is described by the three translations u_1, u_2 and w where

u_1 translation in the beam direction of the centre of gravity of lamella number 1

u_2 translation in the beam direction of the centre of gravity of lamella number 2

w translation perpendicular to the beam axis (the same for both lamellas).

The strains are ($'$= differentiation with regard to x):

$$\varepsilon_1 = u_1' \text{ and } \varepsilon_2 = u_2' \tag{5}$$

The curvature is

$$\kappa = -w'' \tag{6}$$

For small values of w''

$$u_s = u_2 - u_1 + h_{cg}w' \tag{7}$$

or by differentiation

$$u_s' = u_2' - u_1' + h_{cg}w'' \tag{8}$$

u_s is the slip in the joint between lamella 1 and 2 taken positive as shown in Figure 3.

For elastic materials

$$N_1 = EA_1u_1' \quad \text{and} \quad N_2 = EA_2u_2' \tag{9}$$

$$M_1 = -EI_1w'' \quad \text{and} \quad M_2 = -EI_2w'' \tag{10}$$

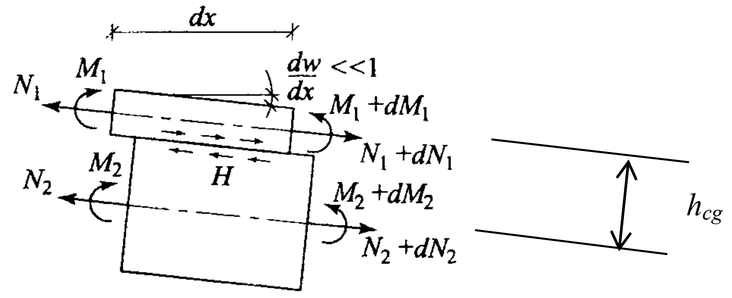

Figure 4. Forces and moments in the deformed situation.

Since there is no external axial force, equilibrium leads to:

$$0 = N = N_1 + N_2 = EA_1u_1' + EA_2u_2'$$

$$u_2' = -\frac{A_1}{A_2}u_1' \tag{11}$$

Moment equilibrium for the total cross-section:

$$M = M_1 + M_2 - h_{cg}N_1 = -E\left(I_1 + I_2\right)w'' - h_{cg}EA_1u_1' = EI_0w'' - h_{cg}EA_1u_1' \tag{12}$$

Equilibrium for Lamella 1:

$$Hdx + N_1 + dN_1 - N_1 = 0$$

$$H = -N_1' \tag{13}$$

H is the shearing force per unit length.

Elastic behaviour of fasteners

With a fastener spacing of a, the load on one fastener is Ha and with a fastener stiffness K:

$$Ha = Ku_s \quad H = \frac{K}{a}u_s \tag{14}$$

Inserting (14) and (10) differentiated in (13) gives

$$u_1'' = -\frac{K}{aEA_1} u_s \tag{15}$$

The marked expressions (8), (11), (12) and (15) are the basic expressions from which the deflection w may be determined.

The following equation is found.

$$w'''' - \left(\frac{\gamma}{\beta}\right)^2 w'' - \frac{1}{EI_0}\left(q + M\gamma^2\right) = 0 \tag{16}$$

with

$$\gamma^2 = \frac{K}{EA_r a} \tag{17}$$

A_r is defined in (5).

Example

Simply supported beam with sinusoidal load

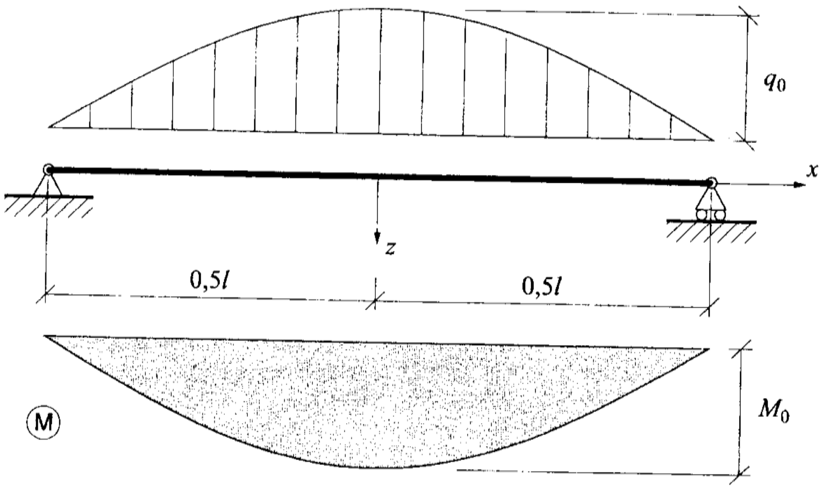

Figure 5. Simply supported beam with sinusoidal load.

The moment from the load $q = q_0 \cos\frac{\pi x}{l}$ is

$$M = \frac{q_0 l^2}{\pi^2}\cos\frac{\pi x}{l} = M_0 \cos\frac{\pi x}{l} \tag{18}$$

By (16)

$$w(x) = \frac{M_0}{EI}\left(\frac{l}{\pi}\right)^2 \frac{1+\left(\frac{\pi}{l\gamma}\right)^2}{1+\beta^2\left(\frac{\pi}{l\gamma}\right)^2}\cos\frac{\pi x}{l} = \frac{1+\mu}{1+\beta^2\mu} w_0(x) \tag{19}$$

where

$$\mu = \left(\frac{\pi}{l\gamma}\right)^2 = \frac{\pi^2 EA_r a}{l^2 K} \tag{20}$$

From this it is seen that

$$\frac{w}{w_0} = \frac{w'}{w'_0} = \frac{w''}{w_0''} = \frac{w'''}{w_0'''} = \frac{1+\mu}{1+\beta^2\mu} \tag{21}$$

The effective moment of inertia is defined as

$$I_{ef} = I\frac{1+\beta^2\mu}{1+\mu} = I_0 + \left(I - I_0\right)\frac{1}{1+\mu} \tag{22}$$

By using the effective moment of inertia, the deflections may be found by the usual methods from the theory of elasticity.

$1/(1+\mu)$ may be regarded as an effectivity factor k_{ef}. For completely stiff fasteners $\mu = 0$, i.e. $k_{ef} = 1$. For very flexible fasteners $\mu = \infty$, i.e. $k_{ef} = 0$.

Plastic behaviour of fasteners

It is assumed that that the load-slip curve is linear elastic-stiff plastic. For structural reasons fasteners are in practice placed over the full beam length, however with a concentration at the length Δl near the ends where the slip is biggest. The fasteners over the rest of the beam length are on the safe side disregarded.

It is assumed that the fastener spacing over the length Δl is constant and that the slip at least corresponds to the yield slip u_y, i.e the load per fastener is R_y . The shearing force per unit length is $H_y = R_y / a$ where a is the spacing.

Examples
A simply supported beams with uniformly distributed load built up of two members jointed by elastic-plastic fasteners with spacing a and yield load R_y is regarded.

$$M = 0,5qx(l-x) \tag{23}$$

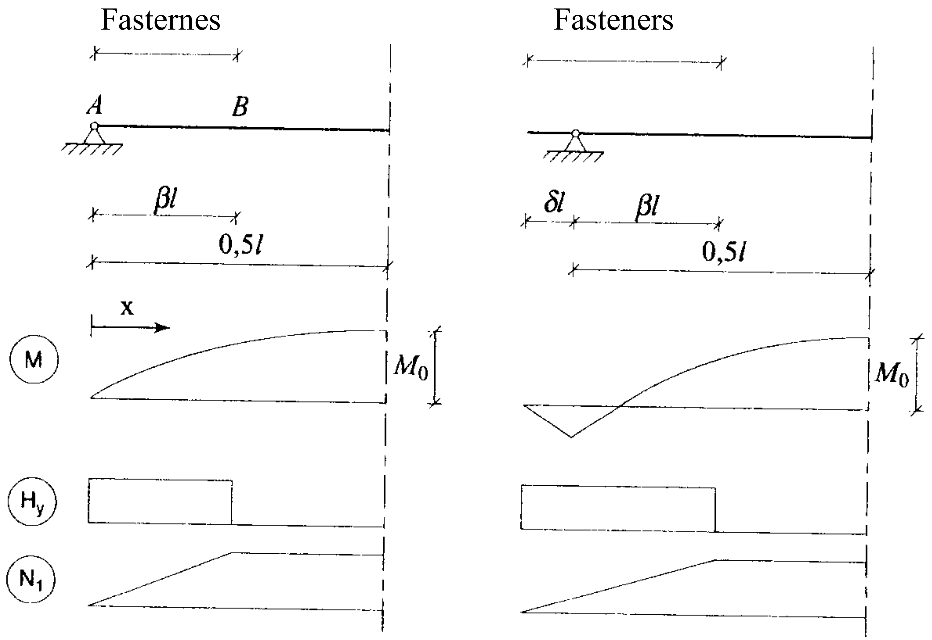

Figure 6. Simply supported beam with constant uniformly distributed load and plastic fastener over the length βl (left) or (δl + βl) (right).

No cantilever, *$\delta l = 0$*
See Figure 6, left.

$$0 \le x \le \beta l \qquad N_1 = -\frac{x}{a} R_y \tag{23}$$

$$\beta l \le x \le 0,5l \quad N_1 = -\frac{\Delta l}{a} R_y \tag{24}$$

The normal stresses in the laminations are found from the axial forces N_1 and $N_2 = - N_1$ (Note that N_1 is negative for downward load) and the moments in the laminations

$$M_1 = (M + N_1 h_{cg}) I_1 / I_0 \tag{25}$$

and

$$M_2 = (M + N_1 h_{cg}) I_2 / I_0 \tag{26}$$

The slip is found by (8):

$$u_s' = u_2' - u_1' + h_{cg} w'' = N_1 \left(\frac{1}{EA_1} + \frac{1}{EA_2} + \frac{h_{cg}^2}{EI_0} \right) - \frac{M}{EI_0} h_{cg} \tag{26}$$

Integrating and using

$u_s = 0 \quad$ for $x = 0,5l$

$u_s^+ = u_s^- \quad$ for $x = \beta l$

$$\text{A:} \quad u_s = \frac{l^2}{24E} \left(\frac{h_{cg}}{I_0} ql - 12 \frac{R_y / a}{A_r \beta^2} (1-\beta) \beta \right) \tag{27}$$

$$\text{B:} \quad u_s = \frac{l^2}{24E} \left(\frac{h_{cg}}{I_0} ql \left(1 - 6\beta^2 + 4\beta^3\right) - 12 \frac{R_y / a}{A_r \beta^2} (1-2\beta) \beta \right)$$

It shall be verified that

$$u_y \le u_s \le u_{failure} \tag{28}$$

where

$$u_{failure} \sim \tag{29}$$

If the beam has a cantilever *δl,* it is a good approximation just to replace Δl by ($\delta l + \beta l$).

I-cross-section
See Figure 7.

The total moment of inertia about the *y*-axis is

$$I = I_0 + \frac{1}{2} A_1 h_{cg}^2 \tag{30}$$

With

$$I_0 = I_1 + I_2 + I_3 = \beta^2 I \tag{31}$$

Because of the double-symmetry $u_2 = 0$, i.e. there is only two parameters u_1 and w and (8) is replaced by

$$u_s' = -u_1' + h_{cg} w'' \qquad (32)$$

The forces become

$$N_1 = -N_3 = EA_1 u_1' \quad \text{and } N_2 = 0 \qquad (33)$$

$$M_1 = M_3 = -EI_1 w'' \quad \text{and } M_2 = -EI_2 w'' \qquad (34)$$

The axial equilibrium is satisfied and moment equilibrium for the total cross-section leads to:

$$M = M_1 + M_2 - h_{cg} N_1 = EI_0 w'' - h_{cg} EA_1 u_1' \qquad (35)$$

that is identical to (12).

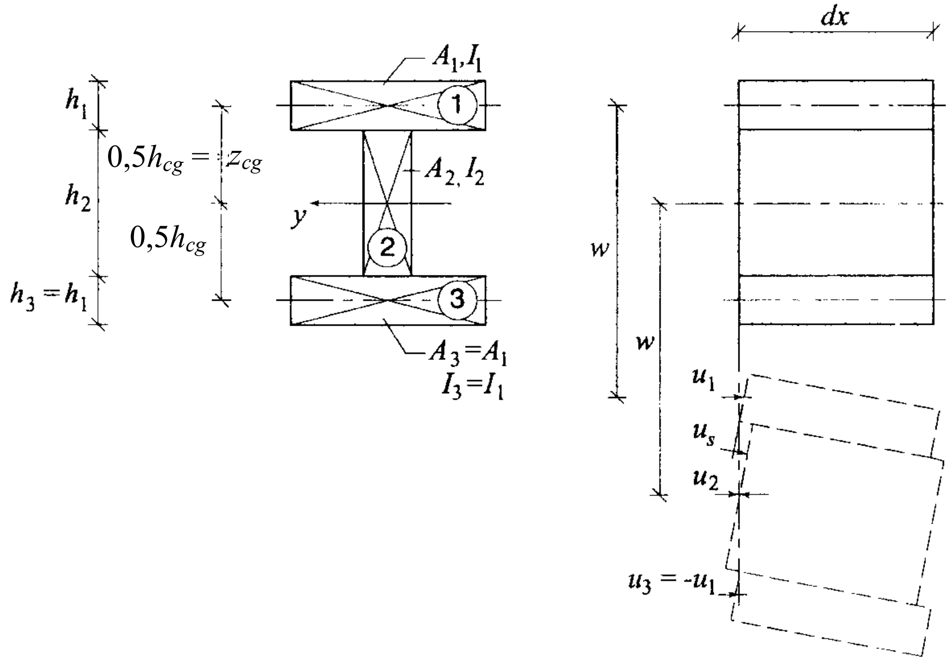

Figure 7. Double symmetrical cross-section. Geometry and deflections.

ESSAY 3.7 H J Larsen
Notched beams in Eurocode 5

The following simple closed-form equation for the strength is derived by means of fracture mechanics.

$$\frac{V_f}{b\alpha d} = \frac{\sqrt{G_{fy} / d}}{\sqrt{0,6(\alpha - \alpha^2) / G} + \beta\sqrt{6\left(1/\alpha - \alpha^2\right) / E_x}} \tag{1}$$

where

V_f shear force at fracture of the notch
G shear modulus
E_x modulus of elasticity
G_{fy} fracture energy in pure tensile splitting perpendicular to grain

To arrive at the Eurocode 5 expressions a few simplifying modifications of (1) are made:
1) The ratio *E/G* is set to 16.
2) It is assumed that $\sqrt{EG}$ is proportional to the shear strength.
3) Test results from Riberholt et al[1] were used to introduce a factor that considers the effect of taper.

----
1. Riberholt, H, Enquist, B, Gustafsson, P.-J. and Jensen, R. B.: Timber beams notched at the support. Report TVSM-7071. Lund University, Sweden. 1999.

ESSAY 3.8 H J Larsen
Plate Buckling

Safe rules for plate buckling are given in Eurocode 5, clause 9.1.1 Glued thin-webbed beams and clause 9.1.2 Glued thin-flanged beams. In cases not covered with the rules a detailed buckling analysis should be made.

Theory
The following is based on **Paper 10-4-**1.

Buckling
An elastic plate loaded in compression or shear in the plane of the plate may for some load levels become unstable and deflect perpendicular to the plane. The phenomenon is called buckling and is an instability phenomenon of the Euler column buckling, however with an important difference: It is in most cases possible to increase the load after initial buckling. Initial buckling is, therefore, often regarded as a serviceability limit state.

When a rather long panel buckles it is divided up by node lines where the deflections are zero. The buckled form depends on plate form and type of loading. Typical examples are shown in figure 1. The critical load is found as for a slender column: A deflected form for the plate is assumed and by energy considerations the conditions for the deflected plate to be stable is found. The calculations will not be given here. Reference is made to e.g. Halasz & Cziesielski[1].

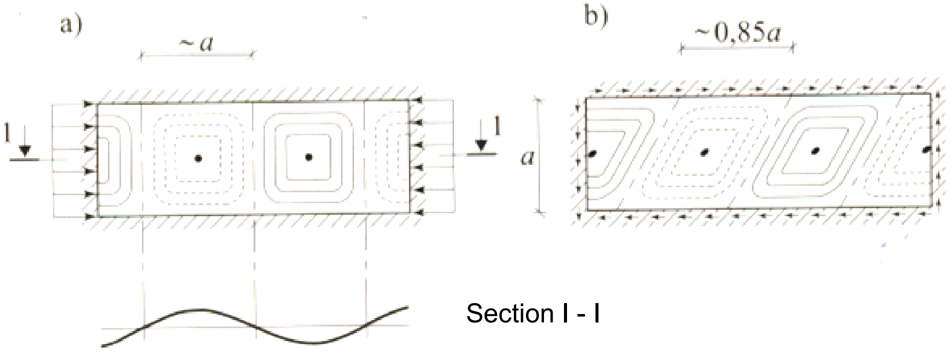

Figure 1. Buckled plate fields. a) for a constant normal (compression)stress. b) for pure shear stresses.

A rather long web may be regarded as composed of a number of fields simply supported by the flanges and webs, and over the node lines. It is loaded by in-plane stresses (σ,τ) from N, M and V.

Buckling – normal stresses
The case shown in Figure 2 is investigated. A plate with length l and width a, simply supported along the edges is loaded in the x-direction with compression stresses varying over the depth from σ to $\mu\sigma$ where $\mu \le 1$. The plate is assumed to be orthotropic with main directions x and y. The critical stress may be written as

$$\sigma_{cr} = k_{buck,\sigma} \frac{\pi^2 \sqrt{(EI)_x (EI)_y}}{ta^2} \tag{1}$$

where

$(EI)_x$ bending stiffness of a strip (with length direction parallel to the y-axis) width unit width by bending about the x-axis

$(EI)_y$ as $(EI)_x$ but for bending by bending about the y-axis for a strip (with length direction parallel to the x-axis)

$k_{buck.\sigma}$ a factor depending on μ and two parameters β_1 and β_2, see figure 3-5

$$\beta_1 = \frac{l}{a} \sqrt[4]{(EI)_x / (EI)_y} \tag{3}$$

$$\beta_2 = 0,5 (GI)_{tor} / \sqrt{(EI)_x (EI)_y} \tag{4}$$

$(GI)_{tor}$ torsional stiffness of a plate strip with unit width.

The stiffness parameters may be calculated from the moduli of elasticity E_x and E_y, the shear modulus G and the Poisson's ratios ν_{xy} and ν_{yx}

$$(EI)_x = \frac{1}{12} E_x t^3 / (1 - \nu_{xy}\nu_{yx}) \tag{5}$$

$$(EI)_y = \frac{1}{12} E_y t^3 / (1 - \nu_{xy}\nu_{yx}) \tag{6}$$

---

1. Halasz, R. & Cziesielski, E.: Berechnung und Konstruktion geleimter Träger mit Stegen aus Furnierholz. Beichte aus der Bauorschung, Heft 47. 1966.

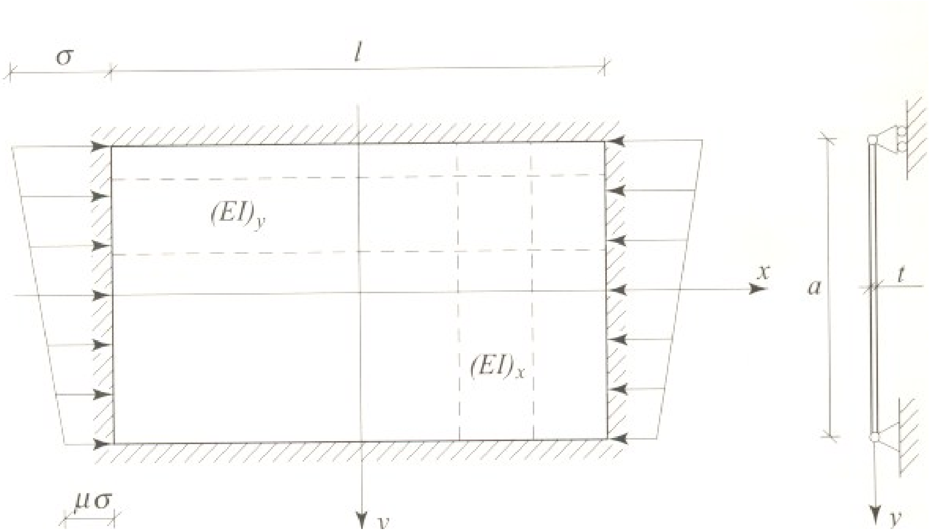

Figure 2. simply supported plate with varying normal stresses.

$$\left(GI\right)_{tor} = Gt^3\big/3 + \left[\nu_{xy}\left(EI\right)_x + \nu_{yx}\left(EI\right)_y\right] \sim \qquad (7)$$

For an isotropic plate is $\beta_1 = l/a$ and $\beta_2 = 2G/E$.

For $\mu = 1$, the theoretical values for $k_{buck,\sigma}$ are shown in Figure 3. The "festoon" form is due to the fact that the total plate length shall be divisible by the length of the buckled plate fields.

In practice the smoothed out curves are used. They are shown in Figure 4 and 5 for $\mu = -1$ and $\mu = 1$. For $\beta > 1$, $k_{buck,\sigma}$ is almost constant. Figure 6 shows $k_{buck,\sigma}$ for μ between +1 and -2.

The following approximations may be used:

Pure bending ($\mu = -1$): $\quad k_{buck,\sigma} = 11{,}1 \cdot \left(1{,}25 + \beta_2\right) \qquad (8)$

Pure compression ($\mu = 1$): $\quad k_{buck,\sigma} = 2 \cdot \left(1 + \beta_2\right) \qquad (9)$

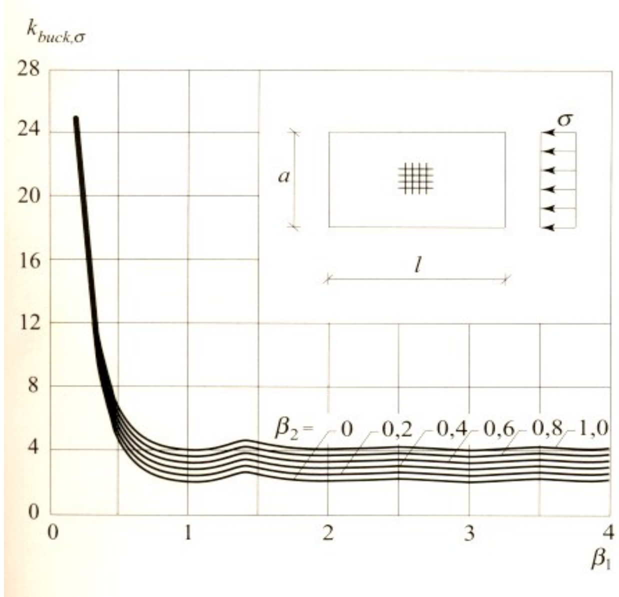

Figure 3. Theoretical values of $k_{buck,\sigma}$ for $\mu = 1$

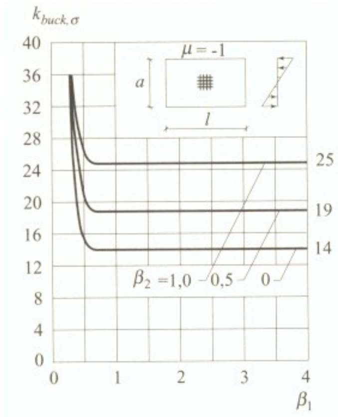

Figure 4. $k_{buck,\sigma}$ for bending ($\mu = -1$)

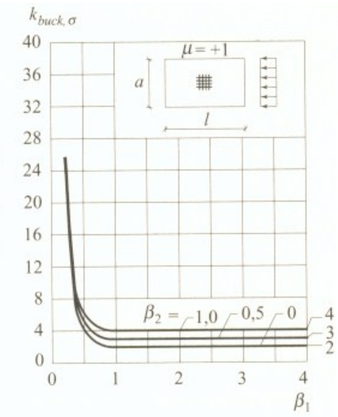

Figure 5. $k_{buck,\sigma}$ for compression ($\mu = 1$)

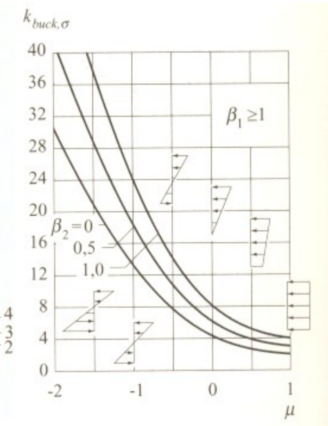

Figure 6. $k_{buck,\sigma}$ for $\beta_1 > 1$

Buckling – shear stresses

For shear stresses alone, see Figure 7, the critical shear stress may be calculated as

$$\tau_{cr} = k_{buck,\tau} \frac{\pi^2 \sqrt[4]{(EI)_x^3 (EI)_y}}{ta^3}$$

Where $k_{buck,\tau}$ is given in Figure 7.

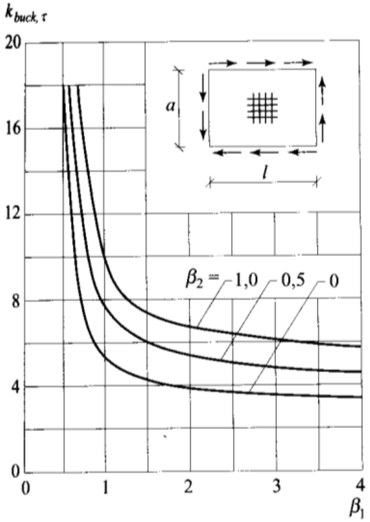

Figure 7. $k_{buck,\tau}$

Buckling – combined stresses

For both stresses according to Figures 4-6 and Figure 7 it should be verified that

$$\frac{\sigma}{\sigma_{cr}} + \left(\frac{\tau}{\tau_{cr}}\right)^2 \leq 1 \tag{10}$$

Minimum thicknesses for particle and fibre boards

In the following the thicknesses necessary to avoid buckling, even when the load-carrying capacities of the panels are fully utilised, are determined.

For isotropic panel e.g. particle boards and fibre boards, $\beta_2 \sim$. For rather long plates, i.e. $\beta_1 > 1$ and for pure compression the conditions become, see Figure 5:

$$\sigma_{cr} = 4\pi^2 \frac{Et^3}{12ta^2} > f_c \tag{11}$$

$$\frac{a}{t} < 1{,}8\sqrt{\frac{E}{f_c}} \tag{12}$$

Correspondingly for pure shear:

$$\tau_{cr} \sim \quad \frac{Et^3}{12ta^2} > f_v \tag{13}$$

$$\frac{a}{t} < 2{,}1\sqrt{\frac{E}{f_v}} \tag{14}$$

Values for t typical values of E/f_c and E/f_v are given in Table 1.

Minimum thicknesses for plywood

For plywood the following notations are used:

$$\varphi = (EI)_y / (EI)_x \tag{15}$$

$$(EI)_x = \frac{1}{1+\varphi}\frac{Et^3}{12} \tag{16}$$

$$(EI)_x = \frac{\varphi}{1+\varphi}\frac{Et^3}{12} \tag{17}$$

where E is the modulus of elasticity. With $E/G \sim$

$$\beta_2 \sim \quad \frac{\quad 3}{20 \quad 3}(1+\varphi) / \left(\frac{Et^3}{12}\sqrt{\varphi}\right) = 0{,}10\frac{1+\varphi}{\sqrt{\varphi}} \tag{18}$$

With $0{,}5 < \varphi < 5$, β_2 will be between 0,27 and 0,20. In the following $\beta_2 = 0{,}25$ is used.

To ensure that failure will not be due to buckling in the case of pure compression

$$\sigma_{cr} \sim \quad \frac{\sqrt{(EI)_x (EI)_y}}{ta^2} > f_c \tag{19}$$

f_c depends on whether the stresses act in or perpendicular to the panel fibre direction. In most cases the former possibility is the worse. The limit for a/t is found by (19)

$$\frac{a}{t} = 5\frac{\sqrt[4]{(EI)_x (EI)_y}}{t\sqrt{f_c}} \tag{20}$$

For pure shear for $\beta_2 = 0,25$ the condition to avoid buckling becomes

$$\tau_{cr} = \frac{4\pi^2}{ta^2}\frac{Et^3}{12}\frac{\sqrt[4]{\varphi}}{1+\varphi} > f_v \tag{21}$$

$$\frac{a}{t} < 1,8\frac{\varphi^{0,125}}{(1+\varphi)^{0,5}}\sqrt{\frac{E}{f_v}} \tag{22}$$

Approximate limits are given in Table 1. They correspond to conservative estimates for the material parameters and to the situation where the panels are fully utilised. It is, therefore often possible to use thinner panels may be used.

Table 1. Limits for the ratio a/t.

<table>
<tr><th></th><th>Pure compression</th><th>Pure shear</th></tr>
<tr><td colspan="3">Plywood with the panel direction</td></tr>
<tr><td>In the stress direction</td><td>20</td><td rowspan="2">$60/(1+0,1\varphi)$</td></tr>
<tr><td>Perpendicular to the stress direction</td><td>25</td></tr>
<tr><td>Particle boards, fibre boards and MDF</td><td>30</td><td>35</td></tr>
</table>

If the buckling load-carrying capacity is insufficient you should
- increase the panel thickness
- put in stiffeners in the length direction to reduce a
- put in stiffeners in the cross direction to reduce l

Generally solution 1) is the most effective; the load-carrying capacity is proportional to t^2.

Solution 2) is also effective; the load-carrying capacity is proportional to $1/a^2$. In practice it may, however be difficult to realise.

Solution 3) is easy to realise but the stiffeners shall be placed rather close (spacing 0,5*a* to 0,7*a*).

ESSAY 3.9 H J Larsen
Vibrations of floors

Vibrations unacceptable to the inhabitant have often been reported for residential floor design outside the very traditional fields with regard to materials and design and the problem have been in focus in CIB-W18.

For vibrations an important parameter is the structure's natural frequency, **Paper 19-8-1** gives 'designer useable' methods for predicting the dynamical behaviour of light-weight wooden joisted floors covered with semi-rigidly attached wood based sheathings of materials such as chipboard or plywood. It is demonstrated that good approximations to the fundamental natural frequencies of floors with practical combinations of edge conditions can be obtained by assuming that a floor behaves as a simple composite beam. This is the background for the simple expression given in Eurocode 5.

It is generally agreed that 8 Hz is a critical value and that a special investigation should be made for residential floors with a fundamental frequency less than 8 Hz. It is also generally agreed that the deflection under a static unit load should be limited either as an absolute value or as a function of the span.

These two parameters are not sufficient to ensure a satisfactory behaviour, and what other criteria should be used has been discussed in several papers.

Based on a Swedish proposal the unit impulse velocity response (v), i.e. the maximum initial value of the vertical floor vibration velocity (in m/s) caused by an ideal unit impulse (1 Ns) applied at the point of the floor giving maximum response has been chosen. Other proposals are

- the mean magnitude of the response caused by human footfall impact
- the frequency-weighted root-mean-square acceleration (A_r) of the response caused by a normal human footfall impact

According to Eurocode 5 it may be assumed that floors with a fundamental frequency greater than 8 Hz are satisfactory provided

$$w/F \le a \text{ mm/kN}$$

and

$$v \le b^{(f_1\zeta - 1)} \text{ m/(Ns}^2\text{)}$$

where

w maximum instantaneous vertical deflection caused by a vertical concentrated static force F applied at any point on the floor, taking account of load distribution

v unit impulse velocity response, i.e. the maximum initial value of the vertical floor vibration velocity (in m/s) caused by an ideal unit impulse (1 Ns) applied at the point of the floor giving maximum response

ζ modal damping ratio.

Eurocode 5 gives recommended ranges of limiting values of a and b. The values to be used in a specific country should be taken from the National Application Document.

The background for the Eurocode 5 clauses may not be found in a CIB-W18 document but in e.g. Ohlsson[1].

---

1. Ohlsson, S: Springiness and Human-Induced Floor Vibrations; A Design Guide, 1988, Swedish Council for Building Research, Stockholm.

ESSAY 3.10 H J Larsen Tapered and curved members

Tapered beams

Figures 1 and 2 show two types of tapered beams commonly used in practice, namely single and double tapered beams.

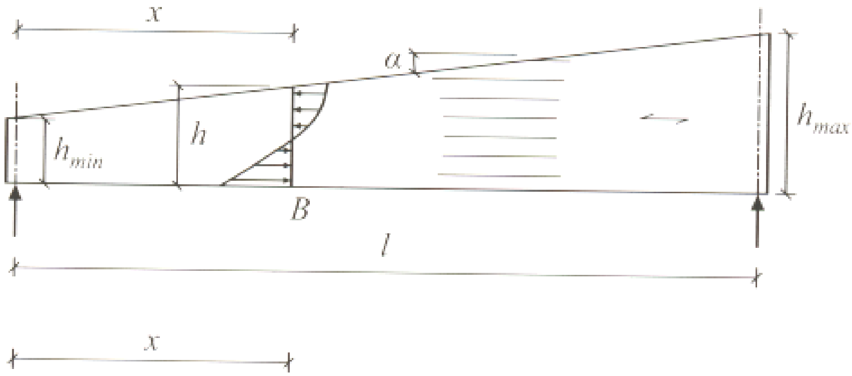

Figure 1. Single tapered beam.

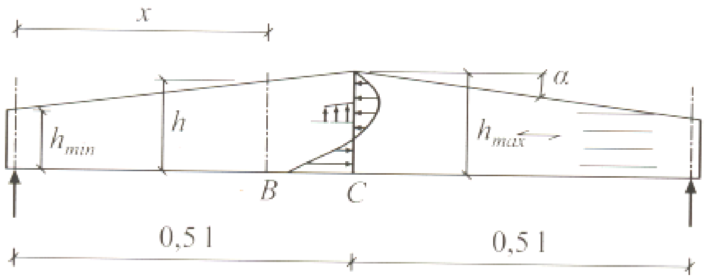

Figure 2. Double tapered beam

The stress distributions in tapered beams differ significantly from those of beams with constant depth. A bending moment results not only in stresses σ_0 in the direction of the beam axis but also in normal stresses σ_{90} perpendicular to this direction and shear stresses. The reason is that the stresses at the top shall be parallel to the surface. At the apex where the stress shall be parallel to both surface, the result is zero normal stresses and stresses – for downward load tensile stresses – perpendicular to grain in a zone under the apex.

The stress distribution is derived in **Paper 11-10-1.** The stresses shall satisfy the normal failure condition according to Hankinsson.

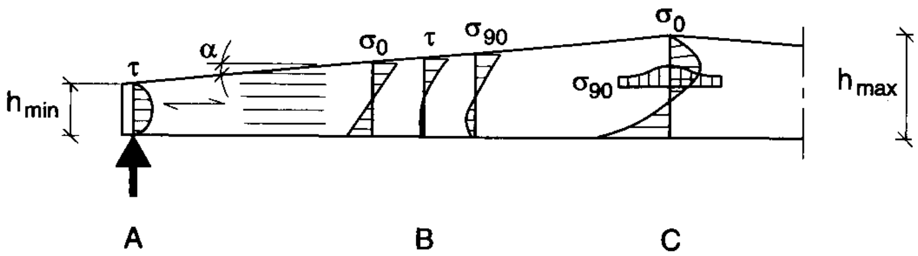

Figure 3. Stresses in a tapered beam

In the final version of Eurocode 5, the requirements are simplified. The normal stresses are calculated as for a beam with constant depth and they shall fulfil the following empirical expressions:

$$\frac{\sigma_m}{k_{m,\alpha} f_m} \leq 1 \tag{1}$$

where σ_m is the bending stress:

$$\sigma_m = \frac{6M}{bh^2} \tag{2}$$

For tensile stresses parallel to the tapered side:

$$k_{m,\alpha,t} = \frac{1}{\sqrt{1 + \left(\frac{f_m}{0.75 f_v} \tan\alpha\right)^2 + \left(\frac{f_m}{f_{t,90}} \tan\alpha\right)^2}} \tag{3}$$

For compressive stresses parallel to the tapered side:

$$k_{m,\alpha,c} = \frac{1}{\sqrt{1 + \left(\frac{f_m}{1.5 f_v} \tan\alpha\right)^2 + \left(\frac{f_m}{f_{c,90}} \tan\alpha\right)^2}} \tag{4}$$

The reduction factors $k_{m,\alpha}$ for compression and tension are shown in Figure 4 for glulam GL32h and GL24c. The reduction factors for other grades of glulam will fall between the two grades.

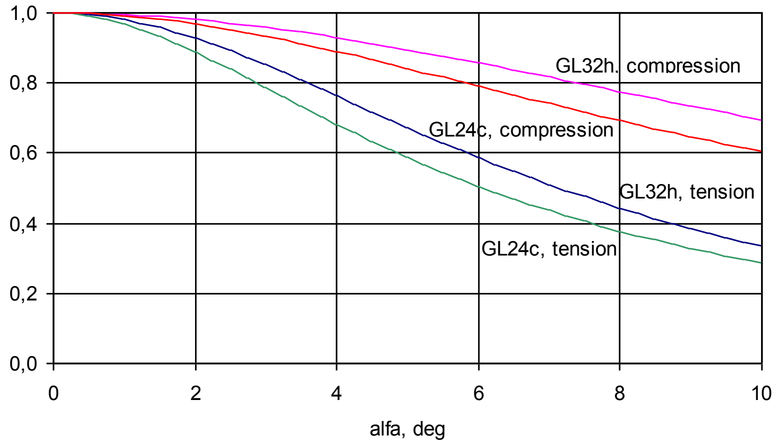

Figure 4. Reduction factors for glulam.

Curved beams

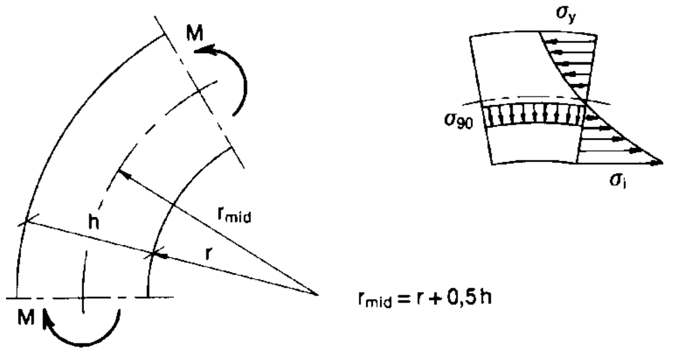

Figure 5. Stress variation in a plane curved beam with constant bending moment.

Loading a curved beam in bending will result in stresses both parallel and perpendicular to the beam, see Figure 5. The normal stresses in the convex side of the beam are smaller than the stresses at the concave side and the stresses at the concave side are larger than the stresses in a corresponding straight beam. The reason is that even if the deformations vary linearly, the strains will not because of the varying fibre lengths. This effect is disregarded in Eurocode 5, i.e. the stress is for a rectangular cross-section calculated as for a straight beam

$$\sigma_{ou} = \sigma_{in} = 6M/bh^2 \tag{5}$$

The bending stresses σ_m developed during the fabrication when the laminations with thickness t are formed to a curvature $1/r$ are theoretically rather high. In the outermost fibres

$$\sigma_m = Et/(2r) \tag{6}$$

These internal stresses reduce the load-bearing capacity of the cross-section.
For an elastic modulus $E = 12000$ N/mm^2, a lamella thickness $t = 33$ mm and a radius $r = 5000$ mm the bending stress becomes $\sigma_m = 40$ N/mm^2, i.e. corresponding to the characteristic strength. Experimental results show, however, that the built-in stresses become significantly smaller, probably due to creep that occur during the hardening process where moisture from the adhesive is added. In the ENV version of Eurocode it was that the strength values for bending, tension and compression for $r/t < 240$ should be reduced by the factor:

$$k_{curve} = 0,76 + 0,001\frac{r}{t} \ (\leq 1) \tag{7}$$

In the final version this effect is disregarded.

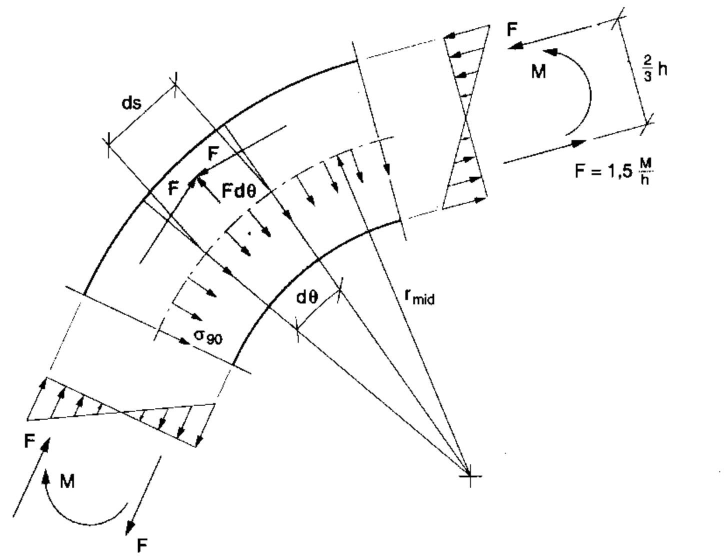

Figure 6. Internal forces and tension stresses perpendicular to the grain direction in a curved beam.

The bending moment results also in stresses perpendicular to grain. The following simplified derivation of the transversal stresses illustrates this effect. It is assumed that the normal stresses vary linearly over the beam depth, see Figure 6, i.e. the influence of the non-linear stress distribution is disregarded. The force resultant F on one half of the cross-section is $F = 1,5M/h$. Equilibrium of the marked element loaded by F on both cross-sections and the stress σ_{90} requires

$$Fd\theta = \sigma_{90} b r_{mid} d\theta$$

$$\sigma_{90} = \frac{F}{br_{mid}} = 1,5\frac{M}{bhr_{mid}} \qquad (8)$$

where b is the thickness (width) of the beam.

When the moment distribution tends to reduce the curvature, as is the case in Figure 8, the stresses perpendicular to the grain are tensile stresses and it is necessary to take into account that the strength perpendicular to grain depends on the stressed volume by multiplying the tensile strength perpendicular to grain by:

$$\frac{\sigma_{t,90,d}}{f_{t,90,d}} \le k_{dis}\left(\frac{V_{ref}}{V}\right)^{0.2} \qquad (9)$$

where V is the stressed volume and V_{ref} is a reference volume. For glulam, $V_{ref} = 0,01\ \text{m}^3$. The factor k_{dis} takes into account the stress variation over the depth. For a parabolic variation from zero at the surface to a maximum value in the middle $k_{dis} = 1,4$.

Pitched cambered beams

The stresses in the "triangle" correspond in principal to those in a curved beam – the axial stresses do not vary linearly and the moment also induces stresses perpendicular to grain – but these effects are much more pronounced especially near the apex where the normal stresses are zero because of the apex point. It is, therefore, not unusual to replace the construction by a curved beam with a separate "triangle".

The maximum normal stress is found in the bottom side of the apex section and should be calculated as

$$\sigma_{m,i} = k_0\frac{6M_{ap}}{bh_{ap}^2} \qquad (10)$$

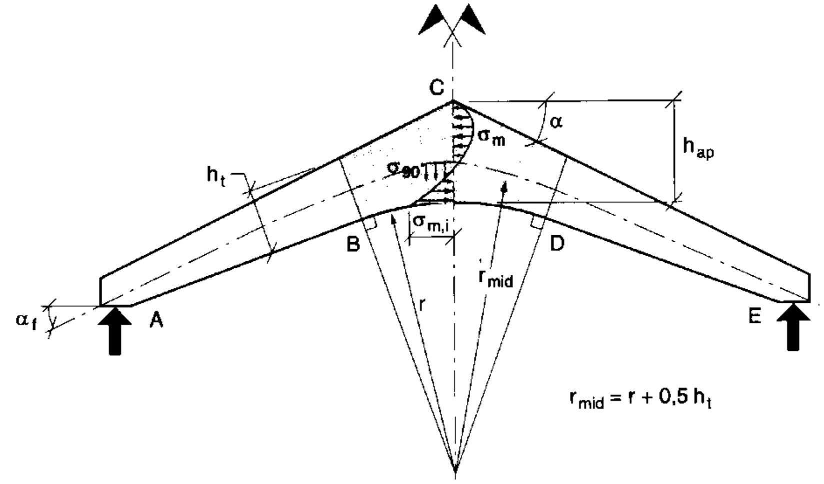

Figure 7. Pitched beam consisting in principle of two tapered beams joined by a "triangle" with curved underside.

The maximum tensile stress perpendicular to the grain direction is found just under centre line in the apex section and should be calculated as

$$\sigma_{t,90,\max} = k_{90}\frac{6M_{ap}}{bh_{ap}^2} - 0,6\frac{p}{b} \qquad (11)$$

M_{ap} is the moment in the apex section where the beam depth is h_{ap}. The factors k_0 and k_{90} are:

$$k_0 = k_1 + k_2\left(\frac{h_{ap}}{r_{mid}}\right) + k_3\left(\frac{h_{ap}}{r_{mid}}\right)^2 + k_4\left(\frac{h_{ap}}{r_{mid}}\right)^3 \qquad (12)$$

$$k_{90} = k_5 + k_6\left(\frac{h_{ap}}{r_{mid}}\right) + k_7\left(\frac{h_{ap}}{r_{mid}}\right)^2 \qquad (13)$$

with

$$k_1 = 1 + 1,4\tan\alpha + 5,4\tan^2\alpha$$

$$
\begin{aligned}
k_2 &= 0{,}35 - 8\tan\alpha \\
k_3 &= 0{,}6 + 8{,}3\tan\alpha - 7{,}8\tan^2\alpha \\
k_4 &= 6\tan^2\alpha \\
k_5 &= 0{,}2\tan\alpha \\
k_6 &= 0{,}25 - 1{,}5\tan\alpha + 2{,}6\tan^2\alpha \\
k_7 &= 2{,}1\tan\alpha - 4\tan^2\alpha
\end{aligned}
\qquad (14)
$$

For a curved beam with $\alpha = 0 : k_5 = 0,\ k_6 = 0{,}25$ and $k_7 = 0$, and in accordance with equation 4.4 the transversal stress becomes

$\sigma_{t,90} = 0{,}25 \cdot 6M/(r_{mid}bh)$.

where:
p is the uniformly distributed load acting on the top of the beam over the apex area;
b is the width of the beam;

The derivation of these expressions is given in Paper 14-12-1.

The term with p in (11) is questioned by some member countries and it is optional in the National Application Document to permit it or not. Although it is small it increases the load-carrying capacity considerably because $f_{t,90}$ is small.

ESSAY 3.11 H J Larsen
Racking resistance of walls

According to Eurocode 5, the racking resistance of a wall shall be determined either by test according to EN 594 or by calculations, employing appropriate analytical methods or design models.

Extract from EN 594: Timber structures - Test methods - Racking strength and stiffness of timber frame wall panels:

1 Scope
This standard specifies the test method to be used in determining the racking strength and stiffness of timber frame wall panels.
The test method is intended, primarily for panels as described, to provide:
- comparative performance values for the materials used in the manufacture of the panels and
- datum information for use in structural design.

……

5 Requirements for test panels
The dimensions of panels shall be given as given in figure 1. The edges of all sheathing materials shall be supported.

6 Test method
6.1 Principle
The test method measures the resistance to racking load of panels which can deform both vertically and horizontally in the plane of the panel.
In this test method, the bottom rail of the panel is bolted to the test rig and uplift is resisted by the sheathing fixings and also by the vertical loads on the top rail of the panel.

6.2 Apparatus
6.2.1 General
The test apparatus shall be as shown in figure 2, and shall he capable of applying, separately, both racking load F, and vertical loads F_v,. The method of application of the loads shall be such that no significant resistance to movement in the panel is induced.

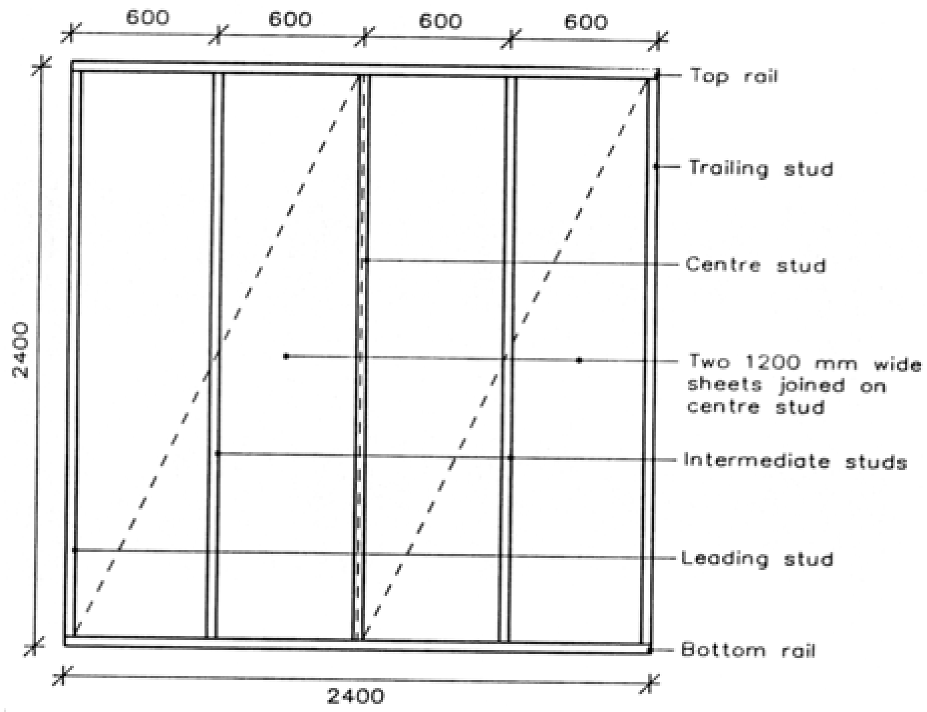

Figure 1. Detalis of test panels (sizes in mm).

……

The apparatus shall be capable of continuously recording the loads F and F_v, with an accuracy of ± 3 % of the applied loads ….

6.2.2 Base and loading frame
The base of the test rig shall provide a level bed to receive the test panel and packer. The base shall be sufficiently stiff so as not to distort during, the test.

……

6.2.3 Mounting of test panel
The panel shall be bolted through a packer to the base of the test rig with holding down bolts positioned as shown in figure 2.

……

The head binder shall be rigidly attached to the top rail of the panel. The cross-sectional dimensions and position shall be such as to provide a firm interface between the loads and the panel and to allow the free movement of the panel sheathing, during the test.

Experience has shown that the strength and stiffness depends very much on the materials, and details in build-up and load application, and the the test method is, therefore primarily intended, to provide comparative performance values for the materials used in the manufacture of the panels, and it is difficult to see how the results can be applied in practice. In an annex guidelines are given for testing of units other than according to clause 5.

Extract from EN 594:

Annex A. The testing of units of dimensions other than 2,4 x 2,4 m

A.1 General
The purpose of this Annex is to adapt the principle of the test method:
- to other sizes of panel and;
- to combinations of panels and,
- to panels which are partially sheathed and;
- to other panel fixings.

It is intended primarily to provide performance data which may be used for quality assurance or for structural design.

A.2 Requirements for panels
The wall panels tested shall generally correspond to those used in practice as far as the essential structural details and service conditions are concerned.
…..

A.3 Apparatus
The apparatus used …. shall generally be as described in clause 6.

Testing may be relevant where there are many identical walls, but in most cases the load-carrying capacity is determined by calculation.

Eurocode 5 gives two alternative simplified methods of calculation, Method A and B. The member states decides which method should be used. With the exception of Denmark where both methods are accepted, and the UK where method B is compulsory, the member states have chosen Method A.

Method A is a very simple equilibrium method and it is clearly required that the there is a tie-down at their end, that is the vertical member at the end shall be directly connected to the construction below. The anchoring in the foundation may in many modern structures be difficult to make in practice due to heat isolation layers needed due to increased heat isolation requirements.

Method B is based on tests and do not explicitely require that the end stud is anchored but the text on this point is obscure The vertical forces necessary to ensure equilibrium is assumed to be taken by the fixing of the bottom rail to the underlying structure. The fixings shall in addition to the vertical forces prevent the sliding of the bottom rail.

Generally Method B gives lower load-carrying capacity than method A, especially for wall without vertical loads.

In **Paper 38-15-9** a unified method is proposed that gives higher load-carrying capacity than the present Method B without requiring full anchoring.

ESSAY 4.1 H J Larsen
Block Shear

When a member is loaded by a group of mechanical fasteners close to the end there is a risk for failure because a plug or a block is torn out, see Figure 1.

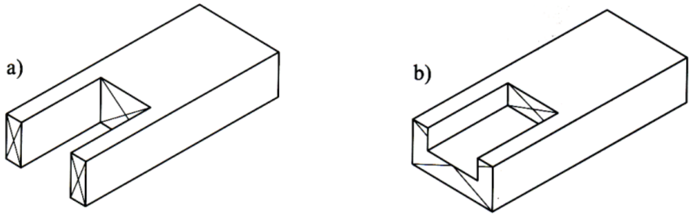

Figure 1. a) Plug shear. b) Block shear

There are two contributions to the load-carrying capacity: tension failure in end cross-section of the plug/block and shear failure in the rest of the failure surface. The deformations at failure are very different for te two failures. The strain-stress curve for tension is short and brittle and failure will take place long before a substantial part of the shear strength has been developed. Two failures are, therefore, investigated:

Tensile failure
Eurocode 5 recommends that the tensile strength is taken as $1{,}5f_{t0}$, i.e. the tension load-carrying capacity of the cross-section through the end nail line is ($_{bs}$ = block shear):

$$R_{bs} = 1,5 f_{t,0} t_{pen} l_{net} \text{ where, see Figure 1, } l_{net} = \sum_i l_{t,i}$$

Often this capacity will be the bigger, but in some cases, the shear capacity is the.bigger.

According to Eurocode 5, the shear strength along the two sides and along the bottom may be added. This is, however, a doubtful assumption.

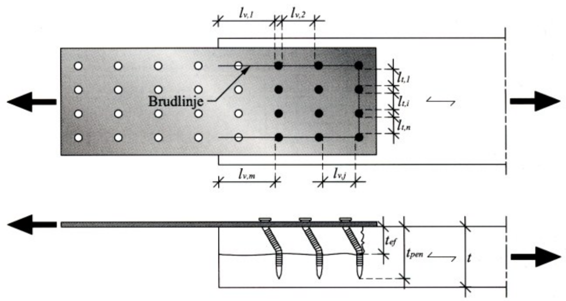

Figure 2. Block shear with tear out along the perimeter of the fasteners

Shear failure
Eurocode 5 recommends that the shear strength to take into account uneven stress distribution is taken as $0{,}75f_v$, i.e. the load-carrying for plug shear is:

$$R_{ps} = 0,7 f_v t l_{net,v} \quad \text{where, see Figure 1,} \quad l_{net,v} = \sum_j l_{v,j}$$

For block shear the shear contribution is:

$$R_{bs} = 0,7 f_{v,k} 0,5 l_{net,v} \left(l_{net} + 2t_{ef} \right)$$

The effective thickness for thin steel plate is determined as

$$t_{ef} = \begin{cases} 0,4 t_{pen} \\ 1,4\sqrt{\dfrac{M_y}{f_h d}} \end{cases}$$

The effective thickness for thick steel plate is determined as

$$t_{ef} = \begin{cases} 2\sqrt{\dfrac{M_y}{f_h d}} \\ t_{pen}\left[\sqrt{2 + \dfrac{M_y}{f_h d t_{pen}^2}} - 1\right] \end{cases}$$

ESSAY 4.2 H J Larsen
Dowel type fasteners

Load-carrying capacity, general

The design of laterally loaded dowel-type fasteners in Eurocode 5 is based on the work of K. W. Johansen[1,2], first described in Danish in 1941. The theory often called The European Yield Model (EYM) is mentioned in **Paper 12-7-2**, but since it plays an important role for Eurocode 5 and many CIB-W18 papers it is briefly described in the following.

The very simple theory assumes that failure is ductile and caused by yielding in the fastener or by compression failure of the wood and not by brittle failure e.g. by splitting of the wood. This is normally ensured by requirements to timber sizes and to minimum spacings and distances to end and edge.

The principal behaviour is illustrated in Figure 1 for a so-called double shear connection (two side members and one middle member). The main part of the load is transferred by contact pressure between the timber members and the dowel that is exposed to shear and bending. Part of the load may be taken by direct tension in the inclined dowels and by friction between the timber members.

It is assumed that the dowel acts as a beam laterally loaded by a constant contact pressure q per unit length. The relation between the contact pressure and the deformation may be found by the test set-up sketched in Figure 2: A stiff steel cylinder in a hole in a timber member is loaded by a force F. The figure shows a typical load-deformation curve. At the beginning there is a linear relation between load and impression, followed by a curved part after which the load falls slightly by increased deformation. In practice a stiff-ideal plastic behaviour with yield value F_y may be assumed.

The so-called embedding is defined by:

$$f_h = \frac{F_y}{d\,t} = \frac{q_y}{d} \tag{1}$$

where F_y is the total load and q_y is the load per unit length when the wood material starts to yield (to get permanent deformation because of some type of fibre damage) and d is the dowel diameter.

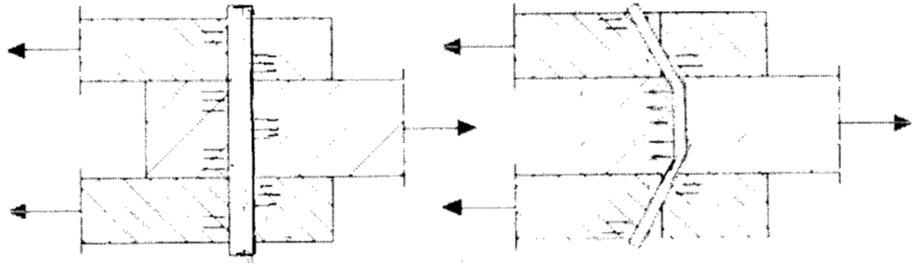

Figure 1. Double shear dowel connections. Thick dowels remain straight and the load is transferred almost solely by shear in the dowel. Slender dowels bend and part of the load may be taken by tension in the inclined dowel parts and by friction between the timber parts that are pressed together by the tension forces.

The embedding strength depends first and foremost on the compression strength (and thereby on the density ρ of the wood) and on the angle α between the load and the fibre direction. Also the dowel form, surface and diameter play a significant role.

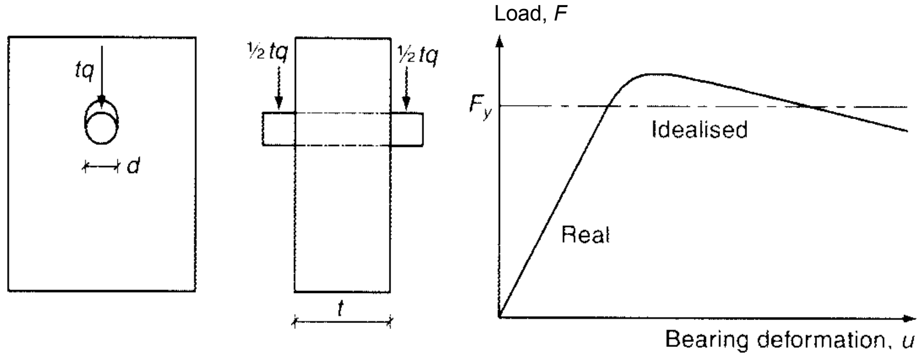

Figure 2. Dowel pressed into a timber member, and the real and ideal-plastic load-deformation curve.

---

1. Johansen, K.W.: Forsøg med Træforbindelser. Bygningsstatiske Meddelelser. Vol. XII, Nr. 2, pp. 29-86, 1941..
2. Johansen, K.W.: Theory of timber connections, International Association of Bridge and Structural Engineering (IABSE), Basel, Publication 9, 1949.

The load-carrying capacity also depends on the yield moment M_y of the dowel. Assuming ideal-plastic behaviour of both wood and dowel, the dowel behaves either as a stiff unit without bending deformation or as stiff dowel parts that are joined by yield hinges. The possible failure modes for single and double shear joints are shown in Figure 3.

In the single shear joint, the dowel will either remain straight (failure modes 1) or bend in one or two yield hinges (failure modes 2 or 3 respectively). For the double shear joint failure, modes 1 correspond to a translation of the dowel either in the side members or the middle member. In failure mode 2, two yield hinges occur in the middle member while the dowel remains straight in the side members. In failure mode 3 four yield hinges are formed within the dowel, two in the middle member and one in each outer part.

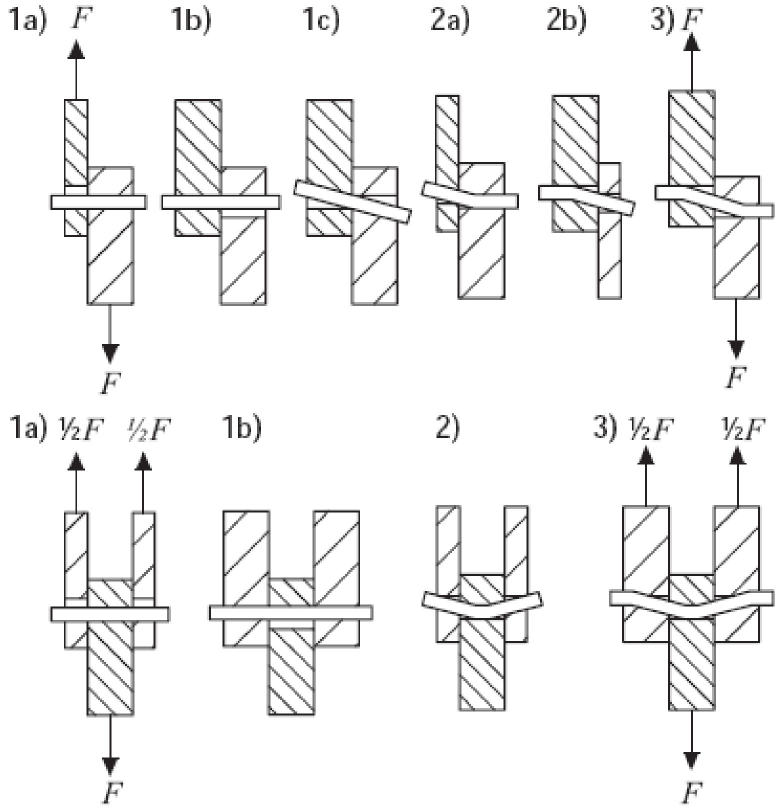

Figure 3. Failure modes for single (upper row) and double shear joints (lower row).

Figures 4 and 5 show examples of K.W. Johansen's test specimens opened after failure. The difference in failure modes in figure 3 is due to the embedding strength being considerably higher for oak than for spruce.

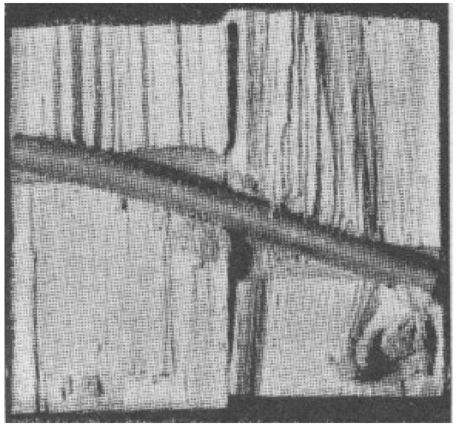

a) Single shear joint, 10 mm dowel in spruce

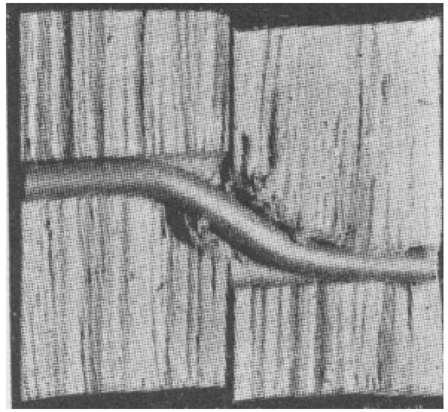

b) Single shear joint,10 mm dowel in oak

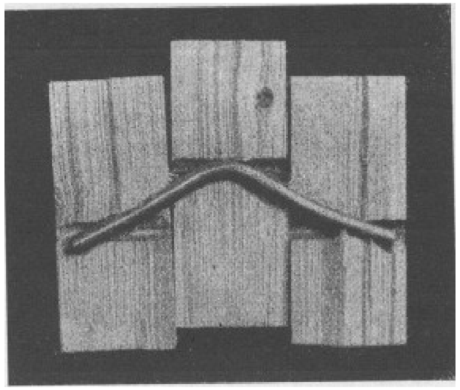

c) Double shear joint, 10 mm dowel in spruce

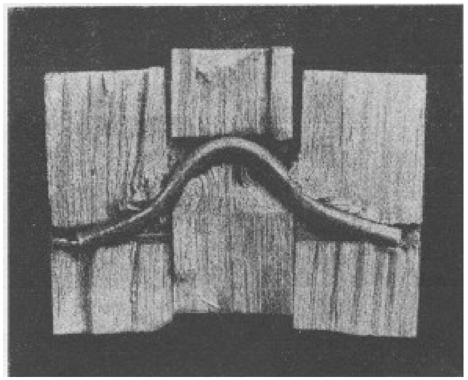

d) Double shear joint,10 mm dowel in oak

Figure J.2.4. Photos from tests with dowels in different wood species. From Johansen[1].

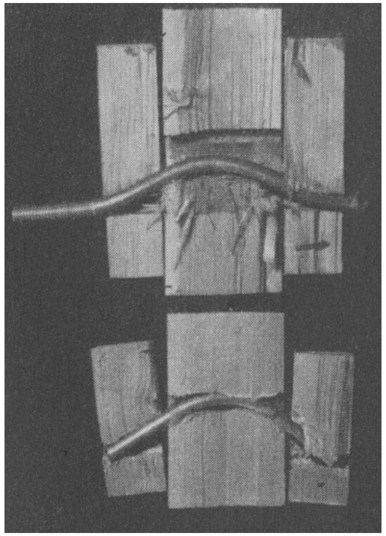

Figure 5. Failure modes for bolt (top) and dowel (bottom). From Johansen[1].

Figure 5 illustrates the difference between a bolt and a dowel. For bolts, head and nut with washers reduce the deformation at the surface. This may change the failure mode to one with a higher load-carrying capacity. This is however not taken into consideration in Eurocode 5.
With increasing load first elastic deformation develops creating tension in the fastener due to an inclination of the fastener axis. A prerequisite for significant tensile forces in the fastener is the anchorage of the fastener in the member, e.g. by head and nut in bolts or by thread and head in nails or screws. This tensile force in the fastener presses the members together and causes friction between the members.

The derivation of the "rope effect" is shown in **Paper 35-7-4**. The rope effect is present in all failure modes.

Near failure the deformations become big resulting in additional tension in the fastener, which becomes inclined so that part of the load may be taken by a direct tension component parallel to the load. Both effects are proportional to the tension force and are taken into account in Eurocode 5 for failure modes 1c, 2 and 3. The effect is demonstrated in figure 5.

Load-deformation curves are shown in Figure 6. For a joint with a dowel (bolt without tension) the slip limit is $P = 0$. Between the slip limit and the yield load P_F the dowel is pressed against the wood and making it

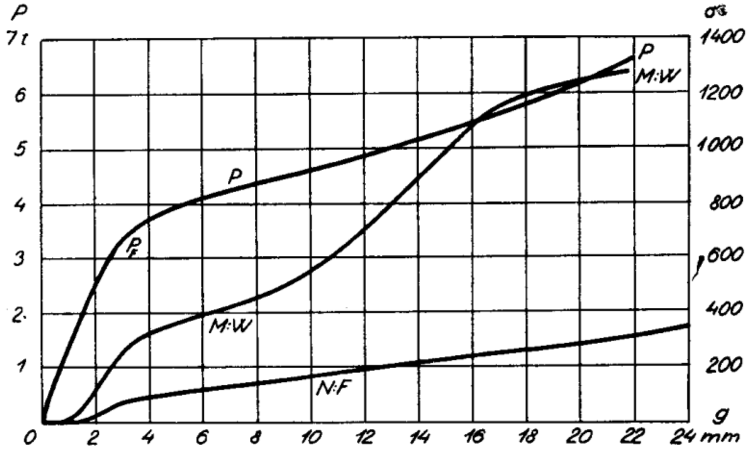

a) Dowel

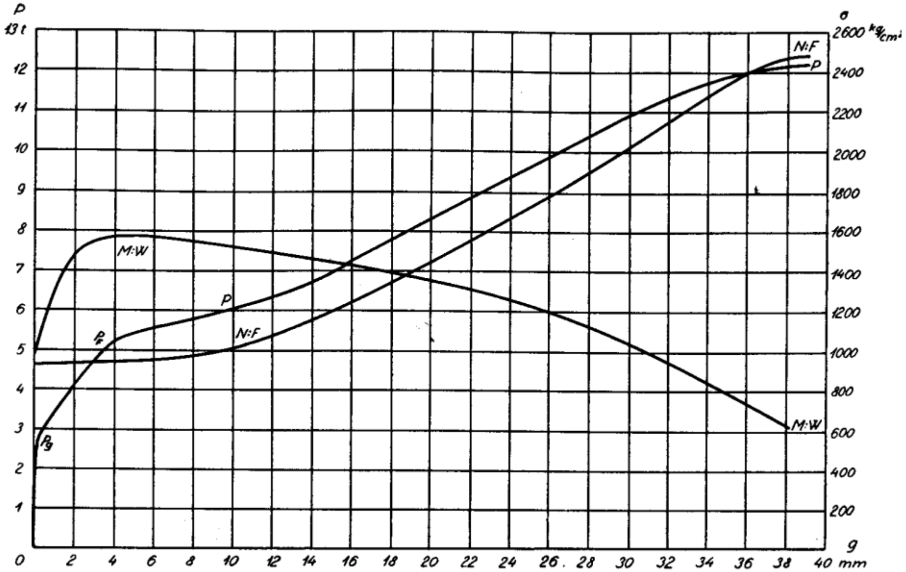

b) Prestressed bolt

Figure 6. Load-slip curves and bending and axial stresses for a dowel and a prestressed bolt. g is deformation (slip), P is the load, N:F is the axial stress in the dowel and M:W is the bending stress in the dowel. From Johansen[1].

possible to take an axial force N resulting in friction between the dowel and the wood.

For joints with a (prestressed) bolt the slip is 0 until $P = P_F$ where P_F is the friction load corresponding to the prestress and the load-deformation curve is shifted upwards by the friction load, resulting in an increase in load-carrying capacity.

It is relatively simple to derive expressions for the load-carrying capacities for the described failure modes using only the equilibrium conditions. see Annex: Theoretical load-carrying capacity expressions.

Wood-to wood or wood-based panel-to-wood connections

Single shear joints: (2)

$$R_{v,k} = \min \begin{cases} f_{h,k,1} t_1 d \\ f_{h,2,k} t_2 d \\ \dfrac{f_{h,1,k} t_1 d}{1+\beta} \left[\sqrt{\beta + 2\beta^2 \left[1 + \dfrac{t_2}{t_1} + \left(\dfrac{t_2}{t_1}\right)^2 \right] + \beta^3 \left(\dfrac{t_2}{t_1}\right)^2} - \beta \left(1 + \dfrac{t_2}{t_1}\right) \right] + T \\ 1,05 \dfrac{f_{h,1,k} t_1 d}{2+\beta} \left[2\beta(1+\beta) + \dfrac{4\beta(2+\beta) M_{y.k}}{f_{h,1,k} d\, t_1^2} - \beta \right] + T \\ 1,05 \dfrac{f_{h,1,k} t_2 d}{1+2\beta} \left[2\beta^2(1+\beta) + \dfrac{4\beta(1+2\beta) M_{y.k}}{f_{h,1,k} d\, t_2^2} - \beta \right] + T \\ 1,15 \sqrt{\dfrac{2\beta}{1+\beta}} \sqrt{2 M_{y,k} f_{h,1,k} d} + T \end{cases}$$

Double shear joints: (3)

$$R_{v,k} = \begin{cases} f_{h,k,1} t_1 d \\ 0,5 f_{h,2,k} t_2 d \\ 1,05 \dfrac{f_{h,1,k} t_1 d}{2+\beta} \left[2\beta(1+\beta) + \dfrac{4\beta(2+\beta) M_{y.k}}{f_{h,1,k} d\, t_1^2} - \beta \right] + T \\ 1,15 \sqrt{\dfrac{2\beta}{1+\beta}} \sqrt{2 M_{y,k} f_{h,1,k} d} + T \end{cases}$$

with

$$\beta = \frac{f_{h,2,k}}{f_{h,1,k}} \tag{4}$$

$$T = \frac{F_{ax,k}}{4} \tag{5}$$

where

$R_{v,k}$ the characteristic load-carrying capacity per shear plane per fastener
t_i the timber or wood-based panel thickness or penetration depth, with i either 1 or 2
$f_{h,k,i}$ the characteristic embedding strength in timber member i
d the fastener diameter
$M_{y,k}$ the characteristic fastener yield moment
β the ratio between the embedding strength of the members
T the contribution from the rope effect
$R_{ax,k}$ the characteristic axial withdrawal capacity of the fastener.

Correction factors

In the expressions (J.2.2) and (J.2.3), the first terms on the right hand side without the factors 1,05 and 1,15 are the load-carrying capacities according to the Johansen yield theory, whilst the second term $T = F_{ax} / 4$ is the contribution from the rope effect.

The factors are correction factors to compensate for the very simple way the design values are derived from the characteristic value, viz.

$$R_{y,d} = k_{\text{mod}} R_{y,k} / \gamma_M \tag{6}$$

whether the load-carrying capacity depends solely on the wood properties or partly also on the steel properties. In the latter case it would be more correct to introduce k_{mod} and the partial safety factors directly on the material parameters;

$$R_y \approx \sqrt{M_y f_y} \sim \sqrt{\frac{M_y}{\gamma_{M,steel}} \frac{k_{\text{mod},wood} f_{h,k}}{\gamma_{M,wood}}} = \frac{R_k}{\sqrt{\gamma_{M,steel} \gamma_{M,wood} / k_{\text{mod},wood}}} \tag{7}$$

Typically $\dfrac{\gamma_{M,wood}}{\gamma_{M,steel}}$ is about 1,2 and k_{mod} about 0,9 i.e.

$$R_{y,d} \approx 1,15 \frac{k_{\text{mod},wood} R_k}{\gamma_{M,wood}}$$

For the other failure modes with bending in the dowel, the effect is smaller and a factor of 1,05 has been chosen.

In **Paper 27-7-2** the corrections are (wrongly) explained as special system factors.

Limitation of rope effect

The contribution to the load-carrying capacity due to the rope effect should be limited to the following percentages of the Johansen part of the load carrying capacity:

Round smooth nails	15 %
Square smooth nails	25 %
Other (threaded) nails	50 %
Screws	100%
Bolts	25 %
Dowels	0 %

If $R_{ax,k}$ is not known, then the contribution from the rope effect should be taken as zero.

For single shear fasteners the characteristic withdrawal capacity $R_{ax,k}$ is taken as the lower of the capacities in the two members.

For the withdrawal capacity $R_{ax,k}$ of bolts the resistance provided by the washers may be taken into account

Steel-to-wood connections

The characteristic load-carrying capacity of a steel-to-timber connection depends on the thickness of the steel plates. Steel plates of thickness less than or equal to $0,5d$ are classified as thin plates and steel plates of thickness greater than or equal to d with the tolerance on hole diameters being less than $0,1d$ are classified as thick plates.

The difference between thick and thin plates is that for thick plates as outer members, it is assumed that the dowel can be restrained at the surface by a moment $M = M_y$. For thin plates $M = 0$.

In **Paper 28-7-3** it is shown that for many connector nails it may be assume that they act as fully restrained in steel plates down to a thickness of $0,5d$.

Thin steel plate in single shear:

$$R_{y,k} = \min \begin{cases} 0.4 f_{h,k} t_1 d \\ 1.15\sqrt{2M_{y,k} f_{h,k} d} + T \end{cases} \tag{8}$$

Thick steel plate in single shear:

$$R_{v,k} = \min \begin{cases} f_{h,k} t_1 d \\ f_{h,k} t_1 d \left[\sqrt{2 + \dfrac{4M_{y,k}}{f_{h,k} d\, t_1^2}} - 1 \right] + T \\ 2.3\left[\sqrt{M_{y,k} f_{h,k} d} + 1\right] + T \end{cases} \tag{9}$$

Steel plate of any thickness as middle member in a double shear connection:

$$R_{v,k} = \min \begin{cases} f_{h,1,k} t_1 d \\ f_{h,1,k} t_1 d \left[\sqrt{2 + \dfrac{4M_{y,k}}{f_{h,1,k} t_1^2 d}} - 1 \right] + T \\ 2.3\sqrt{M_{y,k} f_{h.1.k} d} + T \end{cases} \tag{10}$$

Thin steel plates as the outer members in double shear connection:

$$R_{v,k} = \min \begin{cases} 0,5 f_{h,2,k} t_2 d \\ 1,15\sqrt{2M_{y,k} f_{h,2,k} d} + T \end{cases} \tag{11}$$

Thick steel plates as outer members of a double shear connection:

$$R_{v,k} = \min \begin{cases} 0,5 f_{h,2,k} t_2 d \\ 2,3\sqrt{M_{y,k} f_{h,2,k} d} + T \end{cases} \tag{12}$$

$$T = \frac{F_{ax,k}}{4} \qquad (13)$$

where

$R_{y,k}$ characteristic load-carrying capacity per shear plane per fastener
$f_{h,k}$ characteristic embedding strength in the timber member
t_1 the smaller of the thickness of the timber side member or the penetration depth
t_2 thickness of the timber middle member
d fastener diameter
$M_{y,k}$ characteristic fastener yield moment
T rope effect contribution
$R_{ax,k}$ characteristic withdrawal capacity of the fastener.

Failure modes

The failure modes for steel to timber joints are illustrated in Figure 7.

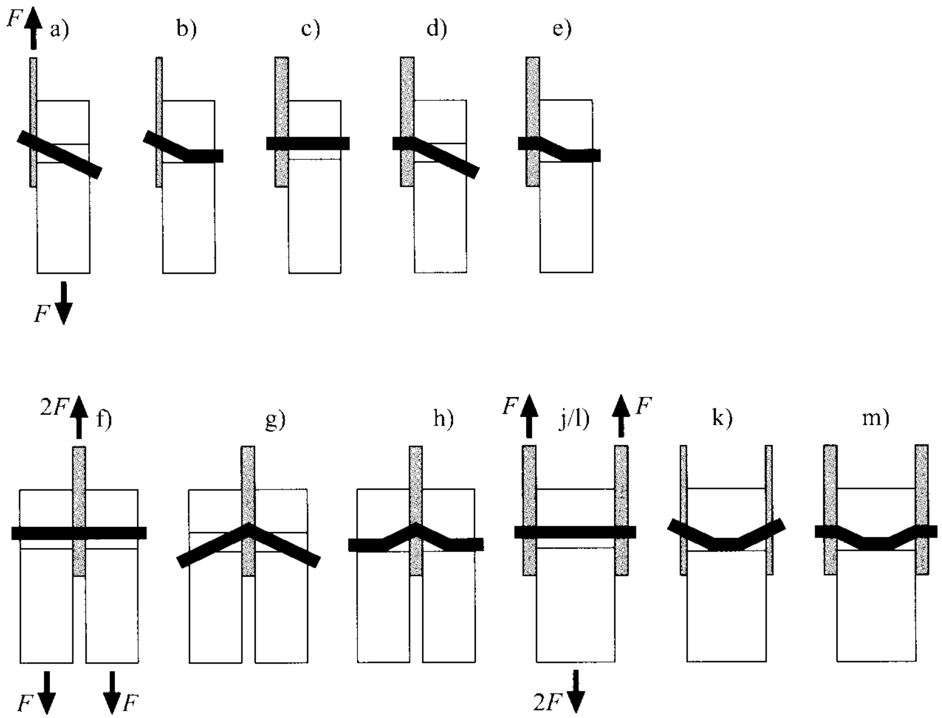

Figure 7. Failure modes for steel-to-timber joints.

Embedding strength

The determination of the embedding strength values in Eurocode 5 for softwoods and panel materials is described in **Paper 20-7-1.**

Other papers on embeddings strength are **Paper 25-7-2** and **Paper 41-7-5**

The embedding strength of fasteners in solid wood panels is treated in **Paper 39-7-5**

Yield moment

One of the important parameters in the expressions for the load-carrying capacity is the yield moment. For nails a standardised test method is described in EN 409[3].

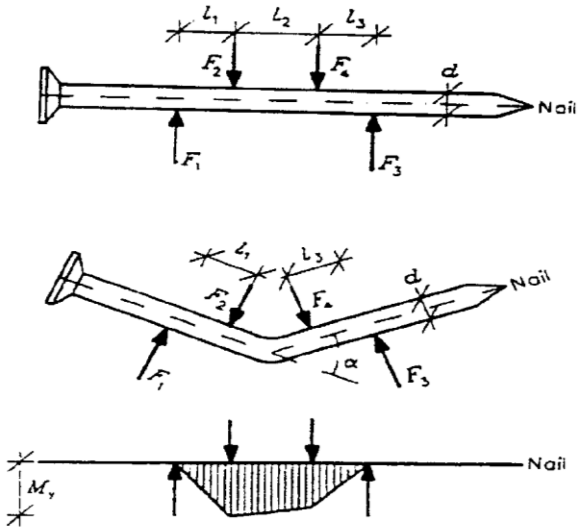

Figure 8. Nail loading, nail deformation and bending moments according to tests described in EN 409. Since F2 and F4 may differ the midsection may also be subjected to shear. There are no tensile force because the loads acts perpendicular to the fastener.

---

3. EN 409 Timber structures – Test methods – Determination of the yield moment of dowel type fasteners

The principle is set out in Figure 8. The test methods aim at reducing the influence of shear, and the effect of the support forces becoming inclined. The yield moment is taken as the maximum moment for a rotation α less than 45º. For thin dowels the method works well, the moment becomes almost constant for increasing values of α.

For bolts K. W. Johansen used the elastic moment

$$M_y = \frac{\pi}{32} d^3 f_y \tag{14}$$

where

M_y yield moment [Nmm]
d diameter [mm]
f_y yield strength in tension [Nmm^2]

Also the moment corresponding to full plastic behaviour

$$M_y = \frac{d^3}{6} f_y \tag{15}$$

has been used.

However it was pointed out in **Paper 31-7-6** and **Paper 31-7-7** that neither of these moments or a moment found by EN 409 are relevant for large diameters: They disregard the influence of strain hardening and in practice a bending angle of 10-20º is more appropriate than 45º. Based on tests a moment of

$$M_{y,k} = 0,3 f_{u,k} d^{2,6} \tag{16}$$

was introduced in Eurocode 5.

Later equation (16) has also entered Eurocode 5 for the yield capacity of dowels with thin diameters like nails and staples. Whether this is correct is discussed **Paper 38-7-5**. The conclusion is that it is on the safe side to use this equation in general for all diameters. But for small values of d (like stables) the bending capacity according to becomes larger than the fully plastic value.

Load distribution

The load carrying capacity R_n of a connection with n fasteners in line in the load direction, does generally not equal the load carrying capacity of a single fastener multiplied by n. Therefore, an effective number of fasteners $n_{ef} < n$ has been introduced. R_n is calculated as:

$$R_n = n_{ef} R_{single} \tag{17}$$

Even assuming ideal conditions - identical load-slip curves of single fasteners - the distribution of the load in multiple-fastener joints is non-uniform when the fasteners are aligned parallel to the direction of loading, because of the different elongations of the connected members. For example, consider Figure 9: Between the first and second nail member 1 is loaded by force F minus fastener load 1 while member 2 resists only fastener load 1. Assuming the same extensional stiffness for both members, the elongation of member 1 between the first and second nail will be greater than the corresponding elongation of member 2. These different elongations must be compensated for by different displacements of the first and second nail. Different displacements mean - at least as long as the yield load is not yet reached – different fastener loads. This effect is also found in e.g. riveted steel structures where it is called the Volkersen effect.

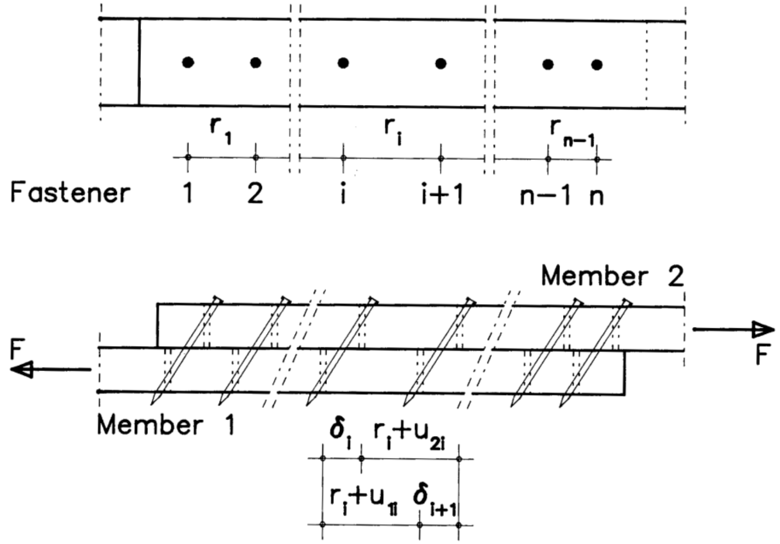

Figure 9. The influence of member elongations. From ***Paper 23-7-2****.*

If the load is increased over a proportional limit, the most highly stressed fasteners at the ends of the joint begin to deform plastically. Moreover, the embedment strength in the contact areas between these connectors and the wood is reached, and redistribution of load from the fasteners at the ends to those in the centre of the joint will result. After each fastener has reached its yield load, the differences in fastener loads become minimal and the joint reaches its yield load.

Since nailed joints are very ductile, load distribution in nailed joints should not affect the load-carrying capacity and this is confirmed by the tests described in **Paper 23-7-2** that concludes: The maximum load of a multiple-nailed joint can be estimated as the sum of those for individual nails, provided joint failure is by nail yielding. Irrespective of this conclusion an effective number $n_{ef} < n$ has without any argument been introduced in Eurocode 5 for nails.

For other fasteners, test results of several researchers indicate, that the ultimate load per fastener decreases, sometimes considerably with increasing number of fasteners arranged parallel to load. This suggests that the failure mode in many connections may not be attaining the joint's yield load. Instead, joint load capacity may be constrained by preliminary wood splitting. Consequently, the potential load capacity of the connection is not realised because load-slip curves of single fasteners break off and ideal redistribution of load is prevented. Oversized and misaligned bolt holes or split ring grooves tend to make the situation even worse: by causing differences in initial slip of single fasteners which makes the load distribution very uneven. This may lead to some single fasteners reaching their maximum load while other fasteners just begin to carry load because of their greater initial slip. In case of long-term or repeated loading, creep deformations and residual plastic deformations after previous higher loading also affect load distribution.

Simplified expressions

The complete set of equations may look a little complicated and many proposals for simplification by omitting some equations or combining two or more. Examples are given in e.g. **7-100-1**, **31-7-7, 31-7-8, 37-7-3** and **40-7-4.** CIB-W18 has, however maintained that with the spread of computers there is no need for such simplified methods. In reality it is easier and safer to use the complete set of equations. An argument is also that none of the simplified methods can cope with the rope effect.

Annex: Theoretical load-carrying capacity expressions

In the following expressions are derived for single-shear and symmetrical double-shear joints. The possible failure modes are shown in Figure A.1.

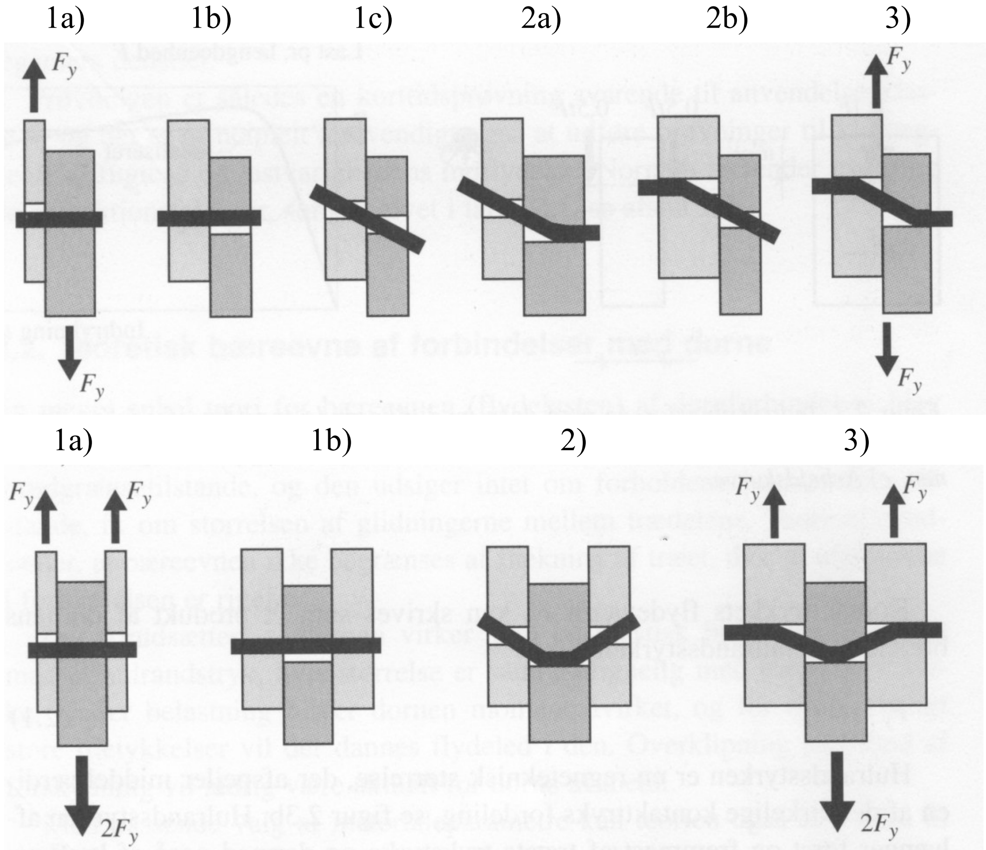

Figure A.1. Possible failure(yield) modes for single-shear and symmetrical double-shear joints.

In the single shear joint, the dowel will either remain straight (failure modes 1) or bend in one or two yield hinges (failure modes 2 or 3 respectively). For the double shear joint failure modes 1 correspond to a movement of the dowel either in the side members or the middle member. In failure mode 2 two yield hinges occur in the middle member while the dowel remains straight in the side members. In failure mode 3 four yield hinges are formed within the dowel, two in the middle member and one in each outer part.

In each member there are the following possibilities:

– the dowel makes a translation without rotation
– the dowel remains straight but rotates
– the dowel bends at a yield hinge.

It is found convenient initially to analyse the situation in one member and then combine the results. The first case – the translation – is so simple that no further mentioning is needed. The other two cases, where a dowel is loaded with a force F_y, resulting in "yielding" in the wood and maybe also in the dowel are shown in Figure A.2.

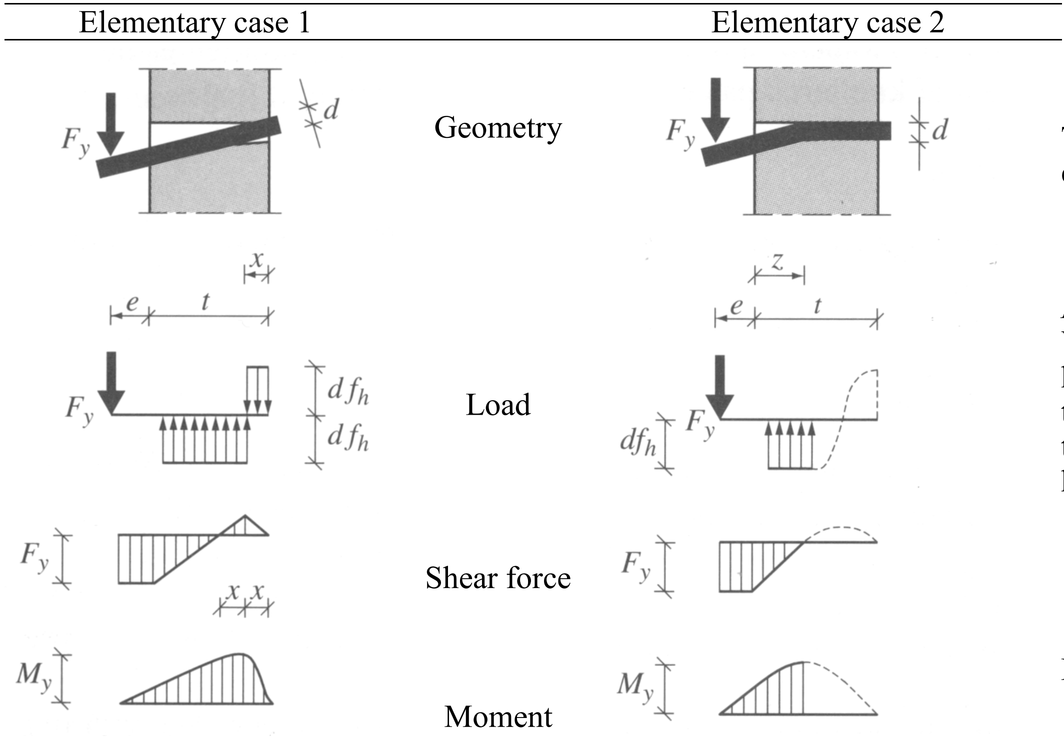

Figure A.2. Dowel loaded by the force F_y in the distance e from the surface. To the left Elementary case 1 (without yield hinge), To the right Elementary case 2 (with one yield hinge).

Elementary case 1

The dowel yield moment is greater than the bending moment. The dowel remains straight and rotates around a point with the distance x from the right surface of the member, see Figure A.2left. By projection and moment around the force

$$F_y = (t-2x)df_h \tag{A.1}$$

$$df_h\left[x\left(t-\frac{x}{2}+e\right)-(t-x)\left(\frac{t-x}{2}+e\right)\right]=0 \tag{A.2}$$

from which

$$x = t+e-\frac{1}{2}\sqrt{(t+2e)^2+t^2} \tag{A.3}$$

$$F_y = \left(\sqrt{(t+2e)^2+t^2}-(t+2e)\right)df_h \tag{A.4}$$

The maximum moments is found where the shear force is zero. Moment equilibrium about the forces on one side of this point renders

$$M_{\max} = x^2 df_h \tag{A.5}$$

Elementary case 2

With the ideal assumptions the dowel will remain straight until a yield hinge is formed at a distance z from the surface, see Figure A.2right. Since the moment M_y is a maximum moment, the shear force is equal to 0 in this point. Vertical equilibrium and moment equilibrium about the yield hinge give

$$F_y - zdf_h = 0 \tag{A.6}$$

$$F_y(e+z) - zdf_h\frac{z}{2} - M_y = 0 \tag{A.7}$$

From these equations

$$z = \sqrt{e^2+\frac{2M_y}{df_h}}-e \tag{A.8}$$

$$F_y = \left(\sqrt{e^2+\frac{2M_y}{df_h}}-e\right)df_h \tag{A.9}$$

Single shear joint

For the single-shear joint shown in Figure A.3 the load-carrying capacity can now be determined for the possible failure modes shown in Figure A.1

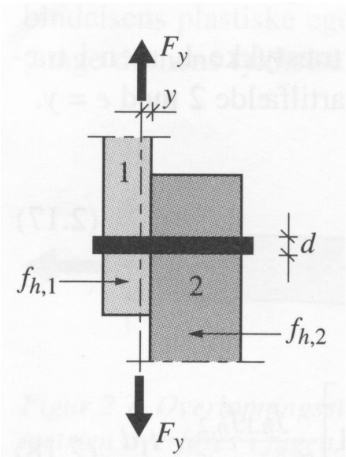

Figur A.3. Single shear joint. It is assumed that the yield hinge i placed in member 1 at a distance y from the joint (positive as shown). Since the shear force is 0 the load is acting in this line.

The member thicknesses are t_1 and t_2 and the embedding strengths $f_{h,1}$ and $f_{h,2}$ with

$$\beta = \frac{f_{h,2}}{f_{h,1}} \tag{A.10}$$

For failure mode 1c the load-carrying capacity yielding takes place simultaneously in the two members , where the situation corresponds to Elementary case 1, i.e. equation (A.4) apply. For member 1 $e = -y$.

$$F_y = \left[\sqrt{(t_1 - 2y) + t_1^2} - (t_1 - 2y)\right] d f_{h,1} \tag{A.11}$$

For member 2 $e = y$.

$$F_y = \left[\sqrt{(t_2 + 2y) + t_2^2} - (t_2 + 2y)\right] d f_{h,2} \tag{A.12}$$

By elimination of y:

$$F_y = \frac{f_{h,1} t_1 d}{1+\beta}\left[\sqrt{\beta + 2\beta^2\left[1 + \frac{t_2}{t_1} + \left(\frac{t_2}{t_1}\right)^2\right] + \beta^3\left(\frac{t_2}{t_1}\right)^2} - \beta\left(1 + \frac{t_2}{t_1}\right)\right] \tag{A.13}$$

For failure mode 2a (A.11) is still valid for member 1; but in member 2 (A.9) apply with $e = y$:

$$F_y = \left(\sqrt{y^2 + \frac{2M_y}{d f_{h,2}}} - y\right) d f_{h,2} \tag{A.14}$$

By elimination of y:

$$F_y = \frac{f_{h,1} t_1 d}{2+\beta}\left[\sqrt{2\beta(1+\beta) + \frac{4\beta(2+\beta)M_y}{f_{h,1} d t_1^2}} - \beta\right] \tag{A.15}$$

For failure mode 2b the yield hinge is placed in member 2 and correspondingly:

$$F_y = \frac{f_{h,1} t_2 d}{1+2\beta}\left[\sqrt{2\beta^2(1+\beta) + \frac{4\beta(1+2\beta)M_y}{f_{h,1} d t_2^2}} - \beta\right] \tag{A.16}$$

For failure mode 3 there is a yield hinge in both members. For member 2, (A.14) still apply, while (A.9) apply for member 1 with $e = -y$.

$$F_y = \left(\sqrt{y^2 + \frac{2M_y}{d f_{h,1}}} + y\right) d f_{h,1} \tag{A.17}$$

By elimination of y:

$$F_y = 2\sqrt{\frac{2\beta}{1+\beta}}\sqrt{2M_y f_{h,1} d} \tag{A.18}$$

The load-carrying capacity is found as the minimum value found by these expressions.

Symmetrical double shear joints

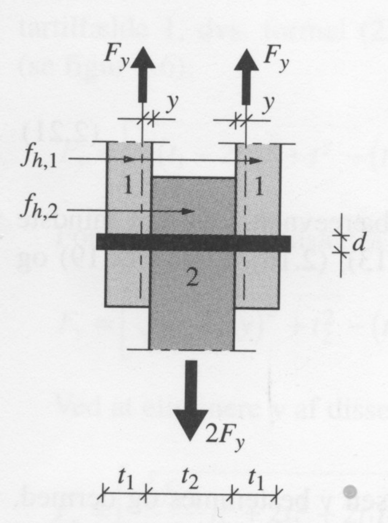

Figure A.4. Symmetrical double shear joint.

The thickness of the outer members is t_1 and of the middle member t_2. The embedding strengths are $f_{h,1}$ and $f_{h,2}$ with $\beta = f_{h,2}/f_{h,1}$.

As shown in Figure A.1 there are 4 failure modes. For failure mode1a:

$$F_y = t_1 d f_{h,1} \tag{A.19}$$

and for failure mode 1b:

$$F_y = 0,5 t_2 d f_{h,2} \tag{A.20}$$

For the failure modes 2 and 3 F_y is the same as for the single-shear joints since F_y is per shear.

ESSAY 4.3 H J Larsen
Glued-in rods

The sad story of glued-in bolts in Eurocode 5
Right from the beginning there was no doubt that glued-in bolt should be included in the Eurocode 5, and clauses were included from 1986 in its predecessor the CIB/W18 Timber Design Code based on **Paper 19-7-2**.

There were however many conflicting views on the draft, and when the time for publication drew near first for ENV 1995-1-1, then for EN 1995-1-1, it became obvious that it would not be possible to come to an agreement. There were many bits of research and all researchers found that their bit overruled all the other bits.

It was agreed to postpone the topic to the bridge Eurocode EN 1995-2. To get a basis for the drafting funding was obtained from the European Commission. Information about the project called GIROD is given in **Paper 34-7-8**. The project was split into several packages.

One was drafting an agreed proposal for a chapter in the Eurocode 5. Unfortunately the partner responsible and paid for this package never delivered the proposal. There was an amateurish draft, but it was never published or discussed in CIB/W18 or in the responsible drafting group. Just before the last meeting in CEN TC 250/ SC5 responsible for the bridge Eurocode some of the GIROD partners come up with a draft that most felt was acceptable, but again some felt that they themselves could have done it better and that some of their pet ideas were not included. And on the spur of the moment it was decided to give up and leave glued-in rods out.

And there it stands until a new generation takes over.

In the following the rejected proposal is shown and compared to two other proposals: The old one set out in **Paper 19-7-2** and for a time included in the drafts for ENV 1995, and a German one given in the National Application Document (DIN V EN 1995-1-1/NA 1:2004-12) to Eurocode 5.

Proposal in prEN 1995-2 discussed for formal vote

Annex C (informative)
Bonded-in steel rods

C.1 General

(1) The use of bonded-in rods should be limited to structural parts assigned to service classes 1 and 2.

(2) It should be verified that the properties of the adhesive and its bond to steel and wood are reliable during the lifetime of the structure within the temperature and moisture ranges envisaged.

(3) Rods should be threaded or deformed bars.

(4) The shear strength of the adhesive and its bond to steel and timber should be verified by tests.

(5) For service class 2, the values of k_{mod} according to EN 1995-1-1 clause 3.1.3 should be reduced by 20 %.

C.2 Axially loaded rods

C.2.1 General
(1) The load-carrying capacity of connections made with bonded-in axially loaded rods should be verified for the following failure modes:
- failure of the steel rod;
- failure of the adhesive and its bond to steel and timber;
- failure of the timber adjacent to the glue-line;
- failure of the timber member (e.g. pull-out failure of a whole timber block with several bonded-in rods).

(2) The design load-carrying capacity should generally be limited by the strength of the rod.

(3) The expressions given are based either on the outer diameter d of the rod; or when strength of the adhesive is not critical, on an equivalent diameter d_{equ} equal to the smaller of the hole diameter, d_h, and 1,15d.

Note: For threaded rods, the outer diameter is equal to the nominal diameter; for most deformed reinforcing bars used as rods, the outer diameter is about 10 % greater than the nominal diameter.

(4) Minimum spacings and edge and end distances should be taken according to figure C.1.

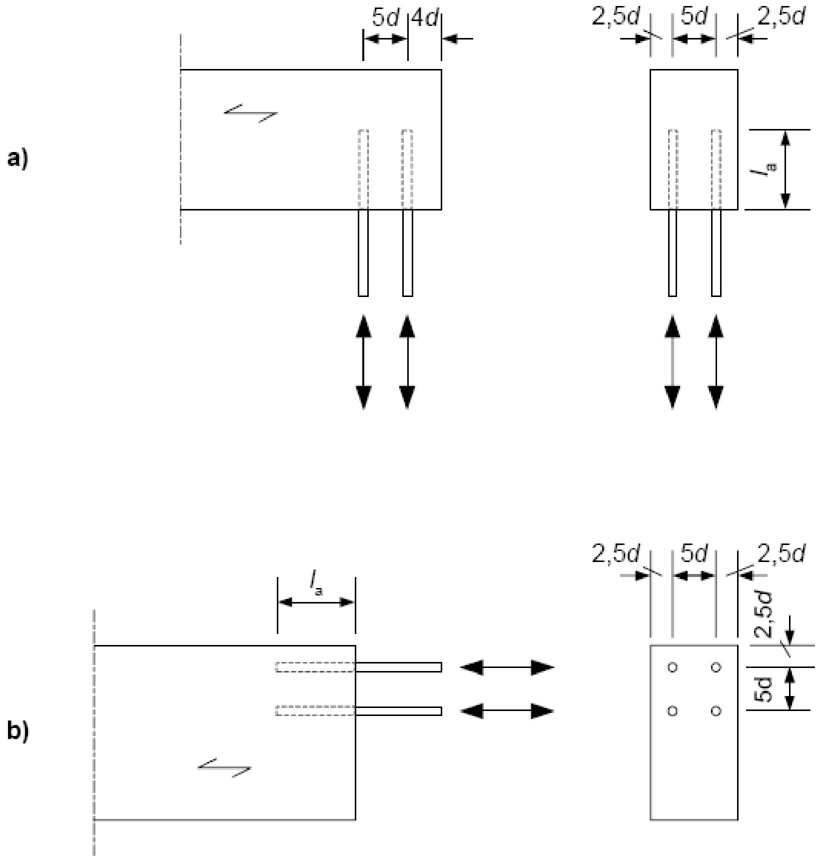

Figure C.1 – Minimum spacings and distances for axially loaded rods loaded a) perpendicular to the grain b) parallel to the grain

(5) The minimum anchorage length $l_{a,\text{min}}$ should be taken as:

$$l_{a,\min} = \max \begin{cases} 0,5d^2 \\ 10d \end{cases} \tag{C.1}$$

where:
$l_{a,min}$ is the minimum anchorage length in mm, see figure C.1;
d is the outer diameter of the rod in mm.

C.2.2 Ultimate limit state

C.2.2.1 Failure of individual rod
(1) The characteristic axial load-bearing capacity in tension of the steel rod, $R_{\text{ax,k}}$ in N, should be taken as:

$$R_{ax,k} = \min \begin{cases} f_{y,k} A_{ef} & \text{(a)} \\ \pi d_{equ} l_a f_{ax,k} \dfrac{\tanh \omega}{\omega} & \text{(b)} \end{cases} \tag{C.2}$$

where:

$f_{y,k}$ is the characteristic yield strength in N/mm^2;
A_{ef} is the effective cross-sectional area of the rod in mm^2;
d_{equ} is the equivalent rod diameter in mm, see C.2.1(3);
l_a is the anchorage length in mm;
$f_{ax,k} = 5,5$ N/mm^2;

$$\omega = \frac{0,016\, l_a}{\sqrt{d_{equ}}}; \tag{C.3}$$

For rods in compression, the possibility of buckling should be taken into account for design compression stresses greater than 300 N/mm^2.

C.2.2.2 Failure in the timber member
(1) The effective timber failure area, A_{ef}, of a rod inserted in direction parallel to the grain, see figure C.2, should be taken as the smaller of
- an effective width, b_{ef}, of 3d on each side of the centre of the rod;
- the area derived from the actual geometry where the distance is smaller than 6d or the edge distance is smaller than 3d.

(2) In a group of rods inserted in direction parallel to the grain, the characteristic resistance parallel to the grain of one rod, $R_{ax,k}$, should be taken as:

$$R_{ax,k} = f_{t,0,k} A_{ef} \tag{C.4}$$

where:

$R_{ax,k}$ is the characteristic load-carrying capacity of one rod;
$f_{t,0,k}$ is the characteristic tensile strength of the wood;
A_{ef} is the effective timber failure area.

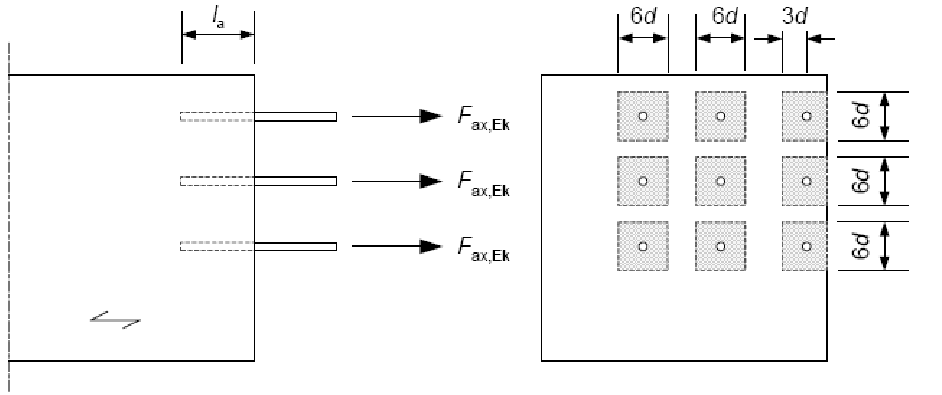

Figure C.2: Effective areas for anchorage forces parallel to the grain with b_{ef} = 6d

(3) For rods inserted at an angle to the grain, EN 1995-1-1 clause 8.1.4 applies where h_e is the loaded edge distance to the end of the rod and b is replaced by b_e.

C.2.3 Serviceability limit states

(1) The instantaneous slip modulus, K_{ser}, in N/mm per rod should be taken as

$$K_{ser} = 0{,}004 d^{1,8} \rho_{mean}^{1,5} \tag{C.3}$$

where:

d is the diameter of the rod, in mm;
ρ_{mean} is the mean density of the wood in kg/m^3.

C.3 Laterally loaded rods

C.3.1 Ultimate limit state

(1) The provisions of EN 1995-1-1 section 8 for laterally loaded dowels apply.

(2) For laterally loaded bonded-in rods inserted parallel to the grain, the embedding strength should be taken as 10 % of the embedding strength perpendicular to the grain.

(3) For bonded-in rods inserted at an angle α to the grain, linear interpolation should be applied.

C.3.2 Serviceability limit states

(1) For rods inserted perpendicular to the grain, the slip modulus K_{ser} in N/mm per rod should be taken as

$$K_{ser} = 0{,}04 d \rho_{mean}^{1,5} \tag{C.4}$$

where:

d is the effective rod diameter, in mm;
ρ_{mean} is the mean density of the wood in kg/m^3.

Note: For threaded rods the effective diameter of the rod corresponds to about 90 % of the outer diameter; for deformed reinforcing bars to the nominal diameter.

(2) For rods inserted parallel to the grain, K_{ser} should correspondingly be taken as

$$K_{ser} = 0{,}08 d \rho_{mean}^{1,5} \tag{C.5}$$

(3) For bonded-in rods inserted at an angle α to the grain, linear interpolation should be applied.

C.4 Combined laterally and axially loaded rods

(1) For combined laterally and axially loaded bonded-in rods, the following condition should be satisfied:

$$\left(\frac{F_{ax,d}}{R_{ax,d}}\right)^2+\left(\frac{F_{la,d}}{R_{la,d}}\right)^2\leq 1 \qquad \text{(C.6)}$$

where:
$F_{ax,d}$ is the axial design load;
$F_{la,d}$ is the lateral design load;
$R_{ax,d}$ is the axial design load-carrying capacity;
$R_{la,d}$ is the lateral design load-carrying capacity.

C.5 Execution

(1) The surfaces of the holes should be clean cut.

(2) With several rods in a group to be tightened, the tightening should be uniform.

(3) It should be insured that the hole is completely filled with adhesive.

(4) At the time of gluing the rods, the moisture content of the timber should not be more than 15 %.

Proposal given in Paper 19-7-2.

The characteristic load-carrying should be taken as

$$F_{ax,k}=\min\begin{cases}k_{thread}\,f_y A_{ef}\\ f_{ax,k}d_{equ}\sqrt{l_a}\end{cases}$$

where
$f_{ax,k}$ = 167 N/mm^{1,5} for polyurethane adhesives and $f_{ax,k}$ = 133 N/mm^{1,5} for epoxy and resorcinol adhesives.

Proposal given in The German National Application Document to EN 1995-1-1

The load-carrying capacity should be taken as

$$F_{ax,k}=\min\begin{cases}f_{y,k}A_{ef}\\ \pi d l_a f_{a,k}\end{cases}$$

where

$$f_{ax,k}=\begin{cases}4 & & l_a\leq 250\text{ mm}\\ 5,25-0,005l_a & \text{for} & 250\text{ mm}<l_a\leq 500\text{ mm}\\ 3,5-0,0015l_a & & 500\text{ mm}<l_a\leq 1000\text{ mm}\end{cases}$$

Example

As an example the load-carrying capacity is calculated for a threaded rod M 20 with $f_{y,k}$ = 240 N/mm^2. A_{ef} = 245 mm^2.

Proposal in EN 1995-2 (bridges)

With a hole diameter of 20 mm, the equivalent diameter is

$$d_{equ}=\min\begin{Bmatrix}22\\ 1,15d=23\end{Bmatrix}=22\ \text{mm}$$

The minimum anchorage length is

$$l_{a,\min}=\max\begin{Bmatrix}0,5d^2=200\\ 10d=200\end{Bmatrix}=200\,\text{mm}$$

With

$$\omega=\frac{0,016l_a}{\sqrt{22}}=3,41\cdot l_a\cdot 10^{-3}$$

the characteristic axial load-carrying capacity is

$$R_{ax,k}=\min\begin{cases}240\cdot 245\cdot 10^{-6}=58,8\\ \pi\cdot 22\cdot l_a\cdot 5,5\cdot\dfrac{\tanh\omega}{\omega}=380\dfrac{\tanh\omega}{\omega}\end{cases}$$

The axial load-carrying capacity depending on $l_a \geq 200\,\text{mm}$ is shown in Table 1 and Figure 1.

Proposal in Paper 19-7-2

For epoxy adhesives

$$F_{ax,adh,k} = f_{ax,k} d_{equ} \sqrt{l_a} = 133 d_{equ} \sqrt{l_a}$$

The load-carrying capacity is shown in Table 1 and Figure 1.

German Proposal

$$F_{ax,shear,k} = \pi d l_a f_{a,k}$$

where

$$f_{ax,k} = \begin{cases} 4 & l_a \leq 250 \text{ mm} \\ 5,25 - 0,005 l_a \quad \text{for} & 250 \text{ mm} < l_a \leq 500 \text{ mm} \\ 3,5 - 0,0015 l_a & 500 \text{ mm} < l_a \leq 1000 \text{ mm} \end{cases}$$

The load-carrying capacity for is also shown in Table 1 and Figure 1.

Table 1. Characteristic load-carrying capacity for epoxy adhesives

Eurocode 5-2 (bridges)					Paper **19-7-2**	German NAD
l_a mm	$F_{ax,steel.k}$ kN	ω	$F_{ax,shear.k}$ kN	$F_{ax.k}$ kN	$F_{ax.k}$ kN	$F_{ax.k}$ kN
160	52,92	0,55			37,1	40,2
180	52,92	0,61			39,3	45,2
200	52,92	0,68	66,1	52,9	41,5	50,3
220	52,92	0,75	70,8	52,9	43,5	53,3
240	52,92	0,82	75,1	52,9	45,4	58,8
260	52,92	0,89	79,1	52,9	47,3	58,8
280	52,92	0,96	82,7	52,9	49,1	58,8
300	52,92	1,02	85,9	52,9	50,8	58,8
320	52,92	1,09	88,9	52,9	52,5	58,8
340	52,92	1,16	91,5	52,9	52,9	58,8
360	52,92	1,23	93,8	52,9	52,9	58,8
380	52,92	1,30	95,9	52,9	52,9	58,8
400	52,92	1,36	97,8	52,9	52,9	58,8

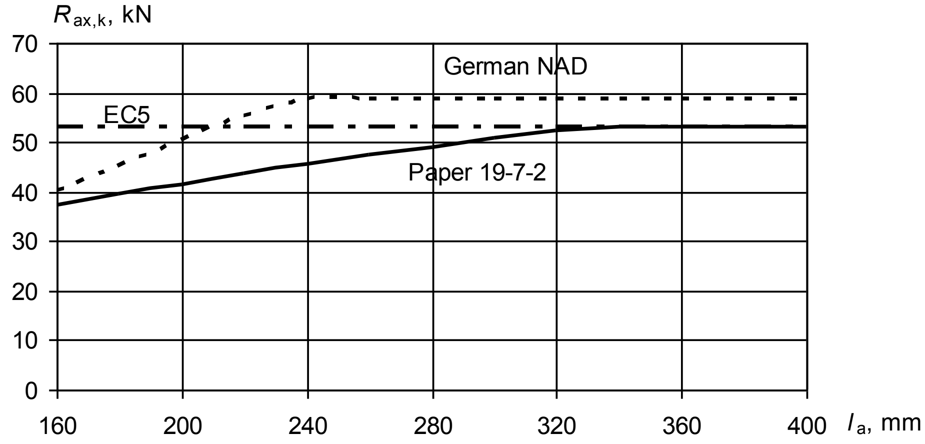

Figure 1. Load-carrying capacities.

If $k_{thread} = 0{,}9$ is used also in the German proposal it gives almost the same result as Eurocode 5 Bridges for $l_a > 200$ mm.

The German proposal differs from the other two by not taking into account the strength reduction given in Eurocode 3 for threaded rods.

The proposal in EN 1995-2 differs from the other two by giving a minimum anchorage length in addition to the general requirement that failure should be due to steel yielding and not adhesion failure.

ESSAY 4.4 H J Larsen
Design rules for screws

A distinction is made between traditional smooth shank screws, where the outer thread diameter is equal to the shank diameter, see Figure 1, and ”modern” self-drilling screws, see Figure 2, with a geometry as shown in Figure 3.

Figure 1. Smooth shank screws. To the left: Lag screws. To the right slotted screw

Figure 2. Top: Self-drilling spun screw. Bottom: SFS- screw with thread both under the head and at the end, (the pitches are a little different resulting in the parts being drawn tight together).

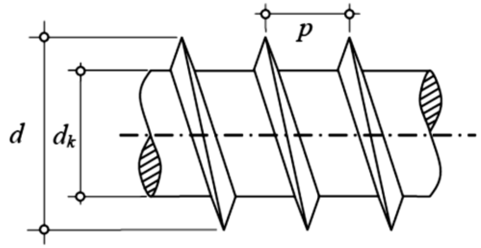

Figure 3. Detail of a screw thread: denotations nominal diameter d (= nominal screw size), thread-root diameter d_k and thread pitch p.

Laterally loaded screwed joints

The load-carrying for screws is assumed to be the same as for dowels, but with an effective diameter d_e, i.e. the characteristic embedding strength should be calculated as:

$$f_{h,k} = 0,082 \rho_k d_e^{-0,3} \tag{1}$$

For smooth shank screws, the effective diameter d_e is taken as the smooth shank diameter. For other screws d_e should be taken as $1,1d_k$. Assuming $d_k/d = 0,65$:

$$f_{h,screw,k} = 0,082 \rho_k \left(1,1 d_e\right)^{-0,3} = 0,082 \rho_k \left(1,1 \cdot 0,65 d\right)^{-0,3} = 0,091 \rho_k d^{-0,3} \tag{2}$$

Tests to determine $f_{h,screw,k}$ are reported in Blass, H J, Bejtka, I and Uibel, T: “Tragfähigkeit von Verbindungen mit selbstbohrenden Holzscrauben mit Vollgewinde”, Karlsruhe Berichte zum Ingenieurholzbau, 2006.

Based on the tests the following expression for the embedding strength is proposed:

$$f_{h,screw,k} = 0,022 \rho_k^{1,24} d^{-0,3} = 0,022 \rho_k^{0,24} \rho_k d^{-0,3} = k \cdot \rho_k d^{-0,3} \tag{3}$$

The factor k is shown below as a function of the strength class/characteristic density.

	C14	C18	C24	C30
ρ_k kg/m^3	290	320	350	380
k	0,086	0,088	0,090	0,092

It is concluded that the Eurocode 5 simple rule seems reasonable.

Axially loaded screwed joints

In Eurocode 5:2004 the characteristic withdrawal load-carrying capacity at an angle α to the grain was originally given as

$$R_{ax,\alpha,k} = n_{ef} \left(\pi d l_{ef}\right)^{0,8} f_{ax,\alpha,k} \tag{4}$$

where

n_{ef} is the effective number of screws
d is the outer diameter measured on the threaded part
l_{ef} is the pointside penetration length of the threaded part minus one screw diameter

$f_{ax,\alpha k}$ is the characteristic withdrawal strength at an angle α to the grain.

The characteristic withdrawal strength at an angle α to the grain should be taken as:

$$f_{ax,\alpha,k} = \frac{f_{ax,k}}{\sin^2 \alpha + 1,5\cos^2 \alpha} \quad (5)$$

with

$$f_{ax,k} = 3,6 \cdot 10^{-3} \rho_k^{1,5} \quad (6)$$

ρ_k is the characteristic density in kg/m^3.

The background for these expressions, taken from DIN 1052:2004, is not given in any CIB W18-paper.

Without any explanation these rules were changed in the 2008 amendment A1 to Eurocode 5. For screws according to EN 14592 and with

6 mm $\leq d \leq$ 12 mm

$0,6 \leq d_k/d \leq 0,75$

where

d is the outer thread diameter;
d_k is the inner thread diameter

Eq. (4)-(6) were replaced by the following:

$$R_{ax,k} = \frac{n_{ef} f_{ax,k} d l_{ef} k_d}{1,2\cos^2 \alpha + \sin^2 \alpha} \quad (7)$$

where

$$f_{ax,k} = 0,52 d^{-0,5} l_{ef}^{-0,1} \rho_k^{0,8} \quad (8)$$

$$k_d = \min \begin{cases} d/8 \\ 1 \end{cases} \quad (9)$$

n_{ef} is the effective number of screws
l_{ef} is the penetration length of the threaded part, in mm
ρ_k is the characteristic density, in kg/m^3

The statistical treatment of the test results is described in **Paper 42-7-3** Models for the Calculation of the Withdrawal Capacity of Self-tapping Screws - M Frese, H J Blass.

It is assumed that the angle, β, between the screw axis and the grain direction, see Figure 4, is greater than 30º.

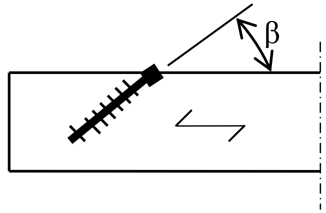

Figure 4. Angle between screw axis and grain direction.

For angles between 30º and 90º, $f_{ax,\alpha,k}$ should be multiplied by

$$k_\beta = \frac{1}{2,5\cos^2 \beta + \sin^2 \beta} \quad (10)$$

It is assumed that the penetration length is as a minimum 6*d.* For smaller lengths, Eurocode 5 gives no load-carrying capacity.

ESSAY 5.1 J König
Structural fire design according to Eurocode 5

This essay is – with the author's kind permission – based on the manuscript for:
König, J.: Structural fire design according to Eurocode 5 – Design rules and their background. Fire and Materials, Volume, 29, Issue 3, Pages 147-163.

Summary
This paper gives a review of design rules of EN 1995-1-2, the future common code of practice for the fire design of timber structures in the Member States of the EU and EFTA, and makes reference to relevant research background. Compared to the European pre-standard ENV 1995-1-2, the new EN 1995-1-2 has undergone considerable changes.

Charring is dealt with in a more systematic way and different stages of protection and charring rates are applied. For the determination of cross-sectional strength and stiffness properties, two alternative rules are given, either by implicitly taking into account their reduction due to elevated temperature by reducing the residual cross-section by a zero-strength zone, or by calculating modification factors for strength and stiffness parameters.

Design rules for charring and modification factors are also given for timber frame members of wall and floor assemblies with cavities filled with insulation. A modified components additive method has been included for the verification of the separating function. The design rules for connections have been systemised by introducing simple relationships between the load-bearing capacity (mechanical resistance) and time.

The code provides for advanced calculation methods for thermal and structural analysis by giving thermal and thermo-mechanical properties for FE analyses. The code also gives some limited design rules for natural fire scenarios using parametric fire curves.

1 Introduction
This paper deals with EN 1995-1-2 [2] containing rules for structural fire design of timber structures. The various Eurocode Parts are not self-containing documents, as almost no information given in one Part is repeated in another Part. Therefore, due to intense crossreferencing, the user of EN 1995-1-2 will also need the following Parts: EN 1990 [1], EN 1991-1-2 [3] giving thermal actions for the fire situation, other EN 1991 Parts with actions, EN 1995-1-1 [4] with common rules for "cold" design of timber structures, and other Parts referenced, e.g. the Fire Parts of other Eurocodes.

As all other Eurocode Parts, EN 1995-1-2 in some cases gives the possibility of a National choice, e.g. regarding safety related parameters or between alternative rules. Information about the Nationally determined parameters (NDP) may be found in a National annex.

ENV 1995-1-2
When ENV 1995-1-2 [5] was published in 1994, for the first time European harmonized structural fire design rules for timber structures were available. Previous National rules, in those member states where such rules existed, were of different complexity, depending on the level of development in the field of fire design of timber structures achieved in respective countries. For example, charring rates given in National codes varied considerably. A common safety philosophy did not exist; sometimes safety factors and/or the effects of elevated temperature on strength and stiffness parameters were included implicitly in the charring rates, in other cases one or both of them were given separately. In ENV 1995-1-2 it was tried to strictly distinguish between material properties and safety factors and to present methods of different levels of complexity. As an alternative to standard fire exposure, also some design rules were given for parametric fire curves representing natural fire scenarios.

2 EN 1995-1-2

2.1 Basis of structural fire design
2.1.1 General.
Section 2 of the Fire Parts of the Eurocodes for each material give rules on requirements, actions, design values of material properties and resistances (that is how design values are established from characteristic values) and verification methods.

2.1.2 Requirements.
The basic requirements for fire design are that, when mechanical resistance in the case of fire is required, the load-bearing function is maintained during the relevant time of fire exposure and, correspondingly for elements forming boundaries of a fire compartment, the separating func-

tion is maintained. For standard fire exposure, the insulation criterion is the well-known temperature rise criterion: the maximum temperature rise averaged over the whole of the non-exposed surface is limited to 140 K and the maximum temperature rise at any point on that surface is limited to 180 K.

For parametric fire exposure, the load-bearing function should be maintained during the complete duration of the decay phase, or for a specified period of time. For verification of the separating function under parametric fire exposure, the temperature criterion given above for the standard fire applies during the heating phase.

During the decay phase the temperature rise should not exceed 200 or 240 K respectively, based on an acceptance criterion used in Sweden since 1975 where the maximum temperature on the unexposed side was limited to 200 or 240°C respectively). Strictly speaking, the requirement for the heating phase is superfluous, since it is covered by the requirement during the decay phase. It should be noted that the 140/180 K criterion for standard fire exposure includes a safety margin taking into account the temperature rise that would occur during the decay phase in a natural fire scenario, but is not explicitly taken into account in the standard fire scenario.

The design values of strength and stiffness properties of timber members are given as

$$f_{d,fi} = k_{mod,fi} \frac{f_{20}}{\gamma_{M,fi}} \tag{1}$$

$$S_{d,fi} = k_{mod,fi} \frac{S_{20}}{\gamma_{M,fi}} \tag{2}$$

where:

$f_{d,fi}$ design strength in fire (bending strength, compressive strength etc of timber members);

$S_{d,fi}$ design stiffness property (modulus of elasticity $E_{d,fi}$ or shear modulus $G_{d,fi}$) in fire;

f_{20} 20 % fractile of a strength property at normal temperature;

S_{20} 20 % fractile of a stiffness property (modulus of elasticity or shear modulus) at normal temperature;

$k_{mod,fi}$ modification factor for fire taking into account the reduction in strength and stiffness properties at elevated temperatures;

$\gamma_{M,fi}$ partial safety factor for timber in fire ($\gamma_{M,fi} = 1$).

The 20 % fractile of a strength, and correspondingly of a stiffness property, is derived from the characteristic (5 % fractile) value as

$$f_{20} = k_{fi}\, f_k \tag{4}$$

where k_{fi} is dependent on the coefficient of variation of the material. For example, for solid timber $k_{fi} = 1.25$, for glued laminated timber $k_{fi} = 1.15$.

As previously in ENV 1995-1-2, the level of the 20 % fractile, although not explicitly specified as such, was chosen in order to achieve a similar safety level as in the National design codes, when the partial factor $\gamma_{M,fi}$ was taken equal to unity.

2.1.3 Verification methods.

EN 1990 states, as an principle, that the structural analysis, among other things, shall consider models for the temperature evolution within the structure as well as models for the mechanical behaviour of the structure at elevated temperature. The application rule, satisfying this principle, says that the required performance should be verified by either global analysis, analysis of sub-assemblies or member analysis. Traditionally, member analysis corresponds to design by performing full-scale furnace tests of members (beams, columns, floors, walls). For timber structures member analysis is sufficient, since thermal elongations of timber members are negligible – due to the large temperature gradient across the cross-section and a sufficiently large cold core in the timber member – and thus have negligible influence on the structural system.

2.2 Charring of timber

2.2.1 Calculation of residual cross-section.

The clauses dealing with charring have undergone considerable revision compared to ENV 1995-1-2 [5]. The charring depth is defined as the position of the 300°C isotherm, which is widely accepted as a rounded value, e.g. [6] and close to 288°C or 550°F given in [7]. As a basic value, the charring rate β_0 has been chosen that is observed for one-dimensional heat transfer under standard fire exposure in a semi-infinite timber slab. The conditions are similar in a slab of limited thickness, or in wide timber crosssections remote from corners.

Figure 1 shows the charring depth for one-dimensional charring of a timber slab. At corners of the cross-section, the radius of the char-line is taken equal to the charring depth. In order to simplify the calculation of cross-sectional properties (area, section modulus and second moment of area) by assuming an equivalent rectangular residual crosssection (see Figure 2), notional charring rates β_n are given such that they implicitly include the effect of corner roundings and approximately give the same results. The ratio of the notional charring rate or depth and the one-dimensional charring rate or depth is:

$$\frac{\beta_n}{\beta_0} = \frac{d_{char,n}}{d_{char,0}} = \begin{cases} 1.23 & \text{for solid timber} \\ 1.08 & \text{for glued laminated timber} \end{cases} \quad (5)$$

Figure 1. One-dimensional charring of wide cross section with fire exposure on one side [2]

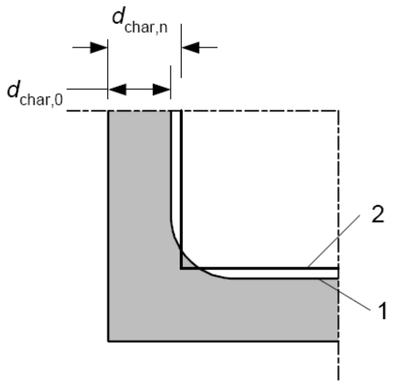

Figure 2. Charring depth $d_{char,0}$ for one-dimensional charring and notional charring depth $d_{char,n}$ [2]

For simplicity, the same value of notional charring rate is used for all sides of a cross-section, although it sometimes would be more accurate to use a greater notional charring rate on the narrow sides of extremely narrow cross-sections. It has been shown [8] that the notional charring rates gives cross-sectional properties (section modulus, second moment of area) that agree well with those calculated for the real shape of the residual cross-section.

Designers sometimes wish to use more complex methods in order to obtain more favourable (economic) results, e.g. by using the one-dimensional charring rates plus corner roundings which is likely to be more exact. Since the corner rounding radius is put equal to the onedimensional charring depth, a minimum width of the cross-section, b_{min}, is given such that the one-dimensional charring rate can be used without unsafe results [8]:

$$b_{min} = \begin{cases} 2\, d_{char,0} + 80 & \text{for } d_{char,0} \geq 13 \text{ mm} \\ 8.15\, d_{char,0} & \text{for } d_{char,0} < 13 \text{ mm} \end{cases} \quad (6)$$

It is assumed that the width of the temperature affected zone, d_Θ, (see Figure 3) increases linearly from 0 to 40 mm during the first 20 minutes of fire exposure (that is after that time the char depth is 13 mm for a charring rate of 0.65 mm/min) and that d_Θ remains constant after 20 minutes.

For softwoods, the (one-dimensional) charring rate of Eurocode 5 is independent of species and densities. This is in contrast to North American experience where different species exhibit considerable influence on the charring rate [7]. For the time being, in Europe these species do not play a major roll in the market place, however increased trade may change this. When Eurocode 5 is used outside Europe, special attention should be paid to species and density.

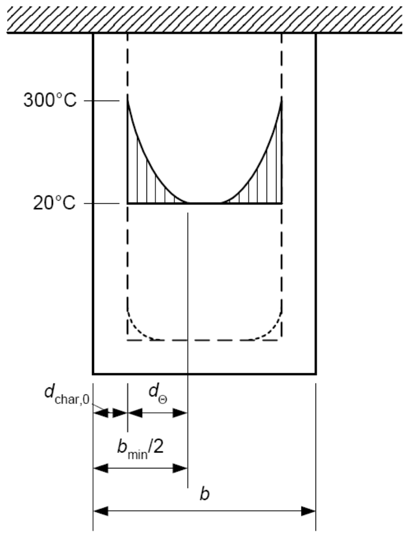

Figure 3. Definition of minimum width for use of one-dimensional charring rate [8] based on temperature profile below the char-line.

2.2.2. Protected surfaces.

The rules on protected surfaces have undergone considerable changes. Based on extensive research [9, 10], it has been shown that different charring rates should be applied during different phases of the fire exposure.

Several cases may occur:

1. The timber surface is protected by a cladding that delays the start of charring until time tf and the cladding is supposed to fall off at that time. Now charring is assumed to take place at double the rate of initially unprotected surfaces, see Figure 4 and Figure 5. The test results of Figure 5 are taken from [9], also showing the simplified bi-linear model adopted by the Eurocode. The reason of the increased charring rate after failure of the cladding is that, at that time, the temperature is already at a high level while no protective char-layer exists to reduce the effect of the temperature. The protection provided by the char-layer is assumed to be built up until its thickness has reached 25 mm. Then the charring rate decreases to the value for initially unprotected surfaces. For simplicity, the 25 mm criterion is adopted for both the one-dimensional and notional charring depth. Typically, claddings made of wood-based panels and regular gypsum plasterboard type A in accordance with EN 520 [11] will give rise to this charring behaviour.

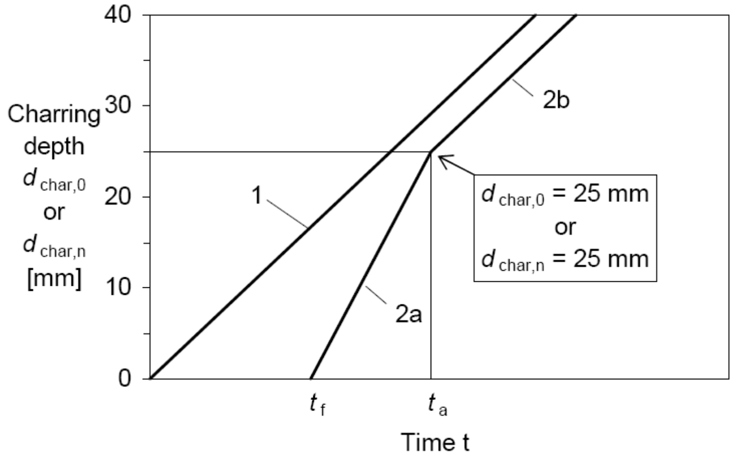

Key:

1 Relationship for members unprotected throughout the time of fire exposure for charring rate β_n (or β_0)

2 Relationship for initially protected members after failure of the fire protection:
2a After protection has fallen off at time t_f, charring starts at increased rate
2c After char depth exceeds 25 mm at time t_a, the charring rate reduces to the rate shown by curve 1

Figure 4. Variation of charring depth with time: Charring starts at failure time of cladding [2].

2. The timber surface is protected by a cladding that delays the start of charring until time tch, however the cladding is supposed to remain in place for a longer time, during which the charring rate is reduced due to the insulation provided by the cladding. When the cladding eventually falls off at time t_f, the charring increases to the double rate described above until a char-layer of 25 mm thickness provides sufficient protection, see Figure 6. Typically, claddings made of gypsum plasterboard type F (with improved core cohesion) and calcium silicate boards will give rise to such charring behaviour. Failure of claddings may take place due to thermal degradation of the boards or pull-out/pull-through failure of fasteners. Unfortunately the code gives no information on failure times of gypsum plasterboard type F due to thermal degradation, since no generic data were available. Such data must be determined by testing (or should be provided by the producer). The code gives a method to calculate the failure time with respect to pull-out failure, assuming that a minimum nominal penetration length of 10 mm is needed for nails or screws in unburned wood (the real penetration length is somewhat smaller, since heat transfer through the fastener will cause increased charring near the tip of the fastener).

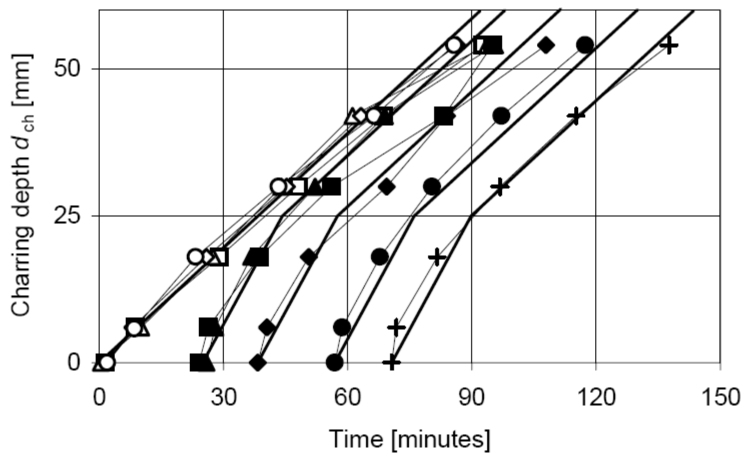

Figure 5. Charring after failure of protection: Comparison of bi-linear model adopted by EN 1995-1-2(bold lines) with test results from [9].

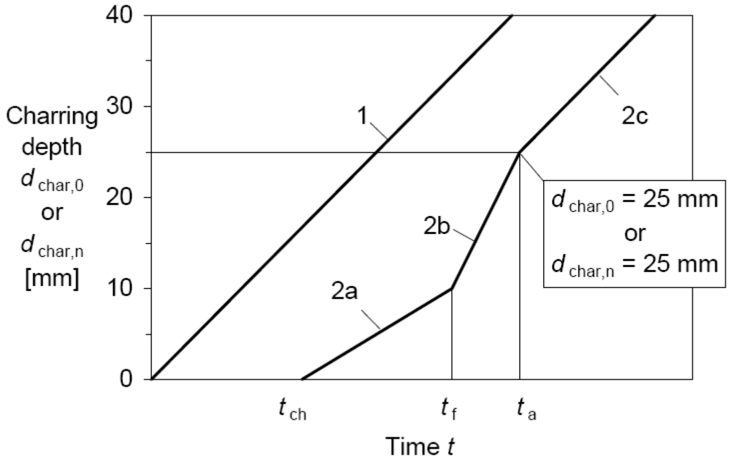

Key:

1 Relationship for members unprotected throughout the time of fire exposure for charring rate β_n (or β_0)

2 Relationship for initially protected members where charring starts before failure of protection:

2a Charring starts at t_{ch} at a reduced rate when protection is still in place

2b After protection has fallen off at time t_f, charring starts at increased rate

2c After char depth exceeds 25 mm at time t_a, the charring rate reduces to the rate shown by curve 1

Figure 6. Variation of charring depth with time: Charring starts before failure time of cladding [2].

Gypsum plasterboard of different types and origin exhibit almost the same thermal properties [12]. Therefore, for the calculation of the delay of the start of charring and the reduction of the charring rate when charring of timber takes place behind the cladding, parameters are given for gypsum plasterboard in general.

Only few experimental data [13] were available for the start of charring and the charring rate of timber which is behind a protective layer of rock fibre batts. The relationship adopted for the start of charring had already been given in ENV 1995-1-2 [5], although it is considerably conservative and describes the effect of insulation layer thickness in an incorrect way. Once charring has started, EN 1995-1-2 reduces the charring rate by 40 % for insulation layer thicknesses of at least 20 mm, provided the rock fibre batts remain in place [13].

2.3 Simplified rules for determining cross-sectional properties

2.3.1. General.

EN 1995-1-1 gives two alternative methods for the determination of cross-sectional properties for the load-bearing capacity of beams and columns. The method recommended in the standard is the method described in 2.3.2 below.

2.3.2. Reduced cross-section method.

This method, permitting the designer to use “cold” strength and stiffness properties (with $k_{mod,fi}$ = 1 in equations (1) and (2)), takes into account the reduction of strength and stiffness in the heat affected zones by removing a further 7 mm thick layer from the residual cross-section. This approach has originally been derived for glued laminated beams [14] where the thickness of the zero strength layer was given as 0.3 inch. In EN 1995-1-2 this concept is also applied to small solid timber cross-sections. For justification, see 2.3.4. It is assumed that this zero strength layer is built up linearly with time during the first 20 minutes of fire exposure, or, in case of a fire protective layer being applied to the timber member, during the time period until the start of charring. For unprotected members, it takes normally about 20 minutes to get stabilised temperature profiles in the zone about 40 mm below the char layer, see e.g. [8]. Fire tests with protected members have shown [15, 16] that bending stiffness decreases linearly until the start of charring. For simplicity, this linear decrease has been applied to the decrease of the reduced residual cross-section.

2.3.3. Reduced properties method.

This method gives values of $k_{mod,fi}$ for compressive, tensile and bending strengths as well as modulus of elasticity of members [17] using expressions (1) and (2). Originally developed for the German standard DIN 4102, the method was modified for ENV 1995-1-2. In the original relationships $k_{mod,fi}$ values were given as functions of the mean temperature of the whole cross-section, while in ENV 1995-1-2 and EN 1995-1-2 the relationships for $k_{mod,fi}$ are given as functions of the section factor (that is the ratio of the perimeter to the area of the residual cross-section) in analogy with the method used for unprotected steel sections. The reduction of cross-sectional strength and stiffness properties in [17] were derived using the test results of [18]. For small cross-sections with large section factors (and correspondingly high mean temperatures) the curves were fitted to test results on small solid timber frame members in bending [19].

2.3.4. Discussion.
Unfortunately only very few test results exist on timber members exposed on three or four sides where the "cold" strength properties were predicted with sufficient accuracy (the only ones known are those of reference [19]), which makes it difficult to compare the two models with test results. Therefore these models were compared with the results according to the advanced method (see 2.7) with thermal and mechanical properties given in annex B of EN 1995-1-2, see [20] (For the background of these properties, see 2.7.2 and 2.7.3 below). Four cross-sections were compared: 200 mm × 800 mm, 140 mm × 300 mm, 100 mm × 200 mm and 45 mm × 120 mm.

For bending, the reduced cross-section method agrees well with the advanced calculation method, while the reduced properties method is non-conservative. For members in compression or tension, both methods are non-conservative, although the results according to the reduced cross-section method are closer to the results of the advanced calculation. A thickness of the zero-strength layer larger than 7 mm would have been more appropriate, however, the method would not be simple because it would require different crosssections for different states of stress.

The section factor is a coarse parameter to determine the reduction of strength and stiffness properties of a cross-section [20], since it does not reflect the physical behaviour of heating (e.g. the insulation provided by the increasing char-layer is not taken into account).

Other draw-backs of the reduced properties method are:

- the gradual increase of strength reduction during the first 20 minutes or until start of charring of protected members is not taken into account;
- no reduction is given for shear strength;
- the section factor depends on whether notional or one-dimensional charring rates are used;
- although the method seems more complex it does not give better accuracy than the reduced cross-section method;
- the method cannot be used for timber slabs.

2.4 Simplified rules for analysis of structural members and components

EN 1995-1-2 gives a few rules for structural members (beams, columns) and bracing. The purpose of these rules is mainly to reduce the need of verifications. To give an example, compression perpendicular to the grain may be disregarded. The justification is that these rules have been applied during many years of design practice without any problems, rather than being the result of scientific research.

2.5 Design procedures for wall and floor assemblies

2.5.1. General.
EN 1995-1-2 gives design rules both for the separating and load-bearing functions. These rules have the potential to reduce the need of fire testing of such elements.

2.5.2. Analysis of the separating function.
The simple components additive method that was already given in ENV 1995-1-2 has been modified by combining it with a method presented in [21] (a short summary was presented in [22] and [23], the latter giving a review of several components additive methods). The total fire resistance, taken as the sum of the contributions from the different layers (claddings, void or insulated cavities) considering different heat transfer paths, see Figure 7, is

$$t_{\text{ins}} = \sum_{\text{i}} t_{\text{ins,0,i}}\, k_{\text{pos}}\, k_{\text{j}} \tag{7}$$

where:
$t_{\text{ins,0,i}}$ is the basic insulation value of layer "i" in minutes;
k_{pos} is a position coefficient;
k_{j} is a joint coefficient.

These contributions firstly depend on the inherent insulation property of each layer, as given by the basic insulation value, and secondly on the position of the respective layer and the materials backing or preceding that layer (in direction of the heat flux), as given by the position coefficient. The method of [21] was modified by extending it to floors, including the effect of joints in claddings that are not backed by members, battens or panels (taken from ENV 1995-1-2) and fitting some of the position coefficients to further test results that have become available during the drafting.

The method [21] is capable of considering claddings made of one or two layers of wood-based panels and gypsum plasterboard, and void or insulation filled cavities. The insulation may be made of glass or rock fiber.

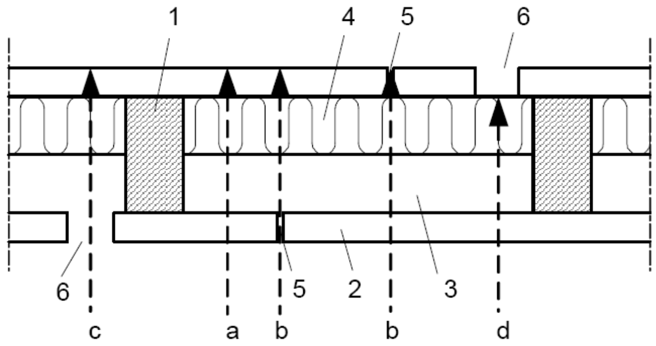

Key:
1 Timber frame member
2 Pannel
3 Void cavity
4 Cavity insulation
5 Panel joint not being backed with a batten, stud or joist
6 Position of services
a - d Heat transfer paths

Figure 7. Illustration of heat transfer paths through a separating construction [2].

2.5.3. Load-bearing floor joists and wall studs in assemblies whose cavities are completely filled with insulation.

The background of the rules for these assemblies (see Figure 8a) is found in [11, 15, 16]. Based on extensive fire tests, thermal and mechanical properties were determined and advanced calculations carried out to determine modification factors $k_{mod,fi.}$ These were expressed by simplified linear expressions to fit the needs of a design code. The heat transfer in the insulation near the timber stud or joist is two-dimensional giving rise to extensive charring near the corners on the fire exposed side. Since the shape of the residual cross-section of the timber frame members is too irregular for design calculations, a notional charring rate is given such that an equivalent residual cross-section can be calculated, see Figure 8b and c. For reduction of strength and stiffness properties, modification factors $k_{mod,fi}$ are given as functions of the ratio $d_{char,n}/h$. The relationships are different for different values of depth h, but for simplicity and on the safe side, the values for small depths of 95 mm may also be used for greater depths.

The concept of the reduced cross-section period, see 2.3.2, was considered as too inaccurate to model the reduction of strength and stiffness properties of timber frame members with partial protection of the sides by insulation material. The assumption of a 7 mm zero strength layer (as for

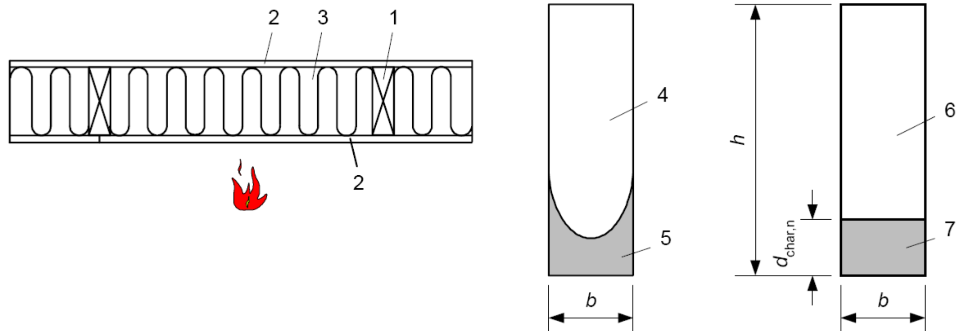

a) Section through assembly

b) Real residual cross-section and char-layer

c) Notional charring depth and equivalent residual cross-section

Key:
1 Timber frame member
2 Cladding
3 Insulation
4 Residual cross-section (real shape)
5 Char-layer (real shape)
6 Equivalent residual cross-section
7 Char-layer with notional charring depth

Figure 8. Charring of timber frame members.

three and four sided fire exposure) on the fire exposed side would lead to non-conservative results.

2.5.4. Charring of members in wall and floor assemblies with void cavities.

Very little information was available when rules for the determination of the charring of the timber members were drafted, mainly because this type of uninsulated construction is not used very much in Europe (requirements regarding thermal insulation and noise protection will normally lead to cavities filled with insulation material). Therefore the rules for this type of structures given in EN 1995-1-2 are coarse; they could be improved considerably. Although comprehensive research on uninsulated walls has been conducted in Australia and Canada, e.g. [24, 25], they have not contributed to simple design rules that would fit into Eurocode 5. The outcome of these research activities were sophisticated computer models helping to analyse the influence of various parameters and to increase our understanding.

2.6 Connections

The rules given in EN 1995-1-2 apply to symmetrical three-member connections made with nails, bolts, dowels, split-ring connectors, shear-plate connectors or toothed plate connectors. The simplified rules of ENV 1995-1-2 were partially adopted with minor modifications. It is stated that unprotected connections designed for normal temperature conditions according to EN 1995-1-1 exhibit a fire resistance of 20 minutes (dowels) or 15 minutes (all other types mentioned above). For greater fire resistances, increased member sizes or applied protection are necessary.

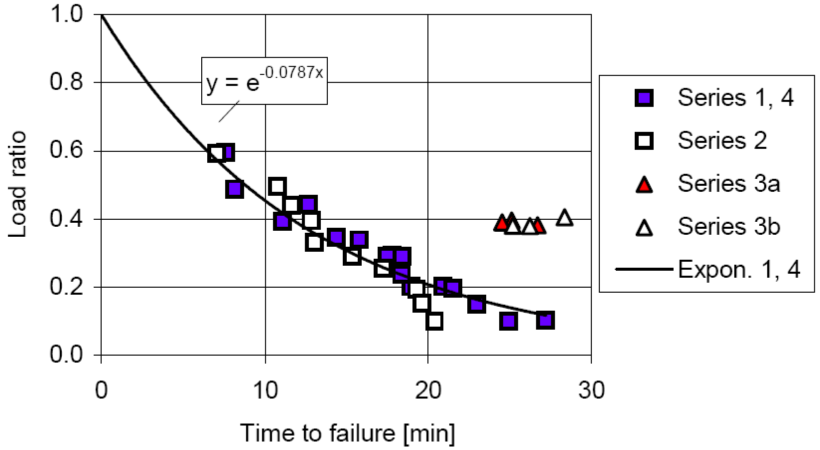

Figure 9. Load ratio versus time to failure for nail connections [21]. The values of series 3a and 3b illustrate the effect of increasing the side member thickness compared to the other series which comprise side members with the minimum thickness required by the Code.

An alternative strategy to increase the fire resistance of a connection is to reduce the load, or to reduce the load with together with increased member sizes or applied protection. The relative load-bearing capacity vs. time is given as an one-parameter exponential model which fits experimental results fairly well [26, 27], see e.g. Figure 9 and 10. The parameters k describing the exponential functions for different connections

$$\eta = e^{-k\, t_{d,fi}} \quad (8)$$

were determined using the test results given in [26, 28, 29], e.g. for nails and screws k = 0.08, for dowels in wood-to-wood connections $k = 0.04$.

The number of test results is still limited. Ongoing and future research will lead to improved design rules. Since longitudinally grooved smooth steel wire nails, common in Sweden, were used in the tests reported in [26], the factor $k = 0.8$ can be assumed to be more conservative for smooth round nails that are used in most countries of Europe, since their rope effect is smaller.

Due to the rope effect (which activates axial forces in the fasteners), the load-carrying capacity of timber connections is increased above the values given by Johansen's yield theory, see [4]. In the fire situation, however, this beneficial effect gradually decreases when, for example, the fastener head is pulled through the char layer. Although advanced calculations [30] on fire exposed timber connections have successfully been carried out by modifying Johansen's yield theory, the results are expected to be non-conservative for connections other than dowelled connections, since they disregard the rope effect.

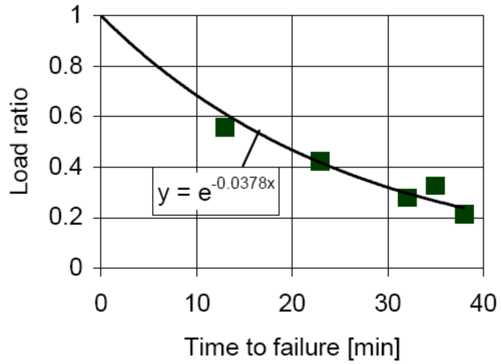

Figure 10. Load ratio versus time to failure for wood-to-wood connections with dowels [29].

For mechanically jointed members, in the fire situation, the slip modulus given in [4] for normal temperature conditions should be multiplied by a conversion factor. This conversion factor (for nails taken as 0.2, for bolts, dowels, and split ring connectors, shear plate connectors and toothed plate connectors taken as 0.67) was derived from test results with timber connections [26, 28, 29].

2.7 Advanced calculation methods

2.7.1. General.

In general, the Fire Parts of the Eurocodes allow for advanced calculation methods, that provide a realistic analysis of structures exposed to fire. For timber structures, EN 1995-1-2 gives more guidance to the user in an informative annex. Advanced calculation methods may be applied for the determination of the char depth, the development and distribution of the temperature within structural members (thermal response model) and the evaluation of the structural behaviour of the structure or any part of it (structural response model). The thermal response model must be based on the theory of heat transfer and take into account the variation of the thermal properties of the material with temperature, where necessary by using effective thermal properties, see 2.7.2. Advanced calculation methods for the structural response should take into account the changes of mechanical properties with temperature and also, where relevant, with moisture. The effects of transient thermal creep should be taken into account. For timber and wood-based materials, special attention should be drawn to transient states of moisture. The thermo-mechanical properties of timber given by EN 1995-1-2 take into account these influences, see 2.7.3.

2.7.2. Thermal properties.

For thermal analysis under standard fire conditions, temperature dependent thermal conductivity, heat capacity and density of wood are given. The thermal properties are effective values rather than real ones. The thermal properties – thermal conductivity and heat capacity values – were proposed in [9] as a result of calibration to test results and discussion of values from other sources. The main difference of these conductivity values compared to other sources, giving rise to a considerable effect on the temperature profiles in the timber member and of the charring depth, is the increase of conductivity for temperatures above 500°C, that is for the char-layer which undergoes cracking – leading to increased heat transfer by convection and radiation – and recession of the char surface.

Previously, a coarse approach to describe these phenomena had been made by Hadvig [6] assuming a sudden increase of the conductivity value at 6 mm below the char-line where the temperature is about 550°C. See also [31]. The relationship of density vs. temperature was taken from [32], however somewhat modified to take into account the recession of the char surface by assuming a linear decrease to zero between 800 and 1200°C.

The thermal properties given in EN 1995-1-2 should not be applied to fire curves other than the standard temperature-time curve. The investigation of [9] showed that temperature histories from tests under parametric fire exposure could not be predicted by the calculations. Since the thermal properties are effective ones rather than real ones – in order to take into account effects of mass transport that are not included in generally available computer models – it was argued that they should vary during different phases of a parametric fire curve, that is, that effective conductivity values could be dependent on the charring rate. Recently, this hypothesis was supported in [33], although it was found that the deviations couldn't solely be explained by different effective conductivity values. During the decay phase, glowing combustion of the char layer, causing high surface temperature considerably above the gas temperature in the fire compartment, was found to have an effect on temperature development in the timber member.

2.7.3. Mechanical properties.

The thermo-mechanical properties that should be used in e.g. a finite element analysis are given as temperature dependent relative values. The relationships are given as bi-linear curves with full strength or stiffness at 20°C and zero strength and stiffness at 300°C, that is at the char-line. All curves have a breakpoint at 100°C, see Figure 11 and 12. The compressive and tensile strengths and the modulus of elasticity in tension and compression were derived [10] from numerous test results on loaded timber frame

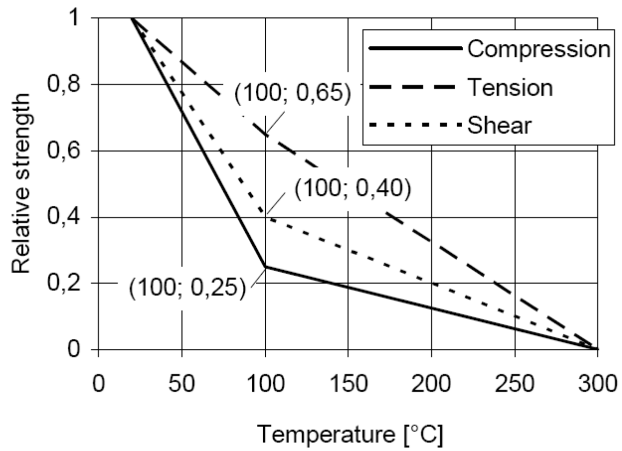

Figure 11. Temperature dependent relative strength of timber [2].

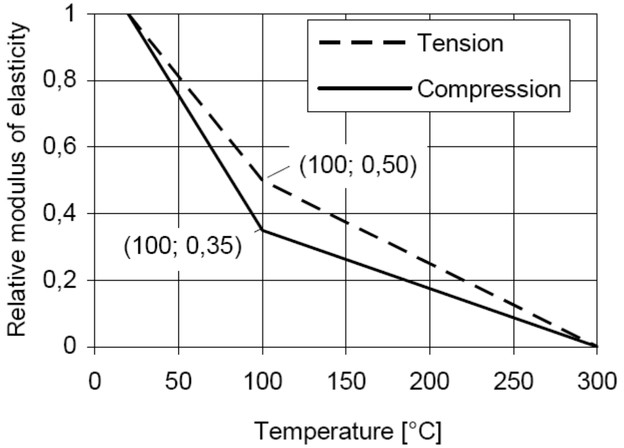

Figure 12. Temperature dependent relative modulus of elasticity [2], [10].

members in bending [15, 16]. By conducting the tests such that the fire exposed side of the members was either in tension or compression, the effect of elevated temperature on the each of above mentioned properties could be determined separately without being influenced by the others.

The relationships of the relative values of strength and modulus of elasticity and temperature were chosen as bi-linear curves. It was not believed that the experimental results could justify more complex curves, although attempts have been made [34]. In [10] relationships from other sources are discussed. It was found that they, in some cases, were in conflict with the derived ones, e.g. [18] which can be explained by the test procedure applied. Factors such as control of moisture content and loading rate play an important role, and the fact that the states of moisture and temperature in the fire situation are transient and not stationary as in the tests in several sources, e.g. [18].

The relationship for shear strength is according to [35]. The values can also be applied to withdrawal failure with respect to shear failure in the timber [36].

2.7.4. Parametric fire curves.

For limited application EN 1995-1-2 gives design rules for natural fire scenarios using parametric fire curves given in EN 1991-1-2 [3]. The rules apply to glued laminated beams in edgewise bending and include the calculation of the charring depth and relative bending strength. The charring rate is taken as constant during a period of t_0, that is approximately equal to the duration of the heating phase, and dependent on the fire load density and the opening factor. During the decay phase (cooling phase), the charring rate decreases linearly to zero at $t = 3t_0$, see Figure 13. The background of the rules for the determination of the charring depth is reported in [6, 37]. The modification factor for the reduction of the bending strength has been taken from [38] and takes into account that the bending strength continues to decrease for a considerable period of time after charring has stopped.

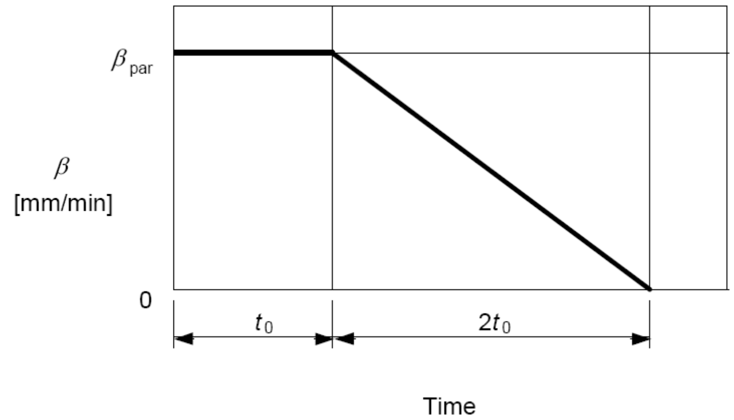

Figure 13. Relationship between charring rate and time for parametric fire curve [2].

References

1. EN 1990:2002, Eurocode 0 – Basis of Structural Design

2. EN 1995-1-2:2004 Eurocode 5: Design of timber structures, Part 1-2: General – Structural fire design

3. EN 1991-1-2:2002 Eurocode 1: Actions on structures – Part 1-2: General actions – Actions on structures exposed to fire

4. EN 1995-1-1:2004 Eurocode 5: Design of timber structures – Part 1-1: General – Common rules and rules for buildings

5. ENV 1995-1-2:1994: Eurocode 5: Design of timber structures – Part 1-2: General rules – Structural fire design

6. Hadvig S, Charring of wood in building fires. Technical University of Denmark, 1981

7. Schaffer E L, Charring rate of selected woods — transverse to grain. Forest Products Laboratory, Research Paper FPL 69, Madison, 1967

8. König J, Basic and notional charring rates. **Paper 35-16-1**, Kyoto, 2002

9. König J, Walleij L, One-dimensional charring of timber exposed to standard and parametric fires in initially unprotected and post-protection fire situations. Swedish Institute for Wood Technology Research, Rapport I 9908029. Stockholm, 1999.

10. König J, Wallleij L, Timber frame assemblies exposed to standard and parametric fires – Part 2: A design model for standard fire exposure. Swedish Institute for Wood Technology Research,

Rapport I 0001001, Stockholm, 2000

11. EN 520, Gypsum plasterboards – Definitons, requirements, test methods. Draft European standard 2003

12. Tsantaridis L, Östman B, König J, Fire protection of wood by different gypsum plasterboards.Fire and Materials 23, 45-48, 1999

13. König J, Rydholm D, Small-scale fire tests of heavy timber components. Swedish Institute for Wood Technology Research, Rapport P 0310036. Stockholm, 2003

14. Schaffer E L, Marx C M, Bender D A, Woeste F E, Strength validation and fire endurance of glued-laminated beams. Forest Products Laboratory, Research Paper FPL 467, Madison, 1986

15. König J, Fire resistance of timber joists and load-bearing wall frames. Swedish Institute for Wood Technology Research, Rapport I 9412071. Stockholm, 1995

16. König J, Norén J, Bolonius Olesen F, Toft Hansen F, Timber frame assemblies exposed to standard and parametric fires – Part 1: Fire tests. Swedish Institute for Wood Technology

Research, Rapport I 9702015. Stockholm, 1997

17. Scheer C, Knauf T, Meyer-Ottens C, Rechnerische Brandschutzbemessung unbekleideter Holzbauteile. Bautechnik 69 (1992), Heft 4

18. Glos P, Henrici D, Festigkeit von Bauholz bei hohen Temperaturen. Institut für Holzforschung, Universität München, Abschlussbericht 87505, 1990

19. Norén J, Failure of structural timber when exposed to fire. Proceedings of 1988 Int. Conf. on Timber Engineering, Seattle

20. König J, Källsner B, Cross-section properties of fire exposed rectangular timber members. **Paper 34-16-2**, Venice, 2001

21. Norén, J, Additionsmetoden – Beräkning av brandmotstånd hos avskiljande väggar (in Swedish). Swedish Institute for Wood Technology Research, Rapport I 9312070. Stockholm, 1994

22. Östman B, König J, Norén J, Contribution to fire resistance of timber frame assemblies by means of fire protective boards. Proceeding of the 3rd International Fire and Materials Conf., Washington D.C.,1994

23. König J, Oksanen T, Towler K, A review of component additive methods used for the determination of fire resistance of separating light timber frame construction. **Paper 33-16-2**, Delft, 2000

24. Clancy P, Time and probability of failure of timber framed walls in fire. Doctoral thesis, Victoria University of Technology, Victoria, Australia, 1999

25. Takeda H, Mehaffey J R, Wall2D: a model for predicting heat transfer through wood-stud walls exposed to fire. Fire and Materials 1998; 22: 133-140

26. Norén J, Load-bearing capacity of nailed joints exposed to fire. Fire and Materials; 1996; 20:133-143

27. König J, Fontana M, The performance of timber connections in fire – Test results and rules of Eurocode 5. Proceedings of International Rilem Symposium “Joints in Timber Structures”, University of Stuttgart, 12/14 September 2001

28. Dhima D, Vérification expérimentale de la résistance au feu des assemblages d´éléments en bois. CTICM, Ref. INC – 99/399 – DD/NB, 1999

29. Kruppa J, Lamadon T, Racher P, Fire resistance tests of timber connections. CTICM, Ref. INC-00/187-JK/NB, 2000

30. Povel D, Tragfähigkeit von Holzverbindungen mit stabförmigen Verbindungsmitteln im Brandfall. Doctoral thesis, Technische Universität Berlin, 2002

31. Källsner B, König J, Thermal and mechanical properties of timber and some other materials used in light timber frame construction. **Paper 33-16-3**, Delft, 2000

32. Janssens, M, Thermo-physical properties for wood pyrolysis models. Pacific Timber Engineering Conference, 1994, Gold Coast, Australia

33. König J, Effective thermal actions and thermal properties of timber members in natural fires. Third International Workshop “Structures in Fire”, Ottawa, 2004

34. Clancy P, A parametric study on the time-to-failure of wood framed walls in fire. Fire Tecchnology, 38, 243-269, 2002

35. Gerhards C C, Effect of moisture content and temperature on the mechanical properties of wood: An analysis of immediate effects. Wood and Fiber 1982; 14:4-36

36. Mischler A, Frangi A, Pull-out tests on glued-in rods at high temperatures. Proceedings of CIB W18, Meeting thirty-four, Venice, 2001

37. Toft Hansen F, Bolonius Olesen F, Full-scale tests on loaded glulam beams exposed to natural fires. Aalborg Universitetscenter, Aalborg, 1992

38. Bolonius Olesen F, König J, Tests on glued laminated beams in bending exposed to natural fires. **Paper 25-16-2**, Åhus, 1992